2022

The Effects Of Platelet Signaling Inhibitors On Clot Development Under Flow

Yiyuan Zhang
University of Pennsylvania

The Effects Of Platelet Signaling Inhibitors On Clot Development Under Flow

Abstract

GPVI is the first responder towards collagen surface and therefore, the role of GPVI in facilitating primary platelet deposition is well studied and unquestionable. However, whether it plays a part in secondary platelet deposition by binding with fibrin, thus facilitating further platelet activation remains a question. Depending on the experiment method and rationale behind it, different results and conclusion could be achieved, thus it calls for a method that could better recapitulate human blood system under in vitro setting with appropriate methods to inhibit GPVI.Indirect method incorporates Syk and Src family kinases (SFK) inhibitors; these molecules interfere with signaling from GPVI, α2β1, αIIbβ3, and GPIb-IX-V to reduce thrombotic risk or induce bleeding episodes. Collagen-mediated clustering of platelet GPVI results in phosphorylation of SFKs such as Lyn and Fyn, and active Lyn is constitutively bound to GPVI to allow rapid signaling. During clotting under flow, the generation of fibrin can have diverse influences on platelet signaling by sequestering thrombin and potentially activating GPVI signaling within the clot interior. These inhibitors tackle the thrombus formation at earlier stages since the platelets reach the activation surface. Direct inhibition of GPVI, which involves using an artificial anti-GPVI fragment, was used to avoid undesirable inhibition and compare the difference between inhibition of subsequent pathways. Using microfluidics, the effects of these inhibitors can be explored under defined hemodynamic flows and procoagulant surface triggers. Additionally, the drug may be present in the blood at desired time of clotting by perfusion switching to drug-treated blood. This experimental design allows exploration of platelet response at different stages of clotting through the measurement of drug potency to modulate clotting on different procoagulant surface conditions, interactions between various coagulation factors in plasma, and the kinetics of several competitive reactions to facilitate platelet recruitment, granule release and fibrin formation.

Degree Type

Dissertation

Degree Name

Doctor of Philosophy (PhD)

Graduate Group

Chemical and Biomolecular Engineering

First Advisor

Scott L. Diamond

Subject Categories

Cell Biology

THE EFFECTS OF PLATELET SIGNALING INHIBITORS ON CLOT DEVELOPMENT UNDER FLOW

Yiyuan Zhang

A DISSERTATION

in

Chemical and Biomolecular Engineering

Presented to the Faculties of the University of Pennsylvania

in

Partial Fulfillment of the Requirements for the

Degree of Doctor of Philosophy

2022

Supervisor of Dissertation

Scott L. Diamond

Arthur E. Humphrey Professor, Department of Chemical and Biomolecular Engineering

Graduate Group Chairperson

John C. Crocker

Professor, Department of Chemical and Biomolecular Engineering

Dissertation Committee

Lawrence F. Brass, Professor, Department of Medicine

Bomyi Lim, Assistant Professor, Department of Chemical and Biomolecular Engineering

Talid R. Sinno, Professor, Department of Chemical and Biomolecular Engineering

THE EFFECTS OF PLATELET SIGNALING INHIBITORS ON CLOT DEVELOPMENT UNDER FLOW

ACKNOWLEDGMENT

First, I would like to thank my advisor, Dr. Scott Diamond, for his consistent mentorship and guidance in scientific field for the past five years. He introduced me to the professional path of being a scientific researcher by teaching me experimental design, critical literature review, and most importantly, how to be a critical thinker. Without whom, I would not have achieved as much in this scientific realm. I would also like to thank my committee, Dr. Lawrence Brass, Dr. Talid Sinno, and Dr. Bomyi Lim for their insightful suggestions and feedback that have constructed the foundation of my thesis.

Second, I would like to thank all the current and former members of the Diamond Lab who I have had the pleasure to work with: Xinren Yu, Chris Verni, Jason Rossi, Jason Chen, Evan Tsiklidis, Kevin Trigani, Michael DeCortin, Jennifer Crossen, Kaushik Shankar, Dr. Noelia Grande Gutierrez, and Yue Liu. I received many ideas, assistance, and chances to collaborate with you for experiments and projects. Many times, you have challenged my ideas that made the experimental design closer to perfection. Beyond that, I also received friendship that made the relationships shine with a bit of personal touch. I would also like to extend some appreciation to regular donors of Diamond Lab, such as Samuel Keller and Dennis Deng, whose kind donations built up the results of my thesis.

Lastly, I would like to thank my mentors and coworkers during my co-op at GlaxoSmithKline, including BanuPriya Sridharan, Katrina Wisdom, Jason Ekert, Prasanna Chandramouleeswaran, Taraka Sai Pavan Grandhi, Terrence Roh and Michelle Ma from Complex In Vitro Models, Lidia Tagliafierro from Novel Human Genomics, as well as Yanzhe ‘Ian’ Gao and Paige Fenn from Protein, Cellular and Structural Sciences, for all your help, guidance and occasional humor that made my short stay an unforgettable life experience. It has been a real pleasure working with you and hopefully our paths cross again for future career development.

ABSTRACT

THE EFFECTS OF PLATELET SIGNALING INHIBITORS ON CLOT DEVELOPMENT UNDER FLOW

Yiyuan Zhang

Scott L. Diamond

GPVI is the first responder towards collagen surface and therefore, the role of GPVI in facilitating primary platelet deposition is well studied and unquestionable. However, whether it plays a part in secondary platelet deposition by binding with fibrin, thus facilitating further platelet activation remains a question. Depending on the experiment method and rationale behind it, different results and conclusion could be achieved, thus it calls for a method that could better recapitulate human blood system under *in vitro* setting with appropriate methods to inhibit GPVI.

Indirect method incorporates Syk and Src family kinases (SFK) inhibitors; these molecules interfere with signaling from GPVI, α2β1, αIIbβ3, and GPIb-IX-V to reduce thrombotic risk or induce bleeding episodes. Collagen-mediated clustering of platelet GPVI results in phosphorylation of SFKs such as Lyn and Fyn, and active Lyn is constitutively bound to GPVI to allow rapid signaling. During clotting under flow, the generation of fibrin can have diverse influences on platelet signaling by sequestering thrombin and potentially activating GPVI signaling within the clot interior. These inhibitors tackle the thrombus formation at earlier stages since the platelets reach the activation surface. Direct inhibition of GPVI, which involves using an artificial anti-GPVI fragment, was used to avoid undesirable inhibition and compare the difference between inhibition of subsequent pathways.

Using microfluidics, the effects of these inhibitors can be explored under defined hemodynamic flows and procoagulant surface triggers. Additionally, the drug may be present in the blood at desired time of clotting by perfusion switching to drug-treated blood. This experimental design allows exploration of platelet response at different stages of clotting through the measurement of drug potency to modulate clotting on different procoagulant surface conditions, interactions between various coagulation factors in plasma, and the kinetics of several competitive reactions to facilitate platelet recruitment, granule release and fibrin formation.

TABLE OF CONTENTS

LIST OF ILLUSTRATIONS

CHAPTER 1 – INTRODUCTION

1.1 Thrombosis and Hemostasis

Depending on the nature of a clot building up in the blood vessel, the process of the clot formation could be defined as thrombosis and hemostasis. Thrombosis occurs when blockage of vessel is caused by pathological reasons, such as rupture of an atherosclerotic plaque or intima erosion under arterial flow, or valve stasis in venous valve pocket (1). Further development of such conditions could lead to severe diseases such as stroke, coronary artery diseases, heart disease and related conditions, which are the leading causes of death around the world (2). A diagram of this process is shown in Figure 1-1 (1).

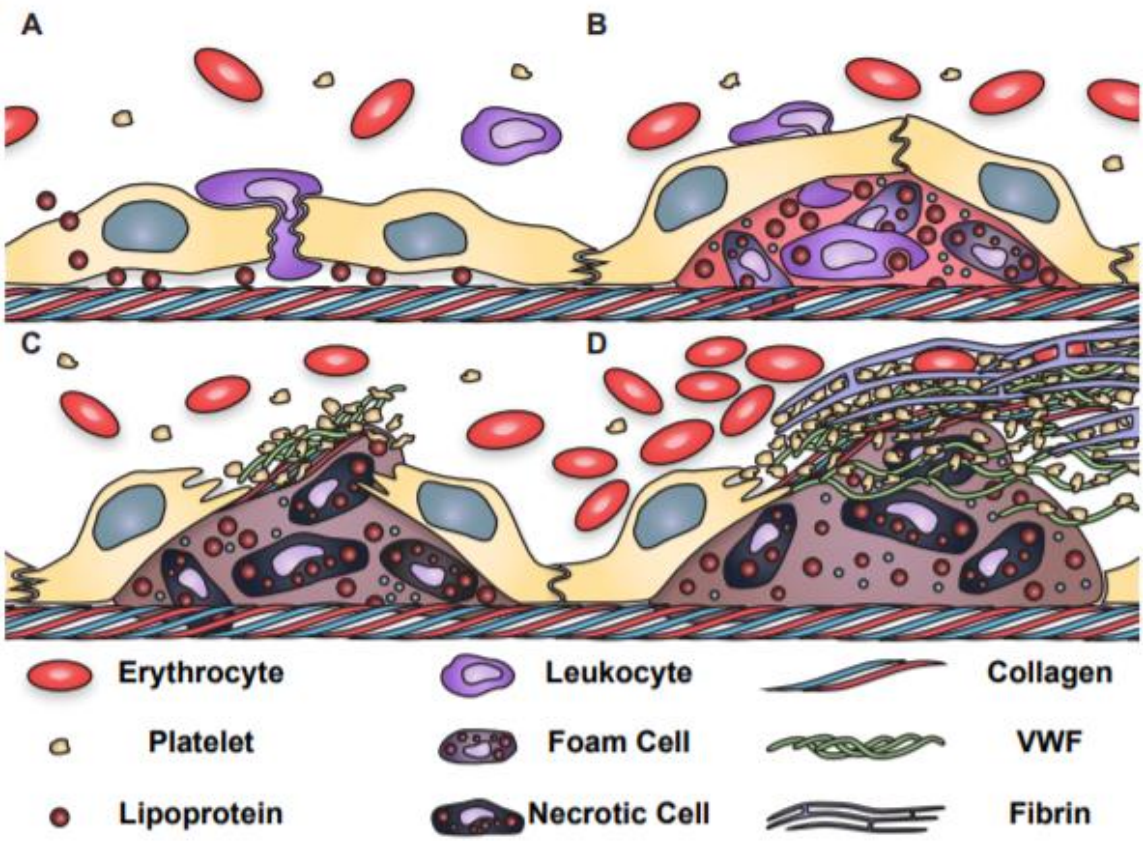

Figure 1-1: Arterial thrombosis formation

Rupture of an atherosclerotic plaque took place (A) and resulted in lipoprotein and leukocyte buildup inside the rupture (B), which later developed into a pathological blockage that induced attachment of VWF and collagen, forming activating surface for platelet (C) and eventually developed into a pathological thrombus plug (D).

In contrast, hemostasis is a normal reaction towards blood vessel injury that involves interruption of blood flow (3). The blood vessel contains endothelium and subendothelial matrix, where endothelium is in contact with blood and the anticoagulant surface maintains the blood flow as liquid (3). Once rupture or injury happened that lead to disintegration of endothelium, blood will be exposed to the procoagulant surface of subendothelial matrix, thus triggering the subsequent coagulation process (4). Primary platelet deposition occurs when the first arriving platelets get exposed to and bind activating surface containing collagen and von Willebrand Factor (VWF) (5). These platelets get activated, releases secondary agonists including ADP, Thromboxane A_2 (TxA_2) and granules which will recruit more platelets in the blood flow and transits into secondary platelet deposition, where major interactions involve platelet binding of fibrinogen and crosslinking of fibrinogen that forms fibrin under the effect of thrombin (6). Thrombin will also further activate platelets on the injury site (7). This process is illustrated in Figure 1-2 (8).

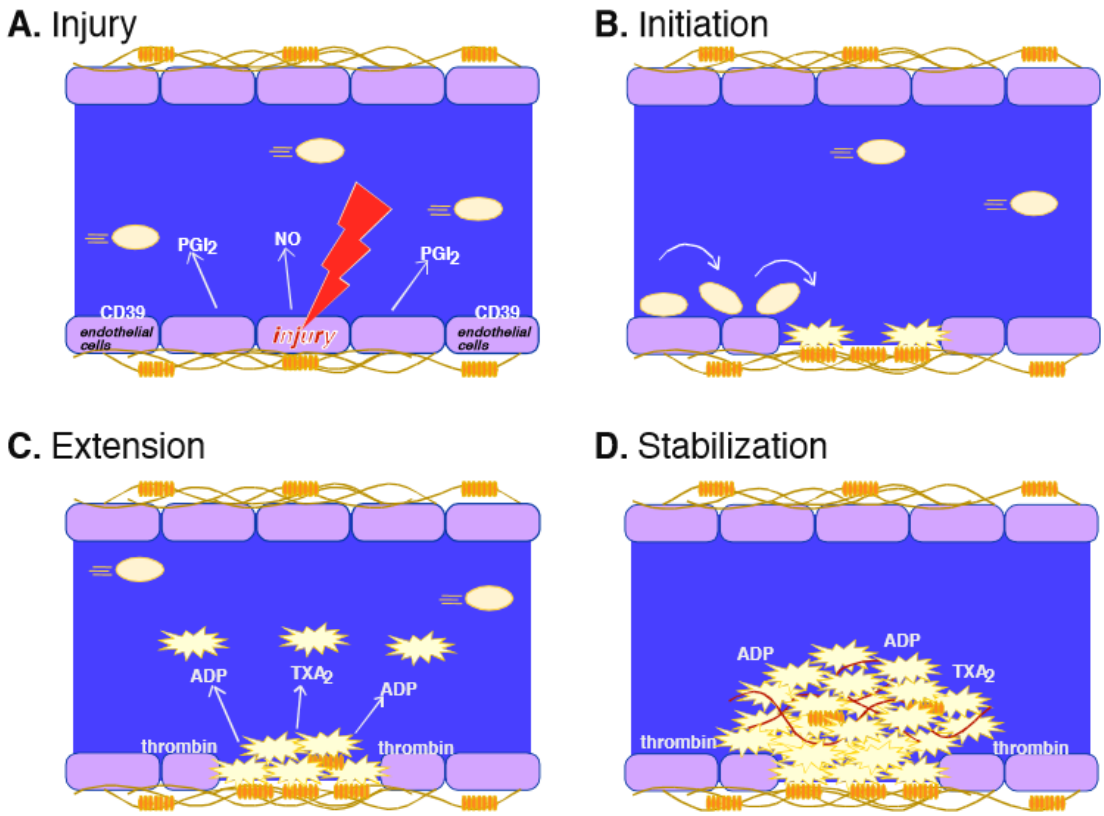

Figure 1-2: Process of hemostasis

When injury happens (A), platelets will get attached to the activation surface (B) and get activated, releasing agonists to recruit more platelets in the blood flow (C). Once fibrin is polymerized, platelets will form a mesh structure and stabilize the blood loss on the injury site (D).

1.2 Platelets and the Coagulation Cascade

Platelets are anucleate cells generated from megakaryocytes and released into blood circulation, which serve as the major participants of coagulation (9). There are many receptors that could trigger the activation of platelets when exposed to different agonists, such as collagen, VWF, thrombin, ADP, and Thromboxane A_2 (10,11). Downstream of these receptors are different activation pathways that involves many kinases such as spleen tyrosine kinase (syk), Src family kinases (SFK) and protein kinase C (PKC), which will be phosphorylated in different manners and regulates calcium ion that drives the process of platelet activation (12). The series of events are illustrated in Figure 1-3 (13).

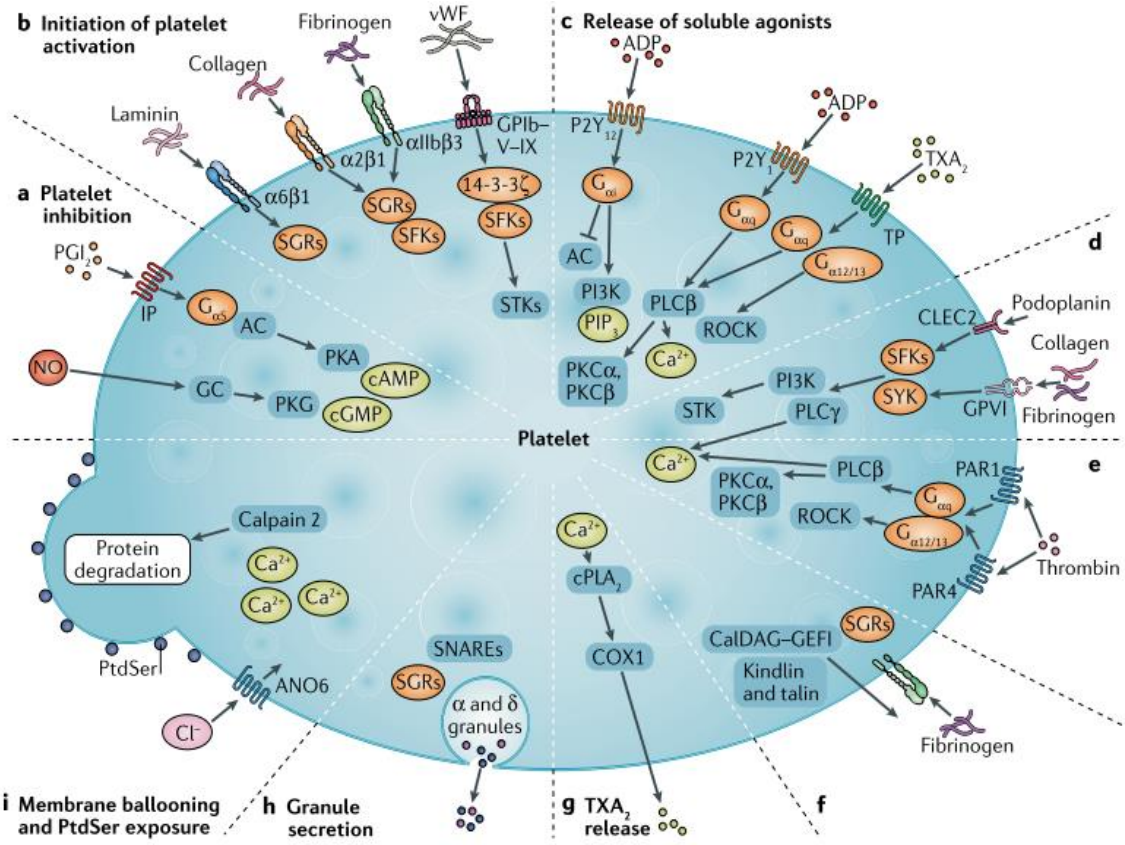

Figure 1-3: Platelet activation and inhibition

Platelets are inhibited under normal conditions, mainly through NO produced from endothelial cells. When needed, platelet can be activated by collagen or VWF from injury site through outside-in signaling, resulting further activation by ADP, TxA2, and thrombin that triggers calcium mobilization which facilitates recruiting and activating other platelets. Then, inside-out signaling would take place, triggers granule release and phosphatidylserine (PS) exposure.

During this process, platelet will release granules that react with quiescent coagulation factors in plasma to convert them into the active form, to recruit other platelets in the blood flow and further reinforce the activation process of platelets (13). This series of reaction is referred as the coagulation cascade, and depending on the initiation event, it could start from the contact activation (intrinsic) pathway and the tissue factor (extrinsic) pathway. The intrinsic pathway is triggered by damaged surface, which coverts FXII to FXIIa with HMW kininogen and prekallekerin (14). The extrinsic pathway is triggered by trauma, that involves exposure of FVII to tissue factor and conversion to FVIIa (15). Through a series of conversion of coagulating factors, these two pathways will eventually undergo the common pathway, which involves conversion of FX and FV to their respective active forms and formation of a complex of FXa, FVa and platelet phospholipids that lead to the conversion of prothrombin (FII) to thrombin (IIa) (16). Thrombin facilitates the cleavage of fibrinogen (FI) and crosslinking to form fibrin (FIa) meshes (6,17). Thrombin also further amplifies the extent of platelet activation by converting FXI, FV and FXIII to their respective active forms (10), showing its critical role in hemostasis and thrombus formation.

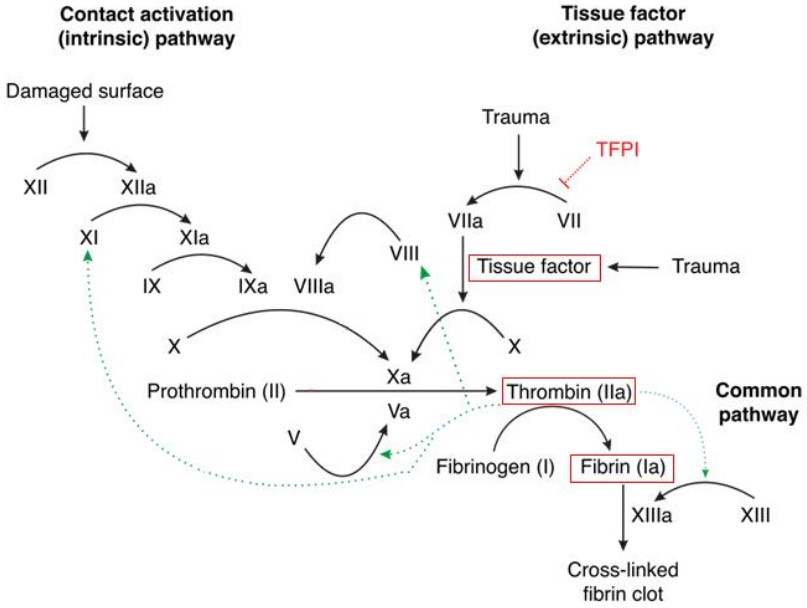

Figure 1-4: Coagulation cascade

Damaged surface and trauma could trigger activation of coagulation factors in different ways, but both leads to formation of Xa-Va complex that converts prothrombin (II) to thrombin (IIa), which plays a part in cleaving fibrinogen to form fibrin polymer and further activates platelets.

1.3 Role of GPVI, Primary Platelet Deposition and Secondary Platelet Deposition

Among all receptors on the surface of platelets, Glycoprotein VI (GPVI) is the first one that responds to exposure of collagen (18,19). Along with GPIb-V-IX complex that responds to VWF upon first exposure, these two receptors will trigger outside-in signaling within platelet through phosphorylation and calcium mobilization to achieve platelet activation and granule release (10,20). Up till this point, most of the interaction happens between platelets and activation surface, and this process is called primary platelet deposition.

Subsequently, through outside-in signaling, $\alpha_2\beta_1$ is converted to its high affinity form to bind with collagen to further anchor the platelet under flow (10), while $\alpha_{IIb}\beta_3$ is converted to their high affinity form and bind with fibrinogen to attract other platelets (10,21). Granules released from first arriving platelets will trigger thrombin generation through the complex of FXa, FVa and platelet phospholipids (16); this will facilitate fibrin crosslinking and reinforce platelet activation through PAR1 and PAR4 (22). TXA_2 and ADP generated through granule release will further activate platelet through TP, $P2Y_1$ and $P2Y_{12}$ receptors (22–24). This process is called secondary platelet deposition, for most of the interactions of platelet involves further recruitment of platelets to the injury site (25).

However, there is no clear conclusion whether fibrin is an agonist of GPVI. Studies have proved that fibrin could act as an activator on GPVI with washed platelets (26,27), but previous studies also showed that fibrin dimer acts as an antagonist of platelet coagulation (28). Neither study was done under the effects of flow with whole blood, thus a more wholistic method that involves human whole blood in a microfluidics context is required to provide another angle for this controversy.

1.4 Microfluidics and “Perfusion-Switch” Assay

To facilitate the *in vitro* experiments with human whole blood under a flow setting to recapitulate a bleeding model in human body, we used our previously developed 8-channel microfluidic device (29). A pre-coated collagen strip on treated glass slide will serve as the activating surface and depending on the need to observe fibrin formation under thrombin, collagen strip will be incubated with tissue factor for 30 mins before the experiment (5). The flow

rate could be controlled by the syringe pump to recapitulate venous (100~200 s^{-1}) or arterial (>500 s^{-1}) wall shear rate (30,31).

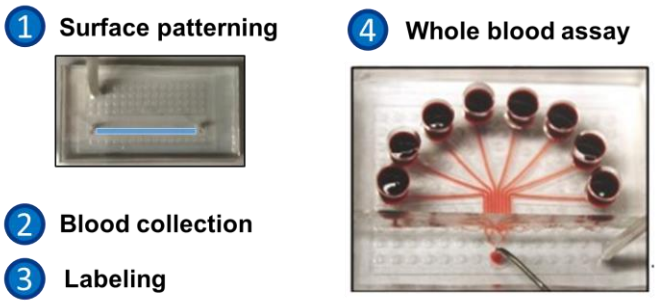

Figure 1-5: General workflow of 8-channel microfluidics experiments

Surface patterning could include tissue factor by incubating with collagen for 30 mins for fibrin formation. Eight wells could load collected whole blood treated with different compounds and ran independent experiments at the same time. Blood switch could happen at wells upstream.

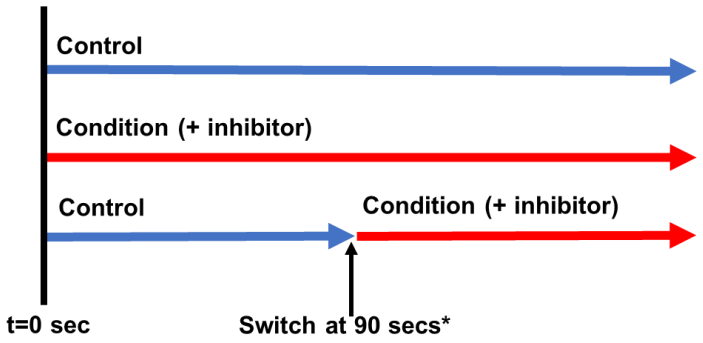

Figure 1-6: "Perfusion-switch" assay layout

Three streams are involved: control, condition with inhibitor, and "switch" streams that has control blood for the first 90 seconds of experiment, then switched to condition blood.

To achieve effective GPVI inhibition during secondary platelet deposition, we introduced the "perfusion-switch" assay. The assay includes three conditions: control (no compound added), condition (compound added at the beginning of the experiment), and "switched" streams where control blood will be flowed for the first 90 seconds to achieve sufficient primary platelet deposition (switch time obtained through experiments), then switch to inhibited blood (condition) instantly by draining and refilling the upstream wells (32). This way, a thin layer of normal platelets is coated on the activating surface, but subsequent clot development is achieved by GPVI-inhibited whole blood, allowing us to study the interaction between GPVI and fibrin.

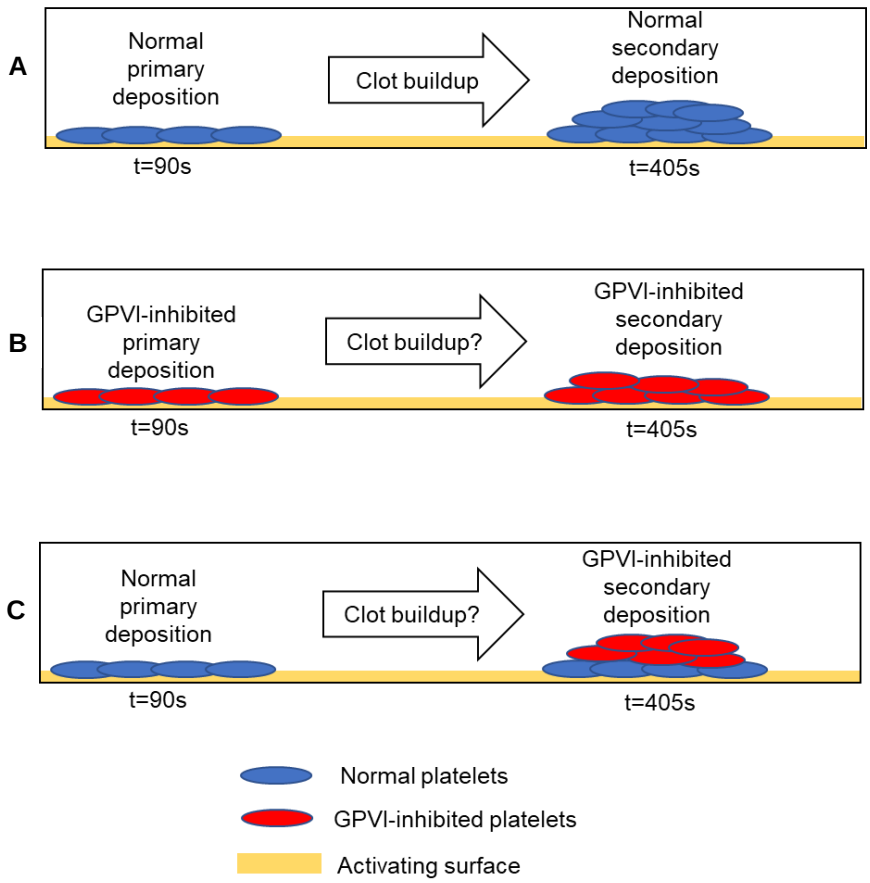

Figure 1-7: Graphic illustration of perfusion switch experiment using GPVI inhibited blood

Control whole blood with normal platelets shows normal clot buildup (A), while inhibited whole blood shows clot formation with GPVI inhibition during primary and secondary deposition (B). Switched stream shows normal primary deposition, then switched to GPVI inhibited whole blood to illustrate differences in clot development during secondary deposition only, thus testify the interaction between fibrin and GPVI.

1.5 GPVI Inhibitors: Dasatinib, GS-9973, and Anti-GPVI Fab

There are two ways to achieve GPVI inhibition: indirect inhibition that is achieved by inhibiting key kinases downstream of GPVI activation pathway, or direct inhibition using selective antibodies. Indirect inhibition of GPVI involves Src family kinase (SFK) inhibition and spleen tyrosine kinase (syk) inhibition.

Dasatinib, as a compound frequently used for treating Philadelphia leukemia, was observed to have a bleeding side among patients (33,34). It is later proven to be a very potent SFK inhibitor that acts on several SFKs including Src, Lyn, and Fyn, which are directly downstream of GPVI (), thus achieving inhibition of GPVI-activation pathway. Downstream of Lyn

and Fyn through immunoreceptor tyrosine-based activation motif (ITAM), syk gets phosphorylated and subsequently, triggers further platelet activation and calcium mobilization (35). GS-9973 (Entospletinib) is a newly discovered molecule that selectively inhibits syk, with a better permeability that requires around five minutes of incubation time for total inhibition (36,37). With dasatinib and GS-9973, SFK and syk could be inhibited respectively, and their role in GPVI-inhibition in primary and secondary platelet deposition could be studied through clot formation under microfluidics.

Direct inhibition will require a specific binding antibody on GPVI which will allow total inhibition of GPVI-activation pathway while avoiding undesired inhibition on activation pathways corresponding to other platelet receptors, such as $\alpha_2\beta_1$, $\alpha_{IIb}\beta_3$, PAR1 and PAR4 (32,38). However, a specific antibody is difficult to come by, so in collaboration with Nieswandt research group from University of Würzburg, we obtained some novel anti-GPVI Fab (the Fab fragment of human GPVI blocking antibody (clone E12)) developed in their group to study the effect of direct inhibition of GPVI and its role in GPVI inhibition for primary and secondary platelet deposition through clot formation under microfluidics. These results will be discussed in the next chapters in detail.

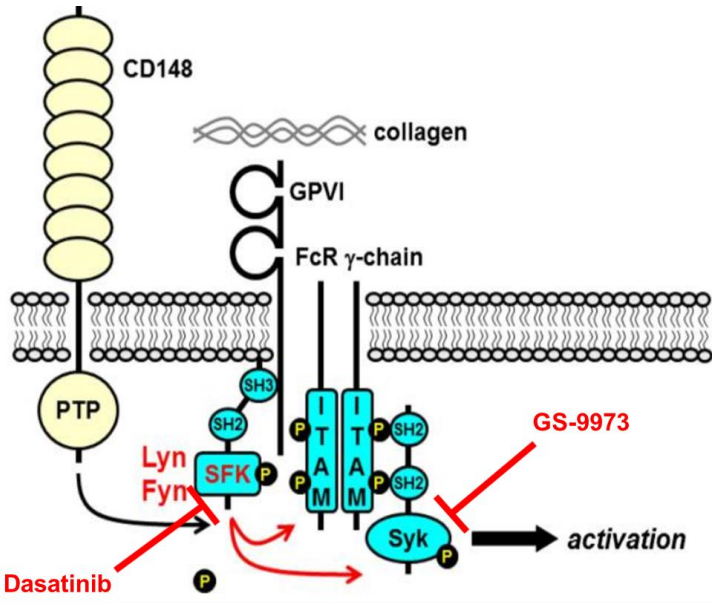

Figure 1-8: Activation pathway downstream of GPVI

Relative location of SFK and syk downstream of GPVI, and their respective inhibitors, dasatinib and GS-9973.

CHAPTER 2 – ACHIEVING GPVI INHIBITION THROUGH DASATINIB AND GS-9973, AND THEIR ROLES ON DIFFERENT STAGES OF CLOT GROWTH

2.1 Introduction: Using dasatinib and GS-9973 to inhibit GPVI signaling pathway at different stages of platelet deposition and observation of subsequent clot growth

Dasatinib is a commonly used kinase inhibitor for imatinib-resistant Philadelphia chromosome-positive leukemias (39), chronic myelogenous leukemia (CML) and acute lymphoblastic leukemia (ALL) (33,40) due to its inhibition of BCR-Abl tyrosine kinase and Src family kinases such as Lyn, Fyn and Src (34). GS-9973 (entospletinib) is another drug targeting Syk for the treatment of various cancers, including diffuse large B cell lymphoma (DLBCL), mantle cell lymphoma (MCL), and non-Hodgkin lymphoma (NHL) (41). Fostamatinib (42), the prodrug of R-406 (tamatinib) (43), as inhibits Syk (42,44,45). However, along with their efficacy in treating various cancers, side effects of Syk or SFK targeting include bleeding (46). Recent research shows that these coagulation risks are caused by the inhibition effects on Syk/Src within platelets that are linked to platelet inhibition (46), and reduced platelet activation mediated by FcγRIIA (47). Alternatively, certain kinase inhibitors may have utility as antithrombotic agents (48,49). For example, a Syk inhibitor could interfere with signaling from GPVI (50), a2b1, $a_{IIb}b_3$, and potentially GPIb-IX-V to reduce thrombotic risk (51).

Platelets can become activated through diverse receptors, depending on the procoagulant surface, the platelet location in the clot, and the elapsed time since the start of the clotting event. For example, the earliest arriving platelets may immediately encounter collagen and thrombin at the triggering surface of clotting. Platelets arriving later may encounter other clot-adherent platelets, fibrin, and diffusible agonists such as ADP and thromboxane, but have no physical contact with collagen. The core-shell architecture of clots is emblematic of this spatiotemporal heterogeneity of receptor engagement as seen in assays of mouse laser injury (21) or microfluidic human blood clotting (17). Similarly, pharmacological agents may engage platelet targets at distinct locations or temporal stages of clotting.

Collagen-mediated clustering of platelet GPVI results in phosphorylation of Src family kinases (SFKs) such as Lyn and Fyn (35). Also, active Lyn is constitutively bound to GPVI to

allow for rapid signaling (52). Lyn phosphorylation of ITAM domains of FcRg drives spleen tyrosine kinase (Syk) binding and phosphorylation at Tyr352 (35). Downstream of GPVI activation, phosphorylated Syk (Syk-pY352) drives activation of phospholipase C_{g2} (PLC_{g2}) and sustained calcium mobilization (53). With fibrinogen binding to activated platelets, outside-in signaling through $a_{IIb}b_3$ results in Src phosphorylation (Src-pY418), ultimately resulting in the generation of phospho-Syk and PLC_{g2} activation. Thrombin activation of protease activated receptors, PAR-1 and PAR-4, drives Gaq activation of PLC_b and transient calcium mobilization. During clotting under flow, the generation of fibrin can have diverse influences on platelet signaling by (i) sequestering thrombin (54,55) and potentially (ii) activating GPVI signaling within the clot interior (27,56,57).

Using microfluidics, the bleeding side effects of drugs can be explored under defined hemodynamic flow, defined procoagulant surface triggers, and in human blood. Additionally, the drug may be present in the blood from the start of the clotting event or can be added acutely at a later time by perfusion switching to drug-treated blood. This “perfusion-switch” experimental design allows exploration of platelet signaling at different stages of clotting through the measurement of kinase inhibitor potency to modulate clotting on different procoagulant surface conditions.

2.2 Materials and Methods

2.2.1 Materials

Reagents were obtained as follows: anti-human CD61 antibody (BD Biosciences, San Jose, CA. Cat#: 555754), Alexa Fluor 647–conjugated human fibrinogen (Life Technologies, Grand Island, NY. Cat#: F35200), Alexa Fluor 488 phospho-Src (Tyr418) polyclonal antibody (ThermoFisher Scientific, Waltham, MA. Cat#: 44-660A1), Dade Innovin prothrombin time (PT) reagent (Siemens, Malvern, PA. Cat#: B4212-40), collagen (type I; Chrono-Log, Havertown, PA. Cat#: 385), Sigmacote® (Millipore Sigma, Burlington, MA. Cat#: SL2-100ML), H-Gly-Pro-Arg-Pro-OH (GPRP; Millipore Sigma, Burlington, MA. Cat#: 03-34-0001), dasatinib (Selleckchem, Houston, TX. Cat#: S1021), GS-9973 (entospletinib) (Selleckchem, Houston, TX. Cat#: S7523), Alexa Fluor 488-conjugated annexin V (ThermoFisher Scientific, Waltham, MA. Cat#: A13201),

GR144053 (Tocris Biosciences, Bristol, UK. Cat#: 1263), Phe-Pro-Arg-chloromethylketone (PPACK, Haematologic Technologies, Essex Junction, VT. Cat#: FPRCK-01) and corn trypsin inhibitor (CTI, Haematologic Technologies, Essex Junction, VT. Cat#: CTI-01).

2.2.2 Preparation and characterization of collagen/TF surface

Glass slides were rinsed with ethanol, then deionized water, and dried with filtered air. Sigmacote® was used to create a hydrophobic surface on the glass. A volume of 5µL of fibrillar collagen was perfused through a patterning channel (250 µm wide × 60 µm high) of a microfluidic device to create a single 250 mm-wide stripe of fibrillar collagen for all experiments, as previously described (29,30). For experiments without thrombin interaction, collagen was rinsed and blocked with 20 mL 0.5% bovine serum albumin buffer (BSA). For experiments that study the effect of thrombin, lipidated TF was sorbed to the collagen surface by perfusing of 5 µL of Dade Innovin PT reagent (20 nM stock concentration), rinsed and blocked with 20 mL 0.5% BSA, then incubated for 30 min without flow, as previously described (29,30).

2.2.3 Blood collection and preparation

Blood was obtained via venipuncture into a syringe containing either PPACK (1:100 v/v; final concentration of 100 µmol/L) or high concentration of CTI (40 mg/mL) from healthy donors who self-reported as free of alcohol use for at least 72 hr and medication for at least a week prior to blood collection. All donors provided informed consent under approval of the University of Pennsylvania Institutional Review Board. Blood was treated with anti-human CD61 antibody (stock concentration, 1:50 v/v [%] in whole blood) and Alexa Fluor 647-conjugated human fibrinogen (1 mg/mL stock solution, 1:80 v/v [%] in whole blood) immediately after blood collection for platelet labelling and fibrin labeling, respectively. While CD61 can bind both platelets and white blood cells, the platelet deposits made on collagen/TF under flow contain essentially no white blood cells until substantially later times. Even at low resolution, white blood cell staining would be morphologically detected if it were present. Annexin V (stock concentration, 1:80 v/v [%] in whole blood) was added for phosphatidylserine labeling when needed. Dasatinib was dissolved in DMSO and diluted in Millipore water, the final concentration was 10 µM (58) (DMSO < 0.1% v/v) after addition to whole blood. The final concentration of DMSO in perfused blood was < 0.1% by

vol. In control experiments, no effect of DMSO at 0.1 % was detected on platelet or fibrin under flow. Additionally, platelet function was essentially unaltered even at 1% DMSO by vol/ (3 donors, 10 clots per condition) (Supp. Fig. S2-5). GPRP was dissolved in Millipore water and the final concentration in whole blood was 5 mM. GR144053 (final concentration, 1 μM) was added to block $\alpha_{2b}\beta_3$ function for forming monolayer of clots. All experiments were initiated within 5 min after phlebotomy. GS-9973 was dissolved in DMSO and the final concentration was 10 μM after addition to whole blood.

2.2.4 Microfluidic clotting assay on collagen surfaces with or without TF

An 8-channel polydimethylsiloxane (PDMS) flow device was vacuum-mounted perpendicularly to collagen/TF surfaces forming 8 parallel-spaced prothrombotic patches (250 × 250 μm), as previously described (23). Treated blood was perfused across the 8 channels by withdrawal through a single outlet. Drug-treated blood was added to the inlet reservoir without stopping flow, thus providing a rapid change in perfusion pharmacology within < 15 sec without hemodynamics crosstalk between channels during the perfusion switch. All clotting events were initiated simultaneously on the chips. Initial wall shear rate was controlled by a syringe pump (Harvard PHD ULTRA; Harvard Apparatus, Holliston, MA) connected to the outlet on the flow device. For experiments using whole blood with CTI, thrombi were formed under constant flow rate (constant *Q*) condition (59). Platelet, fibrin and/or phosphatidylserine activities were monitored simultaneously by epifluorescence microscopy (IX81; Olympus America Inc., Center Valley, PA) at 10× and/or 40× magnification. Each experiment contains three 8-channel devices, so in total 6 independent channels/image streams were used for control, 6 channels/images were used for dasatinib or GS-9973 at t=0s, and 12 channels/images were used for dasatinib or GS-9973 switch at t=90s. For each set of experiments (dasatinib/GS-9973 ± GPRP with PPACK/HCTI blood), blood samples from N=3 donors were taken, so in total 18 samples have been analyzed for control and dasatinib/GS-9973 at t=0s and 36 samples analyzed for dasatinib/GS-9973 at t=90s. Additionally, each clot is extremely well localized on the 250 μm x 250 μm collagen feature and contains tens of thousands of platelets, ideal for obtaining whole clot fluorescence intensities (i.e. total clot mass) with time. However, since we image 24 clots

simultaneously, high magnification single-cell imaging or morphological analysis was not possible. Since we image in real time and under flow conditions, bright field imaging is also more difficult to quantify to obtain clot mass since the thickness of the flowing blood above the clot changes with time and alters the prevailing background signal for brightfield imaging. Images were captured with a charged coupled device camera (Hamamatsu, Bridgewater, NJ) and were analyzed with ImageJ software (National Institutes of Health). To avoid side-wall effects, fluorescence values were taken only from the central 75% of the channel.

In some experiments, clots formed under flow conditions were prepared for fixation and staining to detect Src in cells. After clotting under flow, a solution of 0.5% BSA was perfused in the same manner as whole blood to rinse out blood and then 4% paraformaldehyde was perfused and incubated in the channels. Blocking buffer (3% BSA/TBST/0.1% Triton X-100) was then perfused and incubated for 30 min before clot staining using phospho-Src (pTyr418) polyclonal antibody (1:50 v/v [%] in blocking buffer). Clots were then incubated with phospho-Src antibody for 2 hr under room temperature or overnight under 4C. After rinsing excessive antibody with HBS, images of clots were then taken by the same microscope and camera at 10× and/or 40× magnification and analyzed with ImageJ software.

2.3 Results

2.3.1 Dasatinib inhibits platelet deposition on collagen, but is modulated by thrombin

Using an 8-channel microfluidic device, PPACK-treated whole blood (± dasatinib) was perfused over collagen at 200 s^{-1} wall shear rate. In some channels of the device, perfusion was switched after 90 sec of clotting to PPACK-treated blood with dasatinib (10 mM). Dasatinib present at the start of perfusion potently limited platelet deposition to a sparse monolayer (Figs. 2-1A, 2-2A). Switching to dasatinib-treated blood at 90 sec of flow resulted in an immediate ablation of subsequent platelet deposition, demonstrating the role of SFKs in both the initial platelet activation on collagen as well as later stages of platelet deposition. In this experiment with PPACK-treated whole blood and collagen (no TF) that was designed to prevent thrombin generation, no fibrin was detected (Fig. 2-2B). See Supp. Fig. S2-1 for dasatinib inhibition of phospho-Src staining in a platelet monolayer under thrombin free condition. Clearly, the potency

of dasatinib to block platelet accumulation when added at 90 sec was independent of antagonism of any signaling driven by either thrombin or fibrin, neither of which were present in the experiment.

A similar perfusion-switch experiment was repeated with CTI-treated blood (± dasatinib) perfused over collagen/TF, a condition that robustly generates thrombin and fibrin by engagement of the extrinsic pathway. With thrombin generation promoted in the assay, dasatinib present at t = 0 no longer strongly limited platelet deposition to a monolyer, but instead caused a marked delay and attenuation in platelet accumulation (Figs. 2-1B, 2-2C) as well as a striking inhibition of fibrin deposition (Figs. 2-1B, 2-2C and D). The inhibition of fibrin formation may indicate that dasatinib reduced the procoagulant activity of collagen-bound platelets (to be discussed later). In complete contrast, addition of dasatinib by perfusion-switch at 90 sec had no effect on platelet deposition or fibrin generation. Clearly, the generation of thrombin and/or fibrin modulated the potency of dasatinib (with thrombin being the likely modulator because essentially no fibrin was made with dasatinib present initially at t = 0).

To investigate whether such loss-of-potency behavior was induced by thrombin or fibrin, the experiment was repeated with CTI-treated blood with added GPRP to allow thrombin generation without fibrin polymerization (Figs. 2-1C, 2-2E and F). As seen in the prior experiment with thrombin generation, dasatinib had no effect when added at 90 sec by perfusion switch. As expected, GPRP blocked fibrin polymerization in the clot.

With thrombin generation (± GPRP), dasatinib present at t=0 reduced, but did not limit platelet deposition to a monolayer on collagen/TF. However, once primary deposition had progressed for 90 sec with full SFK signaling (no dasatinib), the subsequent platelet deposition and fibrin generation was completely unaffected by SFK inhibition at 90 sec, implicating the dominance of PAR-1/4 signaling in the growing clot after 90 sec relative to SFK-dependent signaling. In the absence of dasatinib, blocking fibrin polymerization with GPRP had no effect on platelet deposition under flow (Fig. 2-2C vs. 2-2E). Also, see Supp. Fig. S2-2.

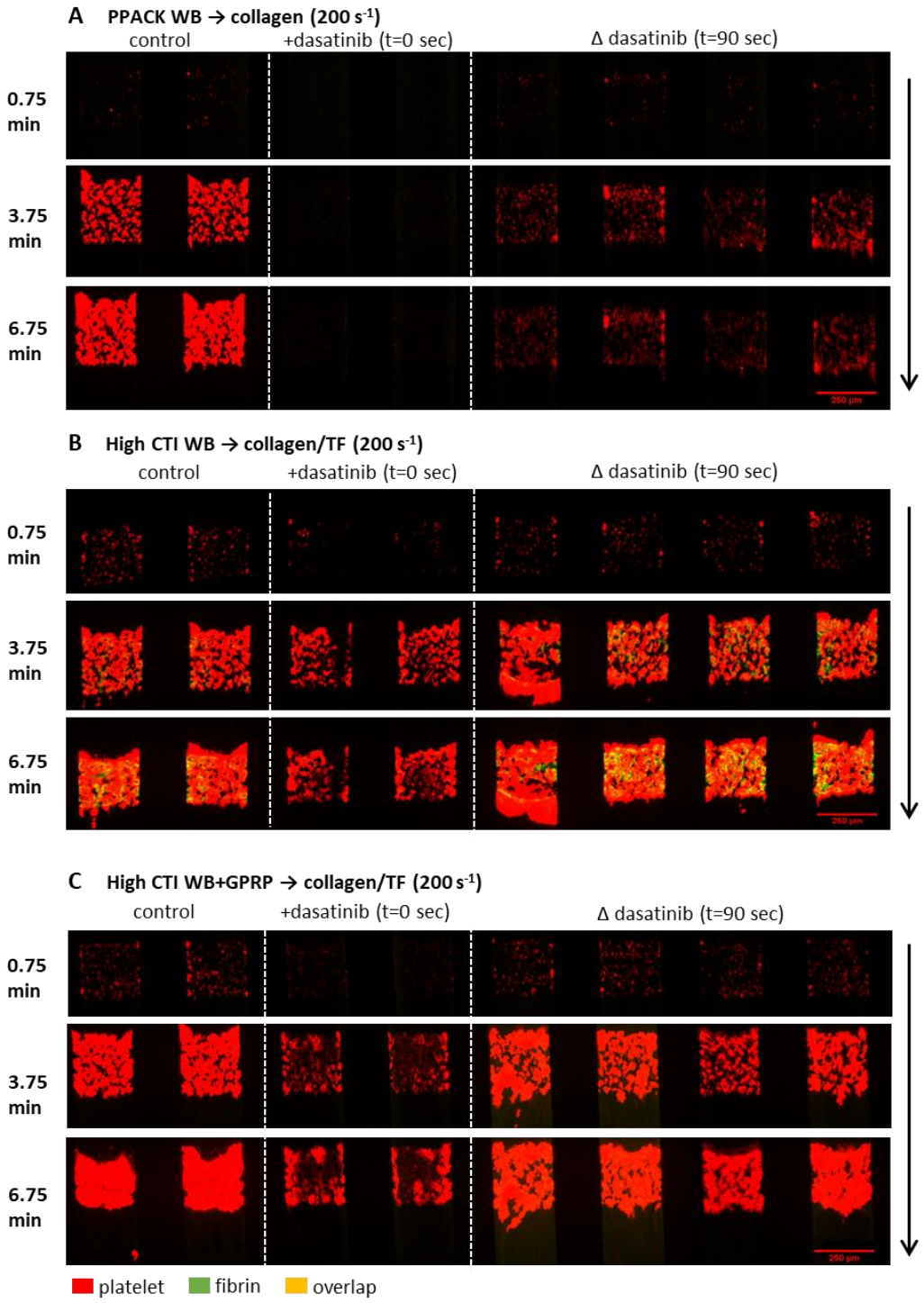

Figure 2-1: The montage image of microfluidic assay at 0.75, 3.75 and 6.75 minute for platelet and fibrin under 10×.

Whole blood with (A) PPACK, (B) high CTI and (C) high CTI with GPRP were perfused over (A) collagen or (B, C) collagen incubated with TF under venous shear rate (200 s^{-1}). The left two channels are control conditions, the next two channels are control conditions with dasatinib at t = 0 sec, and the right four channels are control conditions switched to blood with dasatinib at t = 90 sec. Direction of blood flow is shown as the arrow.

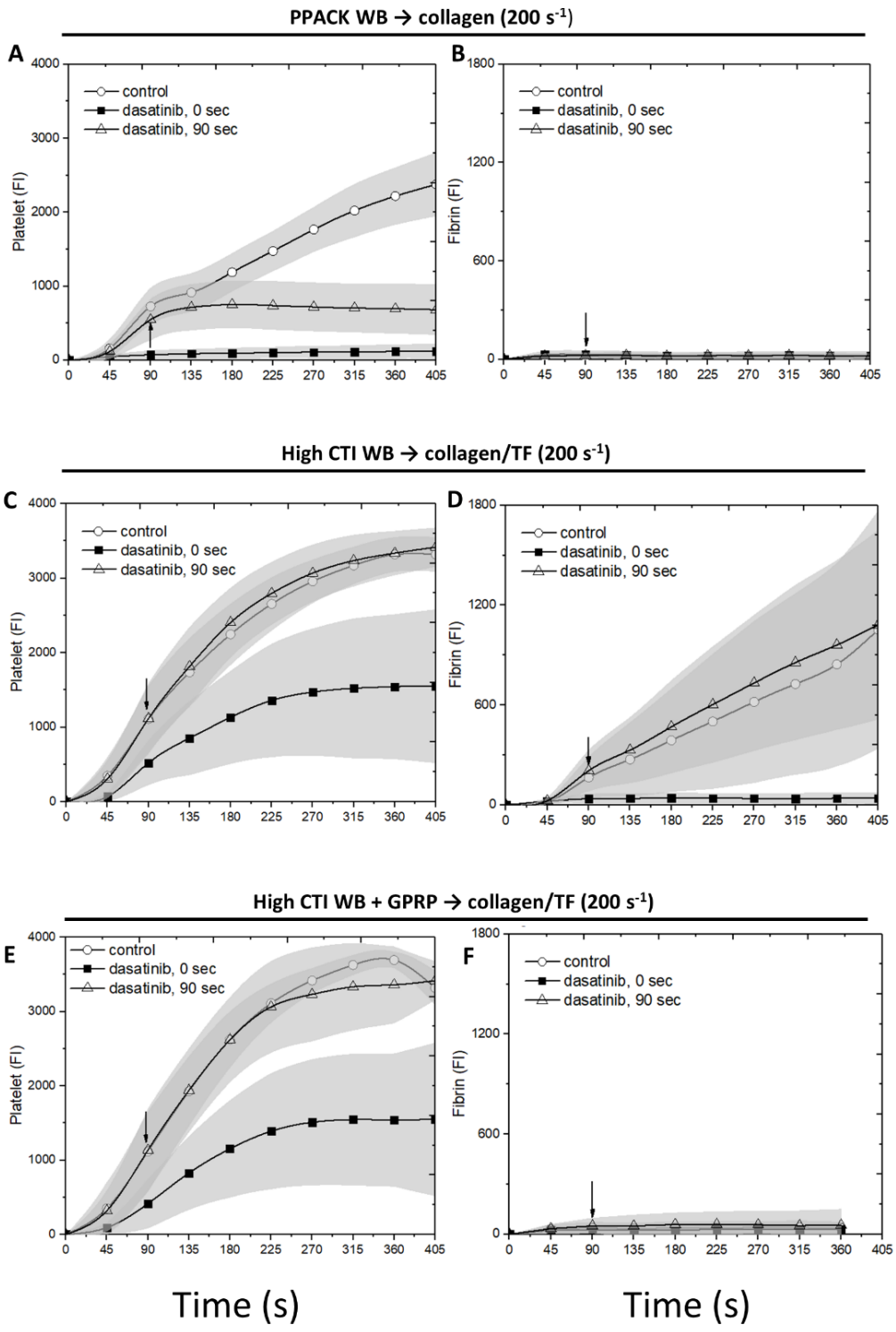

Figure 2-2: The measured intensities for platelet and fibrin as a function of time for whole blood with PPACK, high CTI and high CTI with GPRP.

The experiment conditions are the same as Figure 1. Platelet (A, C, E) and fibrin (B, D, F) intensities are measured after imaging for all conditions, respectively. The arrow in each image shows the time where switching of blood takes place.

2.3.2 The Syk inhibitor GS-9973 inhibited platelet deposition and fibrin generation on collagen

GPVI signaling results in activation of SFKs that drive Syk phosphorylation. We explored the role of direct Syk inhibition using GS-9973 (K_d = 7.6 nM, no other kinase < 100 nM (60)) at clot initiation or added at later stages of clot growth using perfusion-switch. For PPACK-treated whole blood perfused over collagen (no thrombin/fibrin), GS-9973 present initially caused a reduction in platelet deposition (Figs. 2-3A, 2-4A), although clearly not with the potency of dasatinib. However, in contrast to dasatinib, a perfusion-switch at 90 sec to GS-9973-treated blood resulted in a modest reduction in platelet deposition, indicating a role for Syk at later stages of platelet deposition in the absence of thrombin and/or fibrin-driven signaling (Fig. 2-3A, 2-4B).

Repeating this experiment with CTI-treated blood perfused over collagen/TF, GS-9973 reduced platelet deposition and fibrin deposition when the drug was present initially (Figs. 2-3B, 2-4C and D). In contrast to dasatinib, switch to GS-9973-treated blood at 90 sec also reduced platelet secondary accumulation without effect on fibrin deposition.

To investigate the role of thrombin generation without fibrin polymerization, CTI-treated blood with added GPRP was perfused over collagen/TF (Figs. 2-3C, 2-4E and F). GS-9973 reduced platelet deposition when present initiation or when added at 90 sec by perfusion-switch. We conclude that the Syk inhibitor GS-9973 reduced platelet deposition by inhibiting Syk signaling in both collagen-adherent platelets and subsequently arriving platelets, regardless of the presence or absence of either thrombin or fibrin mediated signaling. Again, GPRP to block fibrin generation had no inhibitory effect on platelet deposition (as shown in Fig. 2-4C vs. 2-4E).

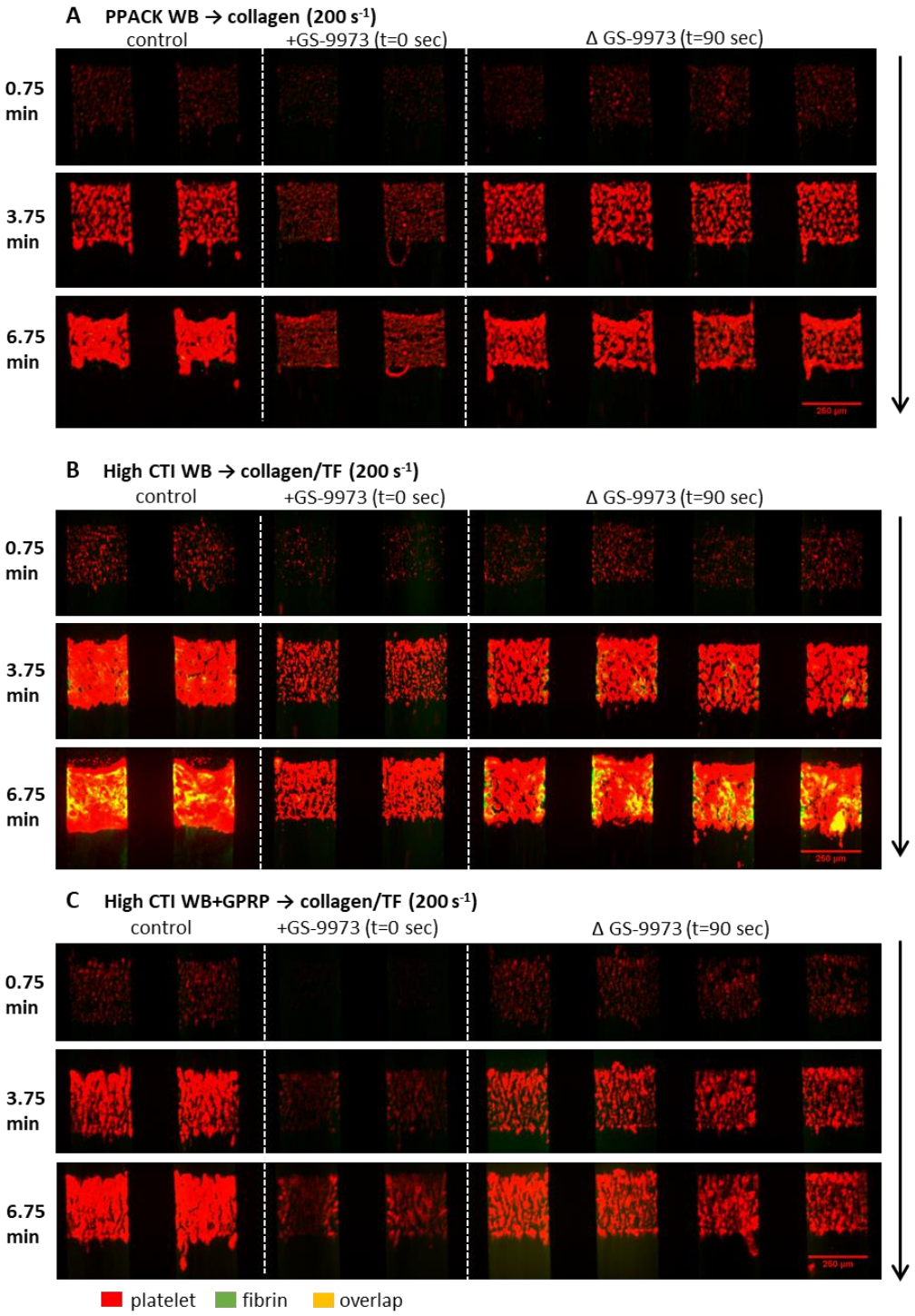

Figure 2-3: The montage image of microfluidic assay at 0.75, 3.75 and 6.75 minute for platelet and fibrin under 10×.

Whole blood with (A) PPACK, (B) high CTI and (C) high CTI with GPRP were perfused over (A) collagen or (B, C) collagen incubated with TF under venous shear rate (200 s^{-1}). The left two channels are control conditions, the next two channels are control conditions with GS-9973 at t = 0 sec, and the right four channels are control conditions switched to blood with GS-9973 at t = 90 sec. Direction of blood flow is shown as the arrow.

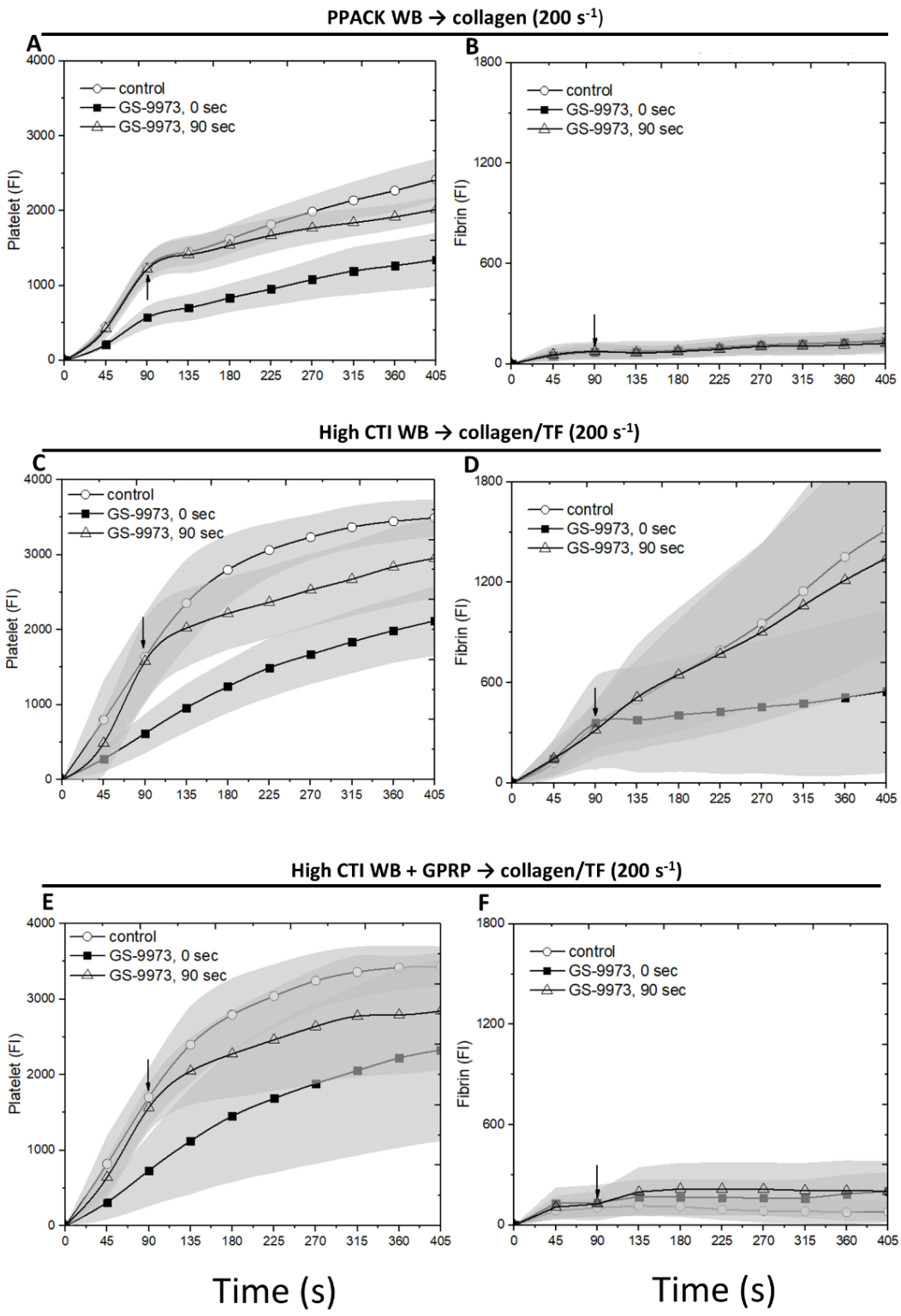

Figure 2-4: The measured intensities for platelet and fibrin as a function of time for whole blood with PPACK, high CTI and high CTI with GPRP.

The experiment conditions are the same as Figure 3. Platelet (A, C, E) and fibrin (B, D, F) intensities are measured after imaging for all conditions, respectively. The arrow in each image shows the time where switching of blood takes place.

2.3.3 Dasatinib and GS-9973 reduce phosphatidylserine (PS) exposure by collagen adherent platelets

Since thrombin and collagen in combination potently induces PS exposure in platelets, CTI-whole blood was perfused over collagen/TF. In some experiments, secondary accumulation was blocked with GR144053 to inhibit fibrinogen binding to $\alpha_{IIb}\beta_3$. Both dasatinib and GR144053 reduced deposition to a single sparse monolayer of platelets (Fig. 2-5). GR144053 had only moderate effects on PS exposure, while SFK inhibition with dasatinib caused a substantial reduction in PS exposure, even on a per-platelet basis (Fig. 2-5F). This could be the source of poor fibrin production in the presence of dasatinib as seen in Fig. 2-2D. While GS-9973 was not as potent of blocker of platelet deposition compared to dasatinib, GS-9973 did cause a marked reduction in PS exposure (Fig. 2-6).

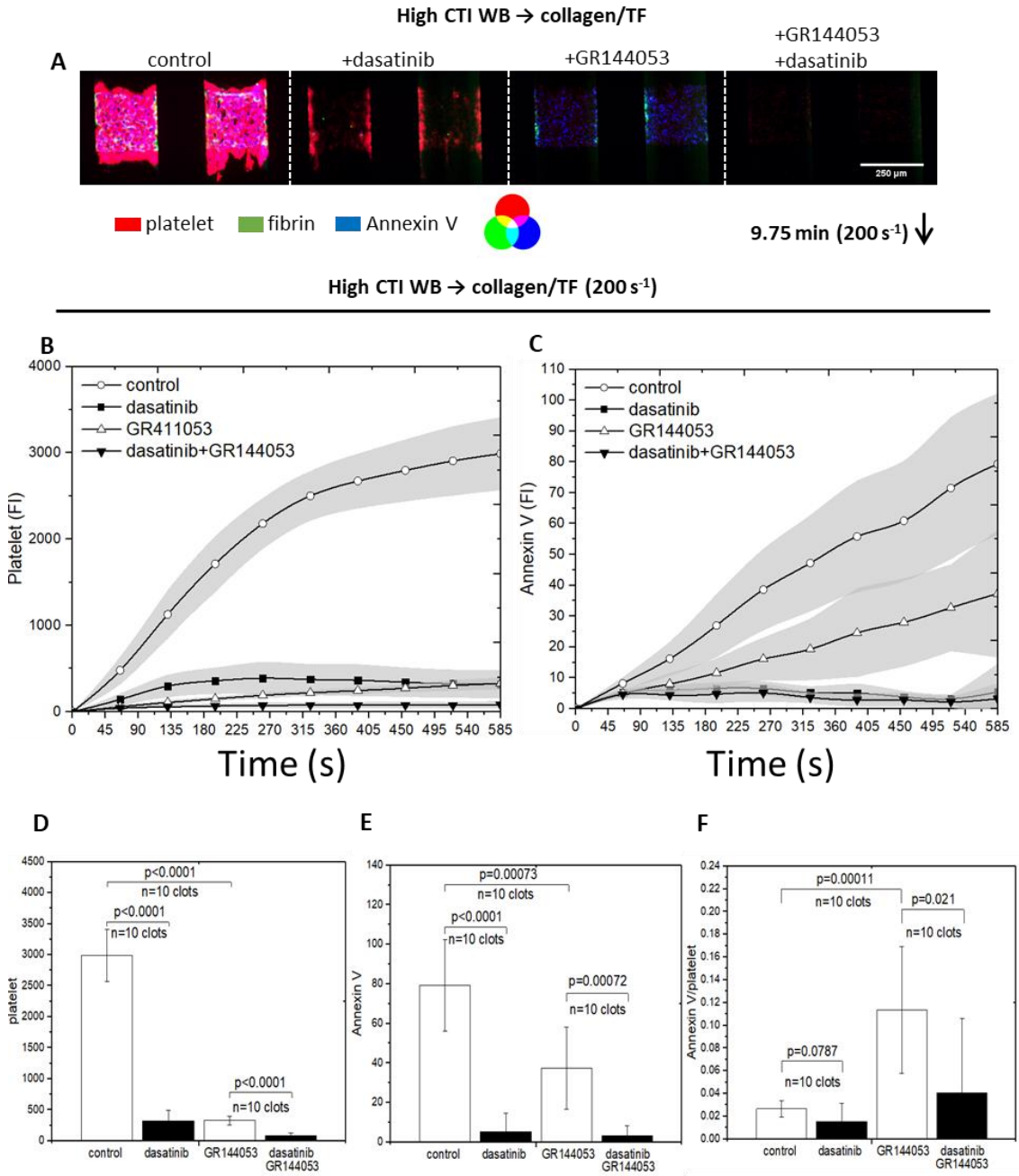

Figure 2-5: The intensities of platelet, fibrin and Annexin V for all conditions under venous shear rate (200 s^{-1}).

High CTI blood was perfused over collagen incubated with TF. Dasatinib was added to inhibit Src and GR144053 was added to form monolayers. The montage images of clots/monolayers were taken for platelet, fibrin and Annexin V at 9.75 minutes under 10× (A), direction of blood flow was shown as the arrow. Fluorescent intensities of platelet (B) and Annexin V (C) were plotted over 9.75 minutes for all conditions. Platelet intensities were inhibited for both presence of dasatinib and GR144053, but Annexin V intensity was not inhibited by the presence of GR144053. Bar charts of fluorescent intensities of platelet (D) and Annexin V (E) at 9.75 minutes for all conditions illustrate the end point comparison; Annexin V signal on per-platelet basis was achieved by obtaining the ratio of Annexin V/platelet signal (C); the highest ratio is obtained by monolayer without dasatinib, implies that primary platelet deposition is crucial for clot development.

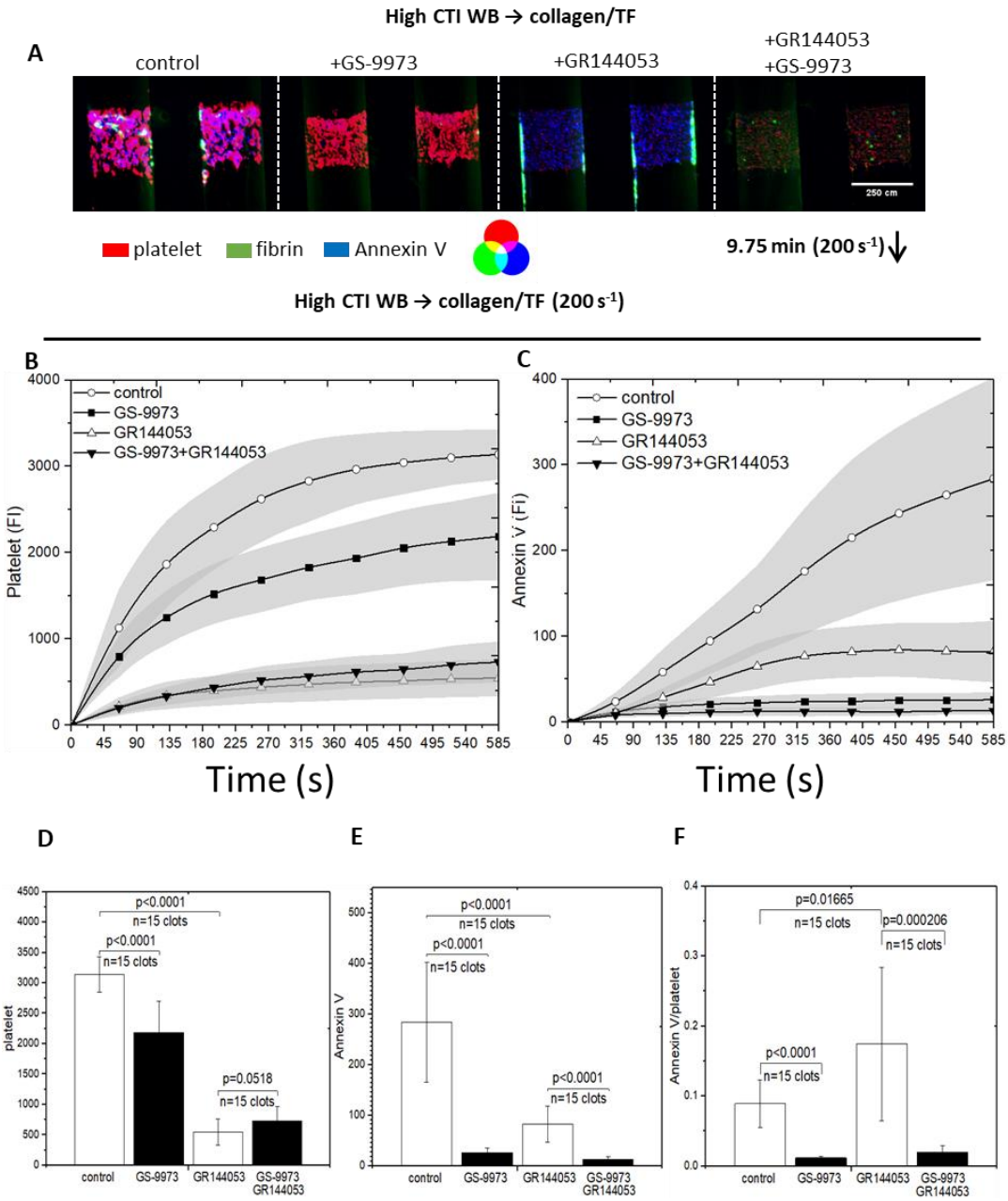

Figure 2-6: The intensities of platelet, fibrin and Annexin V for all conditions under venous shear rate (200 s^{-1}).

High CTI blood was perfused over collagen incubated with TF. GS-9973 was added to inhibit Syk and GR144053 was added to form monolayers. The montage images of clots/monolayers were taken for platelet, fibrin and Annexin V at 9.75 minutes under 10× (A), direction of blood flow was shown as the arrow. and fluorescent intensities of platelet (B) and Annexin V (C) were plotted over 9.75 minutes for all conditions. Platelet intensities were inhibited for both presence of GS-9973 and GR144053, but Annexin V intensity was not inhibited by the presence of GR144053. Bar charts of fluorescent intensities of platelet (D) and Annexin V (E) at 9.75 minutes for all conditions illustrate the end point comparison; Annexin V signal on per-platelet basis was achieved by obtaining the ratio of Annexin V/platelet signal (C); the highest ratio is obtained by monolayer without GS-9973, implies that primary platelet deposition is crucial for clot development.

2.4 Discussion

We used microfluidic assay of human blood to evaluate the potency of kinase inhibitors present at the start of clotting or added acutely at 90 sec once clotting was engaged. This novel experimental design allowed the interrogation of signaling pathways utilized by the initial platelets engaging collagen (± thrombin) relative to the signaling utilized by later arriving platelets (no collagen, ± thrombin). The intent was not to mimic therapy, but rather to use inhibitors to explore signaling pathways at various times and locations during a clotting event with and without thrombin or fibrin. Prior *in vitro* work has deployed 10 μM concentration (58). Interestingly, the anti-platelet action of high concentration dasatinib was mitigated when thrombin is generated.

Strong signaling from the Src/SFK is expected in collagen-adherent platelets via GPVI activation pathway, but other receptors can also drive SFK activation such as a2b1, $a_{IIb}b_3$, $P2Y_{12}$, and even PAR-4 during clotting (35). In the absence of thrombin, dasatinib strongly limited the initial deposition of platelets to a sparse monolayer (Fig. 2-2A). Dasatinib also reduced Src-phosphorylation in collagen-adherent platelet monolayers (Supp. Fig. S2-1) and blocked platelet deposition when added after 90 sec of clotting in the absence of thrombin. However, dasatinib had a striking lack of potency when added after 90 sec of clotting in the presence of thrombin generation. We conclude that thrombin-driven signaling via Gaq drives platelet activation in a manner to substantially bypass SFK inhibition by dasatinib (See Supp. Fig. S2-3 for schematic model). For human blood clotting from 0 to 500 sec, there was little evidence of any role for fibrin-mediated activation of GPVI signaling and SFK signaling: under no conditions did the absence of fibrin using GPRP cause a reduction in platelet deposition. Syk inhibition with GS-9973 in the absence of thrombin was not as potent as dasatinib. GS-9973 may have more Syk selectivity than other small molecule inhibitors (37,61,62). Interestingly, GS-9973 showed a stronger inhibition effect at later stages of clotting than dasatinib, even in the presence of thrombin. Again, none of the observations with GS-9973 indicated a substantial role for fibrin-mediated signaling through platelet GPVI. We also conducted the same experiments with R-406 with only 2 of 5 blood samples responding to R-406 (Supp. Fig. S2-4). The cause of donor variation is unknown, but suggests the possible utility of platelet testing to gage patient-specific risk to kinase inhibitor.

Based on our experiment results, the potency of a kinase inhibitor can depend on both the timing of its addition as well as the nature of the triggering surface to generate thrombin. Fibrin has substantial anti-thrombin I activity. Blocking fibrin with GPRP may increase local PAR1/4 signaling, thrombin-bound GPIb-dependent SFK signaling, or thrombin-mediated feedback pathways (eg. FXI activation). Our observations with thrombin generation modulating the potency of kinase inhibitors on clotting are relevant to both off-target bleeding effects during cancer treatment as well as antithrombotic therapy. These observations may bring more insights on the mechanisms of excessive bleeding during cancer treatment, so undesired phenomena could be better expected and regulated. However, even with fluorescence staining, the true spatiotemporal dynamics of Src phosphorylation and dephosphoryaltion remain challenging to quantify within the small clots formed under flow using microfluidics. At present, microfluidics does not have the molecular resolution expected with western blotting or LCMS phosphoproteomics.

While dasatinib and other kinase inhibitors are known to reduce GPVI-dependent clot growth under flow (47), their effects on late arriving platelets has not been thoroughly studied, and also challenging to conduct in *in vivo* models. For example, inhibitor tests under flow have been previously described (63) where blood pretreated with the BCR-abl inhibitor. The “drug perfusion-switch” allowed interrogation of clot progression after the initial platelets already engaged in surface-driven signaling. This novel assay allows an interrogation of a particular pathway in late arriving platelets that are not interacting with collagen.

Further experiment can be done regarding concurrent medication since other BCR-ABL inhibitors could be used at the same time with dasatinib, and relative work has been done on ponatinib inhibited whole blood under flow (63). Interaction between dasatinib and other BCR-ABL inhibitors may cause a different form of bleeding episode. Some concerns that the specificity of CD61 as platelet marker may not be as good as CD41, since CD61 could bind with cells such as leukocytes. However, the cell count of platelets is 40 times higher than that of leukocytes, and leukocytes do not bind with collagen. Therefore, all the CD61 signal shown on collagen strip could be confidently attributed to platelets. Besides, previous works done on specificity of platelet markers (64) mentioned that in practice CD41 and CD61 can be used interchangeably.

CHAPTER 3 – ACHIEVING GPVI INHIBITION THROUGH ANTI-GPVI FAB AND ITS ROLES ON DIFFERENT STAGES OF CLOT GROWTH[1]

3.1 Introduction: Mechanisms of GPVI activation pathway and advantages of novel anti-GPVI Fab in microfluidic assay

Glycoprotein VI (GPVI) is a known platelet-specific receptor that binds collagen and subsequently activates platelets (27,28). Upon initial vessel injury collagen becomes exposed, allowing for GPVI binding and strong signaling in platelets. This interaction between collagen and platelets is crucial for primary activation and aggregation (65,66), with GPVI as a mediator for this process (18,67). However, recent reports demonstrate that GPVI may bind with other ligands as well, such as fibrin (27,56). Thus, GPVI may have a secondary role in clot formation after collagen is covered by platelets, such as mediating platelet recruitment during secondary deposition (19) or contributing to clot contraction involving fibrin (68).

There are a number of different previous studies that have evaluated GPVI-deficiency in a number of different contexts: using different anti-GPVI antibodies (4,7,15,38,68,69), indirect inhibition of GPVI on human platelets (32,50), *in vivo* GPVI-deficient mouse models (70,71), *in vitro* models with GPVI-deficient mouse blood (15,27,38,69), models with GPVI-deficient human blood (69,72), testing different surface activating materials (68,72), human atherosclerotic plaque material (7,68), microfluidic venous valve model (4), among others. Dubois, et. al. showed a significant decrease in platelet accumulation for GPVI-deficient mouse platelets compared to WT when thrombin is inhibited (70). However, Mangin, et. al. showed that when thrombin is present, this decrease in platelet accumulation is abolished, leading to the conclusion that thrombin is able to overcome GPVI-deficiency and allow thrombus formation to occur normally (71).

Recent research has been focused on developing specific inhibitors of GPVI (18). In previous studies, inhibition of GPVI was mostly achieved through blocking of kinases in subsequent activation pathways, such as inhibition of Src Family Kinases (SFK), spleen tyrosine kinase (Syk) and Bruton's tyrosine kinase (BTK) (7,49,61,73). Some of these inhibitors are irreversible, which serves as a "knockout" condition for GPVI. However, this method has its own

[1] This is a collaborative work with K. T. Trigani, K. N. Shankar and J. Crossen.

limitations. These kinases serve more than one role and function downstream of different platelet receptors (35,74). The recent development of direct inhibition of GPVI, mostly led by Watson (61) and Nieswandt (66,67), alleviates these concerns. Additionally, evaluation of the effects of GPVI inhibition under flow more accurately mimics *in vivo* dynamics compared to static *in vitro* assays (18). To differentiate the role of GPVI at different stages of clot formation under flow, the inhibition of GPVI can be controlled in a microfluidic assay, which is difficult to achieve *in vivo* and in aggregometry assays (50,65).

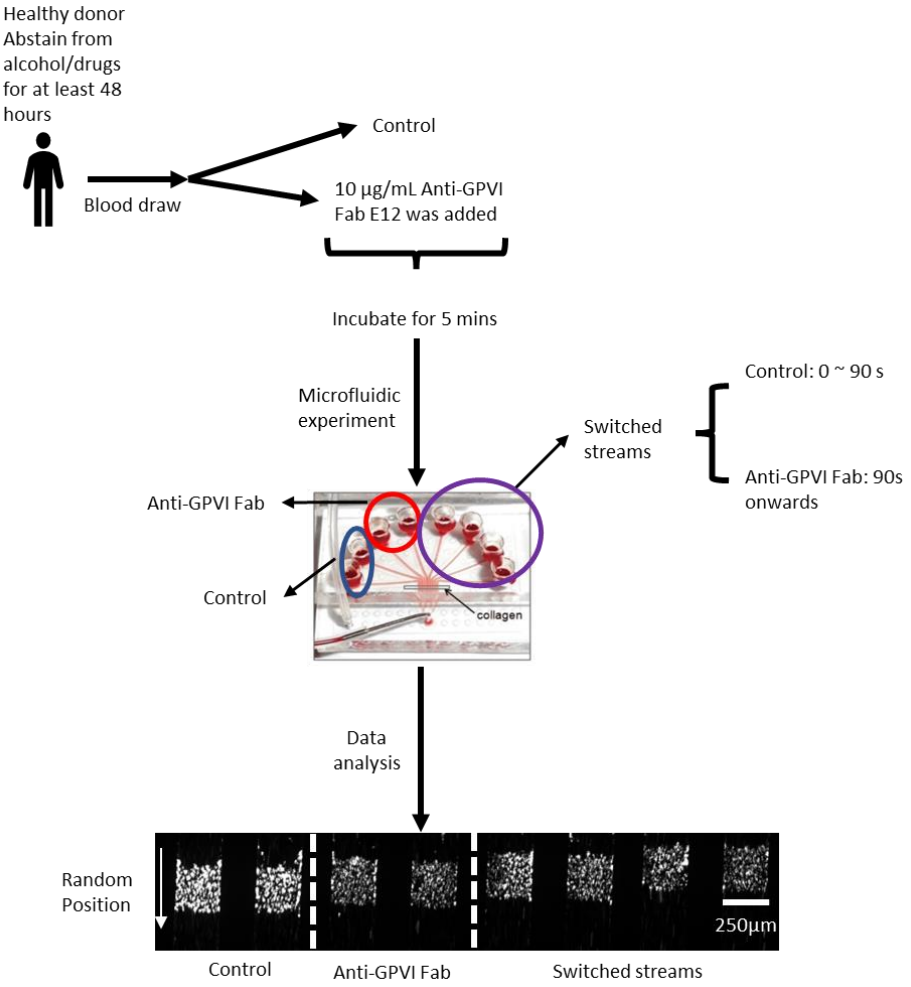

Figure 3-1: Experiment schematic flow chart.

Healthy donors self-reported no medication or alcohol use for 48 hours prior to the blood draw. Blood was collected and either HBS (control) or 10 µg/mL Anti-GPVI Fab E12 were added, followed by a 5-minute incubation. For microfluidic experiments, control blood was loaded into the left two wells, followed by Anti-GPVI Fab in the next two wells. The four wells on the right were switched streams by flowing over control blood for the first 90 seconds of the experiment, then wells were depleted and refilled with blood loaded with Anti-GPVI Fab. Epifluorescence images were taken during the experiment to quantify the change of fluorescent intensity over time.

Therefore, we aimed to investigate the role of a novel anti-GPVI Fab (the Fab fragment of human GPVI blocking antibody (clone E12)) developed by the Nieswandt research group under hemodynamic conditions using our microfluidic assay. GPVI interaction with fibrin(ogen) has previously been reported to play a role in arterial conditions (68,69). Lehmann, et. al. developed a venous thrombosis model with dimensional similarity to venous valves, showing that GPVI is essential for platelet activation and subsequent thrombus propagation (4). Thus, GPVI has been shown to play significant roles in both arterial and venous thrombus formation (26). However, we mostly limited this study to evaluating E12 under venous conditions rather than arterial, as arterial shear rates can cause clot heterogeneity and increased embolization in our microfluidic model. Studies conducted in this *in vitro* microfluidic assay have demonstrated that a perfusion-switch experimental design (Fig. 3-1) can be used to rapidly change conditions (32), fluids, or shear (75) during experiments, and to study the characteristics of clots at different stages of coagulation. We also utilized confocal microscopy as well as a fully resolved 3D computer simulation to validate our *in vitro* microfluidic assay results. We found that GPVI plays a role in primary and secondary platelet deposition, as well as fibrin polymerization, but this role is modulated/obscured by the presence of thrombin generation.

3.2 Methods

3.2.1 Materials

Reagents were obtained as follows: anti-human CD61 antibody (BD Biosciences, San Jose, CA. Cat#: 555754), Alexa Fluor 647–conjugated human fibrinogen (Life Technologies, Grand Island, NY. Cat#: F35200), Alexa Fluor anti-human CD62P (P-Selectin) Antibody (BioLegend, San Diego, CA. Cat#: 304918), Alexa Fluor 546–conjugated human fibrinogen, Alexa Fluor 488-conjugated annexin V (ThermoFisher Scientific, Waltham, MA. Cat#: A13201), Dade Innovin prothrombin time (PT) reagent (Siemens, Malvern, PA. Cat#: B4212-40), collagen (type I; Chrono-Log, Havertown, PA. Cat#: 385), Sigmacote® (Millipore Sigma, Burlington, MA. Cat#: SL2-100ML), H-Gly-Pro-Arg-Pro-OH (GPRP; Millipore Sigma, Burlington, MA. Cat#: 03-34-0001), GR144053 (Tocris Biosciences, Bristol, UK. Cat#: 1263), Phe-Pro-Arg-chloromethylketone (PPACK, Haematologic Technologies, Essex Junction, VT. Cat#: FPRCK-01) and corn trypsin

inhibitor (CTI, Haematologic Technologies, Essex Junction, VT. Cat#: CTI-01). The Fab fragment of human GPVI blocking antibody (clone E12) was generous gift from N. Stefano and Dr. B. Nieswandt from University of Würzburg.

3.2.2 Preparation and characterization of collagen/TF surface

Glass slides were rinsed with ethanol, then deionized water, and dried with filtered air. Sigmacote® was used to create a hydrophobic surface on the glass. A volume of 5µL of fibrillar collagen was perfused through a patterning channel (250 µm wide × 60 µm high) of a microfluidic device to create a single 250 µm-wide stripe of fibrillar collagen for all experiments, as previously described (29,30). For experiments without thrombin interaction, collagen was rinsed and blocked with 20 µL 0.5% bovine serum albumin (BSA) buffer. For experiments that study the effect of thrombin, lipidated TF was absorbed to the collagen surface by perfusing of 5 µL of Dade Innovin PT reagent (20 nM stock concentration), rinsed and blocked with 20 µL 0.5% BSA, then incubated for 30 min without flow, as previously described (29,30).

3.2.3 Blood collection and preparation

Blood was obtained via venipuncture into a syringe containing either PPACK (1:100 v/v; final concentration of 100 µmol/L) or high concentration of CTI (40 µg/mL) from healthy donors who self-reported as free of alcohol use for at least 72 hours and medication for at least a week prior to blood collection. All donors provided informed consent under approval of the University of Pennsylvania Institutional Review Board. Blood was treated with anti-human CD61 antibody (1:50 v/v in whole blood) and Alexa Fluor-conjugated human fibrinogen (1.5 mg/mL stock solution, 1:80 v/v in whole blood) immediately after blood collection for platelet labeling and fibrin labeling, respectively. While CD61 can bind both platelets and white blood cells, the platelet deposits made on collagen/TF under flow contain essentially no white blood cells until substantially later times. Even at low resolution, white blood cell staining would be morphologically detected if it were present. Annexin V (1:80 v/v in whole blood) and P-selectin (1:50 v/v in whole blood) was added for phosphatidylserine labeling and alpha-granule release, respectively, when needed. Anti-GPVI Fab was added to collected whole blood at a final concentration of 10 µg/mL (stock solution 1 mg/mL, dissolved in biology grade water). GPRP (5 mM final concentration in blood)

and GR-144053 (1 μM final concentration in blood) were both dissolved in Millipore water. All experiments were initiated within 5 min after phlebotomy.

3.2.4 Microfluidic clotting assay on collagen surfaces with or without TF

An 8-channel polydimethylsiloxane (PDMS) flow device was vacuum-sealed perpendicularly to collagen/TF surfaces forming 8 parallel-spaced prothrombotic patches (250 × 250 μm), as previously described (29,30). Under appropriate circumstances, the channel height used was either 60 μm or 120 μm depending on the duration of the experiment to prevent occlusion, but the shear rate was kept in the venous level (100 – 200 s^{-1}). Treated blood was perfused across the 8 channels by withdrawal through a single outlet. Drug-treated blood was added to the inlet reservoir without stopping flow, thus providing a rapid change in perfusion pharmacology within < 15 sec without hemodynamic crosstalk between channels during the perfusion switch. All clotting events were initiated simultaneously in the microfluidic device on the collagen strip. Initial wall shear rate was controlled by a syringe pump (Harvard PHD ULTRA / Harvard PHD 2000; Harvard Apparatus, Holliston, MA) connected to the outlet on the flow device. For experiments using whole blood with CTI, thrombi were formed under constant flow rate (constant Q) conditions (30). Platelet, fibrin, alpha granule and/or phosphatidylserine activities were monitored simultaneously by epifluorescence microscopy (IX81; Olympus America Inc., Center Valley, PA) at 10X magnification. For each set of experiments, blood samples from $N \geqslant 3$ donors were taken. Additionally, each clot is extremely well localized on the 250 μm x 250 μm collagen feature and contains tens of thousands of platelets, ideal for obtaining whole clot fluorescence intensities (i.e. total clot mass) with time. However, since we image up to 24 clots simultaneously, high magnification single-cell imaging or morphological analysis was not possible. Since we image in real time and under flow conditions, bright field imaging is also more difficult to quantify to obtain clot mass since the thickness of the flowing blood above the clot changes with time and alters the prevailing background signal for brightfield imaging. Images were captured with a charged coupled device camera (Hamamatsu, Bridgewater, NJ) and were analyzed with

ImageJ software (National Institutes of Health). To avoid side-wall effects, fluorescence values were taken only from the central 75% of the channel.

3.2.5 Confocal Microscopy

To determine the 3-dimensional orientation of platelets, fibrin, and PS exposure, we utilized confocal microscopy to develop images of the clots in the microfluidic device. For confocal images, all clots imaged were formed under high CTI WB perfused over collagen/TF (100 s^{-1}) for 7.5 min. After 7.5 minutes of WB perfusion, WB was switched with BSA (+ 5mM $CaCl_2$) and perfused for about 2 minutes to clear out any remaining blood in the channels. After BSA perfusion, any remaining BSA (+ 5mM $CaCl_2$) in the wells was replaced with 4% paraformaldehyde (+ 5mM $CaCl_2$) and perfused for about 2 minutes to fix clots and prevent contraction. After 2 minutes of perfusion with 4% paraformaldehyde (+ 5mM $CaCl_2$), perfusion was stopped and devices were transferred to the confocal microscope, with clots still maintained in the 8-channel microfluidic device. Z-stack images were taken of fixed clots using the Leica TCS SP8 laser scanning confocal microscope at the CDB Microscopy Core at the University of Pennsylvania. Images were compiled to form a 3C rendering of a clot endpoint in ImageJ.

3.2.6 3D Model of First Platelet Layer of Clot Development

The simulation framework is an extension of a 2D model from previous work (76,77) to a fully spatially resolved 3D model (78) and consists of four modules: neural network (NN), lattice kinetic Monte Carlo (LKMC), lattice Boltzmann (LB), and finite volume method (FVM). The NN module used multicomponent agonist exposure data to determine intra-platelet calcium mobilization, which was then used to determine the extent of integrin activation and adhesiveness of each platelet. The NN was trained using calcium traces obtained for all single and pairwise combinations of six agonists at low, medium and high concentrations: ADP, thrombin, GSNO (NO donor), and mimetics for collagen, thromboxane, and prostacyclin, which were used to quantify P2Y1/P2Y12, PAR1/PAR4, guanylate cyclase, GPVI, TP, IP receptor signaling, respectively (22). The LKMC module constructed a rate database of all possible events, which in this case are platelet motion and binding events. LKMC discretized the domain into uniform hexahedrons, resulting in lattice points upon which platelets were placed. Subsequent platelet motion or binding

events were carried out at these lattice points. The rates of attachment and detachment of platelets to the reactive collagen/TF patch and/or to each other were a function of the activation state of the platelets (NN module) and the local shear rate around the platelets (LB module). The LB module solved the equations which described the blood flow velocity in the domain. The FVM module tracked local agonist concentrations (ADP and thromboxane A2) by solving the convection-diffusion-reaction equation for species transport. To account for the effect of wall-derived TF, a reduced model of the coagulation cascade was used to determine the concentration of thrombin within the clot (79). The thrombin concentration predicted by the reduced model was used as an input to the NN module to estimate intracellular calcium for platelets within the clot core (within 15μm of the TF surface). A detailed description of the model along with model parameters can be obtained from Shankar, et al. (78).

3.4 Results

3.4.1 Direct inhibition of GPVI inhibits secondary platelet deposition without thrombin present, but has no effect on either primary or secondary platelet deposition with thrombin present

Using the 8-channel microfluidic device (60 μm channel height), PPACK/Apixaban-treated whole blood (± anti-GPVI Fab) was perfused over collagen at 200 s^{-1} initial wall shear rate. In some channels of the device, perfusion was switched after 90s of clotting to PPACK/Apixaban-treated blood with anti-GPVI Fab (10 μg/mL). Channels with anti-GPVI Fab present from t=0s showed a very strong inhibition of primary platelet deposition (Fig. 3-2A to D). The 90-sec perfusion-switched channels began to plateau in platelet fluorescence intensity (FI) shortly after switching (Fig. 2D) and the clot morphology appeared to be more heterogeneous compared to control. As expected, there was negligible fibrin polymerization under all conditions since thrombin production was strongly inhibited and tissue factor was absent (Fig. 3-2A to C, E).

However, when similar experiments were repeated to promote thrombin generation using whole blood (WB) treated with high concentration of CTI (HCTI, 40 μg/mL final concentration in WB) perfused over collagen/TF, no difference in platelet deposition was observed in any condition, regardless of the time of anti-GPVI Fab present in blood flow (Fig. 3-3A to D). Interestingly, fibrin polymerization was inhibited when anti-GPVI Fab was present initially at t=0.

However, fibrin generation was not interrupted or inhibited when Fab was added later at 90-sec compared to control (Fig. 3-3A to C, E), consistent with thrombin generation and fibrin deposition being robust by 90 seconds of clotting.

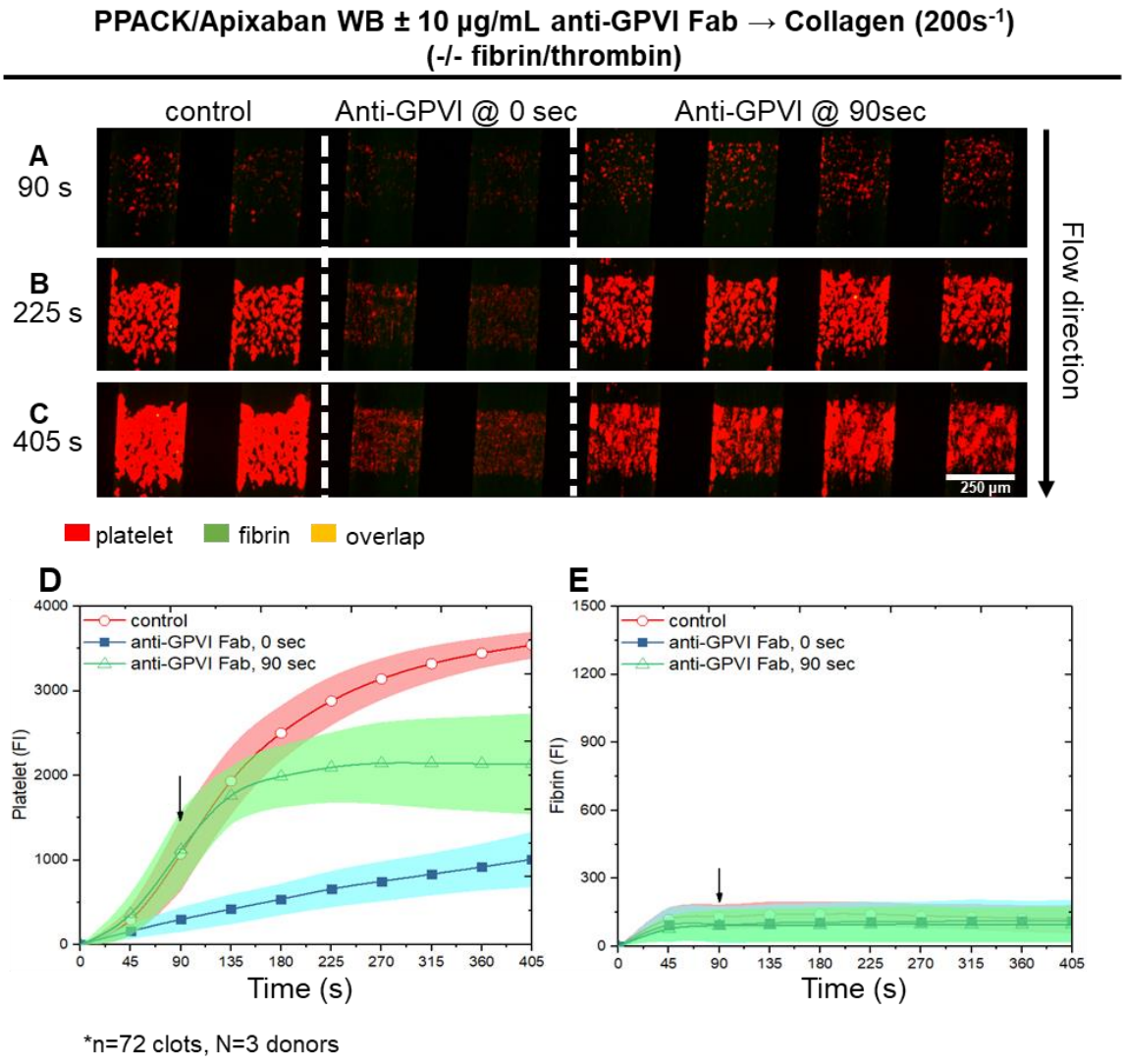

Figure 3-2: Inhibition of GPVI leads to decreased primary and secondary platelet deposition when neither thrombin nor fibrin are present.

PPACK/Apixaban WB with and without anti-GPVI Fab was perfused over collagen at 200s^{-1} for 7 minutes. In the right 4 channels, control WB was perfused for 90 seconds, with a perfusion switch to anti-GPVI WB at 90s. CD61 and fluorescence fibrinogen fluorophores were added to label platelets and fibrin, respectively, with overlay images taken at 90s (A), 225s (B), and 405s (C). Fluorescence intensities for platelets (D) and fibrin (E) were measured throughout the course of the experiments.

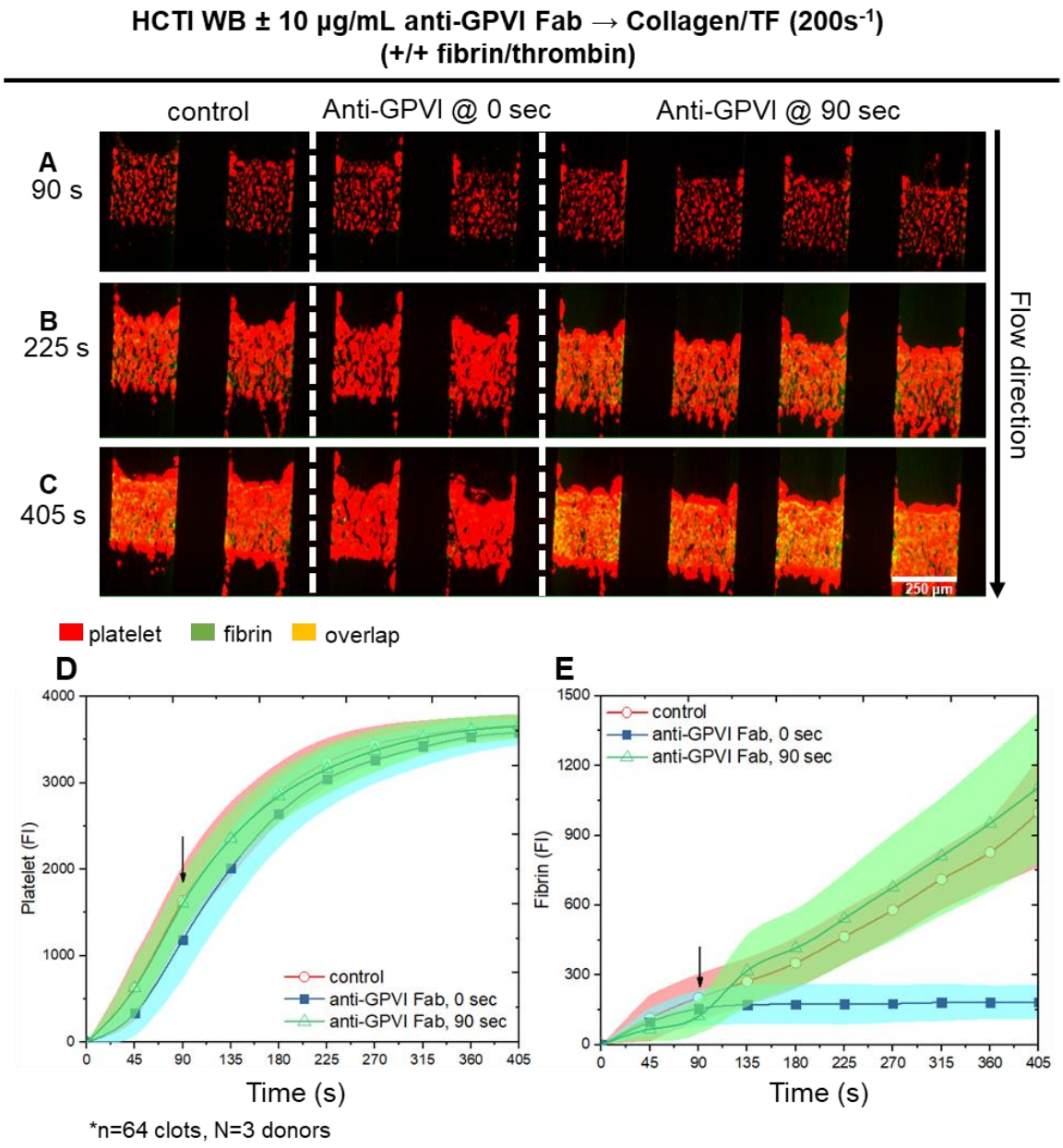

Figure 3-3: Inhibition of GPVI shows no effect on primary and secondary platelet deposition when both thrombin and fibrin are present.

High CTI WB with and without anti-GPVI Fab was perfused over collagen at 200 s^{-1} for 7 minutes. In the right 4 channels, control WB was perfused for 90 seconds, with a perfusion switch to anti-GPVI WB at 90s. CD61 and fluorescence fibrinogen fluorophores were added to label platelets and fibrin, respectively, with overlay images taken at 90s (A), 225s (B), and 405s (C). Fluorescence intensities for platelets (D) and fibrin (E) were measured throughout the course of the experiments.

To confirm that platelet dynamics were mediated by thrombin rather than fibrin, we repeated the same experimental design in Figure 3-3, but this time with 5 mM of gly-pro-arg-pro (GPRP) added to all channels to prevent fibrin polymerization. The same degree of platelet

deposition was observed in all channels regardless of the presence of anti-GPVI Fab (Fig. 3-4A to D), while fibrin was absent in all GPRP conditions, as expected (Fig. 3-4A to C, E). Platelet deposition was insensitive to Fab added at t = 0 or 90 sec when thrombin was robustly generated, even in the absence of fibrin.

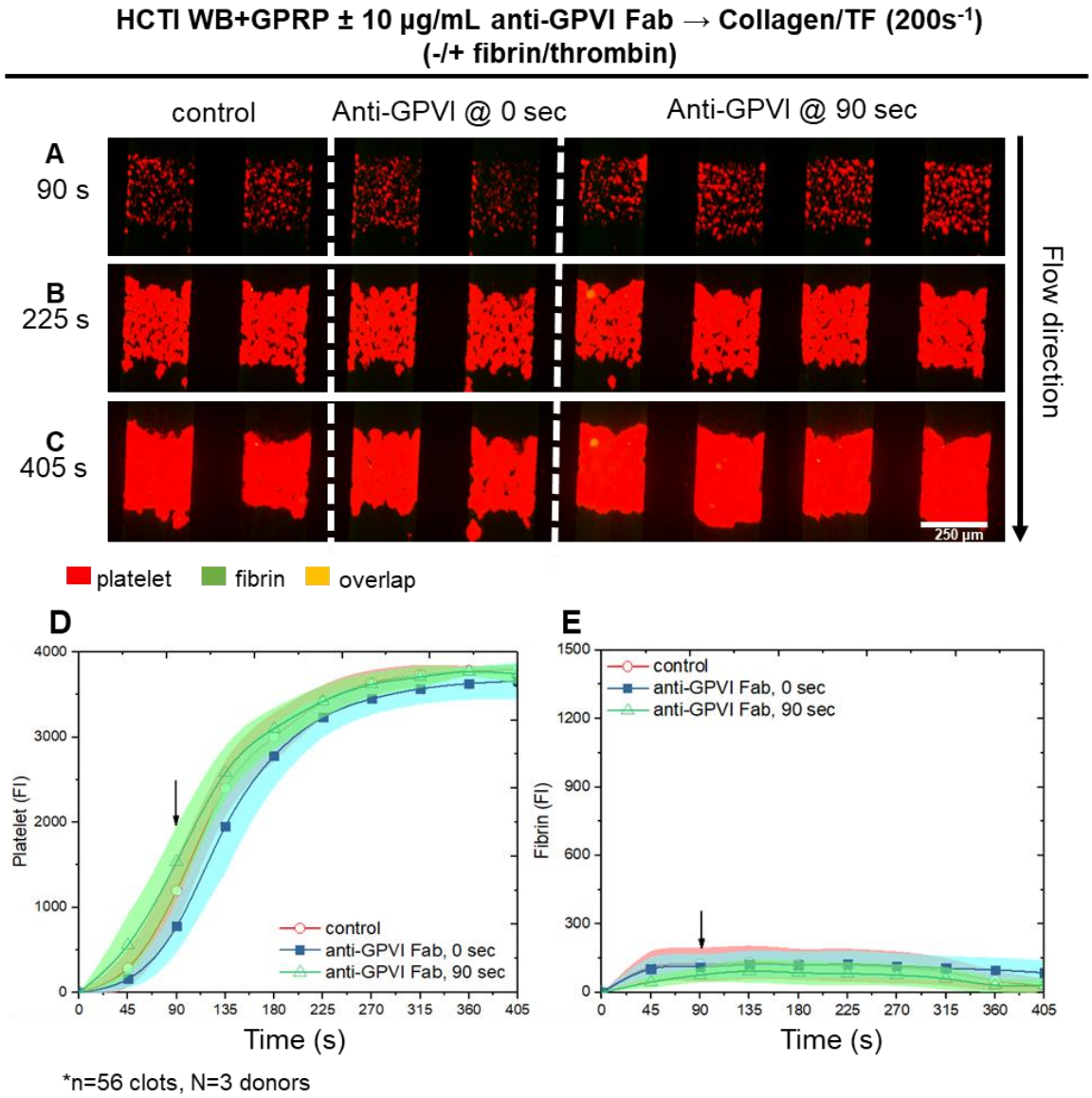

Figure 3-4: Thrombin, instead of fibrin, is the overriding factor for platelet activation when GPVI is inhibited.

High CTI WB treated with GPRP, and with and without anti-GPVI Fab, was perfused over collagen at 200 s^{-1} for 7 minutes. In the right 4 channels, control WB was perfused for 90 seconds, with a perfusion switch to anti-GPVI WB at 90s. CD61 and fluorescence fibrinogen fluorophores were added to label platelets and fibrin, respectively, with overlay images taken at 90s (A), 225s (B), and 405s (C). Fluorescence intensities for platelets (D) and fibrin (E) were measured throughout the course of the experiments.

3.4.2 Role of fibrin in platelet activation in the presence of thrombin and anti-GPVI Fab

To investigate the role of thrombin (± fibrin) in platelet activation and deposition, 5 mM GPRP or 10 µg/mL anti-GPVI Fab was added to CTI-treated WB perfused over collagen/TF without perfusion switching. Anti P-selectin Ab was added to WB, as P-selectin fluorescence is associated with the thrombin-rich inner core of a clot (75), while fluorescent fibrinogen was added to the left two channels to monitor the presence of fibrin under control condition (no P-selectin Ab). Clots with GPRP showed a quicker increase in platelet FI compared to control (Figs. 3-5A to D). One possible explanation for this is that there may be more freely available thrombin to act on platelets in the GPRP channels, since fibrin is a strong inhibitor of thrombin via antithrombin-I activity [27]. In that work, the enhanced generation of elutable F1.2 was observed with GPRP. Control conditions showed similar levels of platelet aggregation compared to WB treated with anti-GPVI (Figs. 3-5A to D). However, while GPRP-treated WB showed significantly ($p<0.0001$) higher P-selectin FI than control, anti-GPVI Fab treated WB showed significantly ($p<0.0001$) lower levels of P-selectin than control (Figs. 3-5C and E).

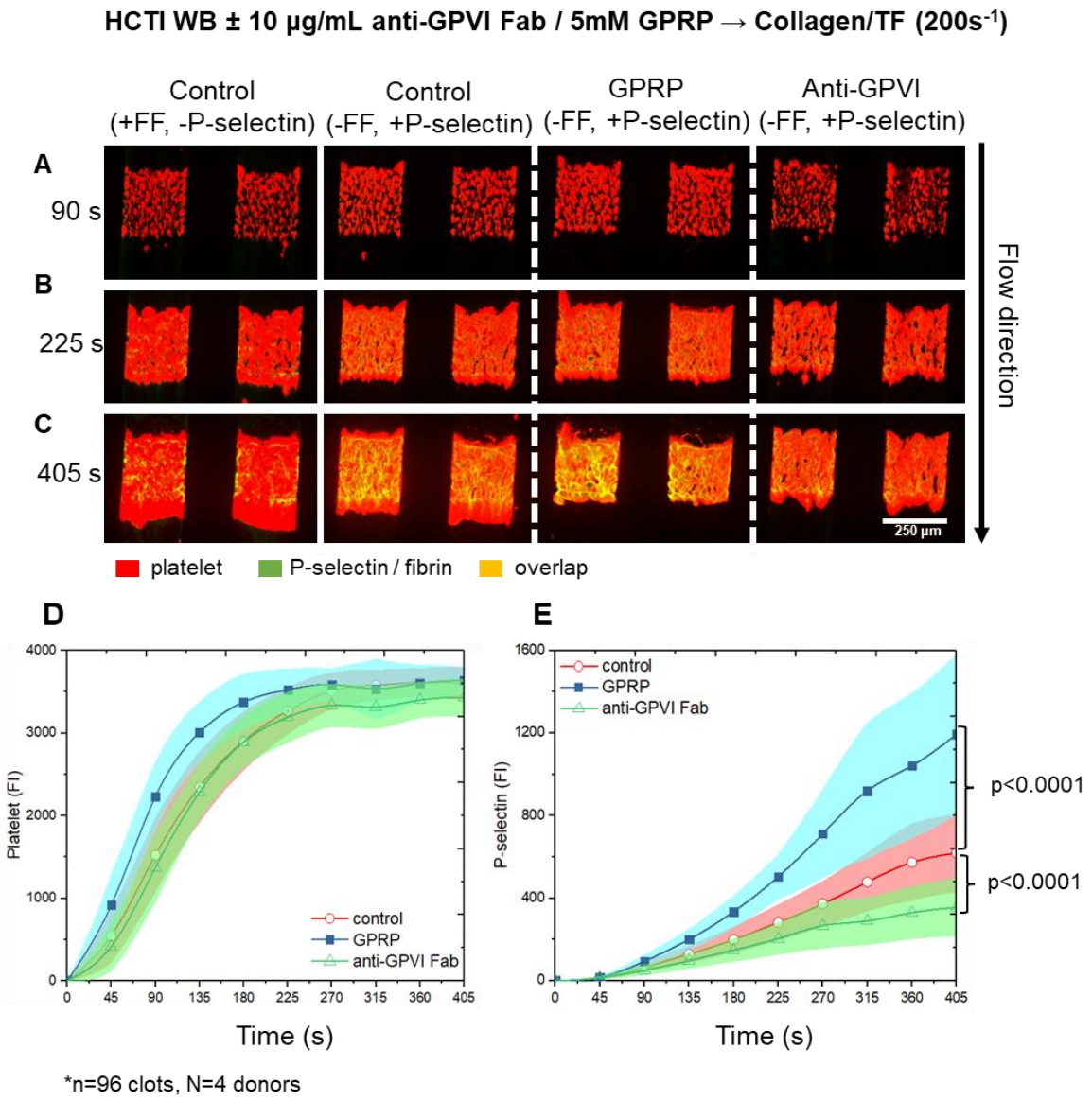

Figure 3-5: P-selectin level is lower for anti-GPVI Fab treated clot when both thrombin and fibrin are present, even though platelet fluorescence is comparable to control.

High CTI WB treated with control (HBS), GPRP, or anti-GPVI Fab, was perfused over collagen at 200 s^{-1} for 7 minutes. CD61 was added to all channels to label for platelets. In the 2 leftmost channels, fluorescent fibrinogen fluorophore was added to confirm the presence of fibrin, while in the 6 rightmost channels, P-selectin fluorophore was added to label α-granule release. Overlay images were taken at 90s (A), 225s (B), and 405s (C). Fluorescence intensities for platelets (D) and P-selectin (E) were measured throughout the course of the experiments.

3.4.3 The combination of annexin V and anti-GPVI Fab significantly impedes platelet deposition in CTI-treated WB perfused over collagen/TF

We next wanted to evaluate the effect of anti-GPVI Fab on PS exposure in clot development. Annexin V binds to exposed PS on the surface of platelets; as a result, this annexin V binding may prevent PS on the platelet surface from fully contributing to platelet procoagulant activity, and ultimately delaying and/or lowering fibrin generation (9). We have previously shown this to be this case in our assay, where annexin V contributed to a delay in fibrin formation compared to when annexin V was absent (80). To investigate the effect of annexin V in the presence of anti-GPVI Fab, we first perfused CTI-treated WB with anti-GPVI alone, with annexin V alone, or with both anti-GPVI Fab and annexin V, over collagen/TF (200 s^{-1}). Results showed that anti-GPVI or annexin V alone had almost no effect on platelet deposition (Fig. 3-6A to C), consistent with the anti-GPVI results of Fig. 3-3 and 3-4. Annexin V channels had a slight delay and decrease in fibrin polymerization (in agreement with ref. (80)), while anti-GPVI Fab channels showed inhibition of fibrin polymerization (Fig. 3-6B and D). However, when both anti-GPVI Fab and annexin V were present, there was a striking decrease in platelet deposition (Fig. 3-6A to C). Fibrin deposition was also reduced in the presence of both anti-GPVI Fab and annexin V, resulting in levels slightly lower than anti-GPVI Fab alone (Fig. 3-6D), all consistent with strong collagen signaling via GPVI in the first platelet layer, along with thrombin enhancing the procoagulant activity of platelets.

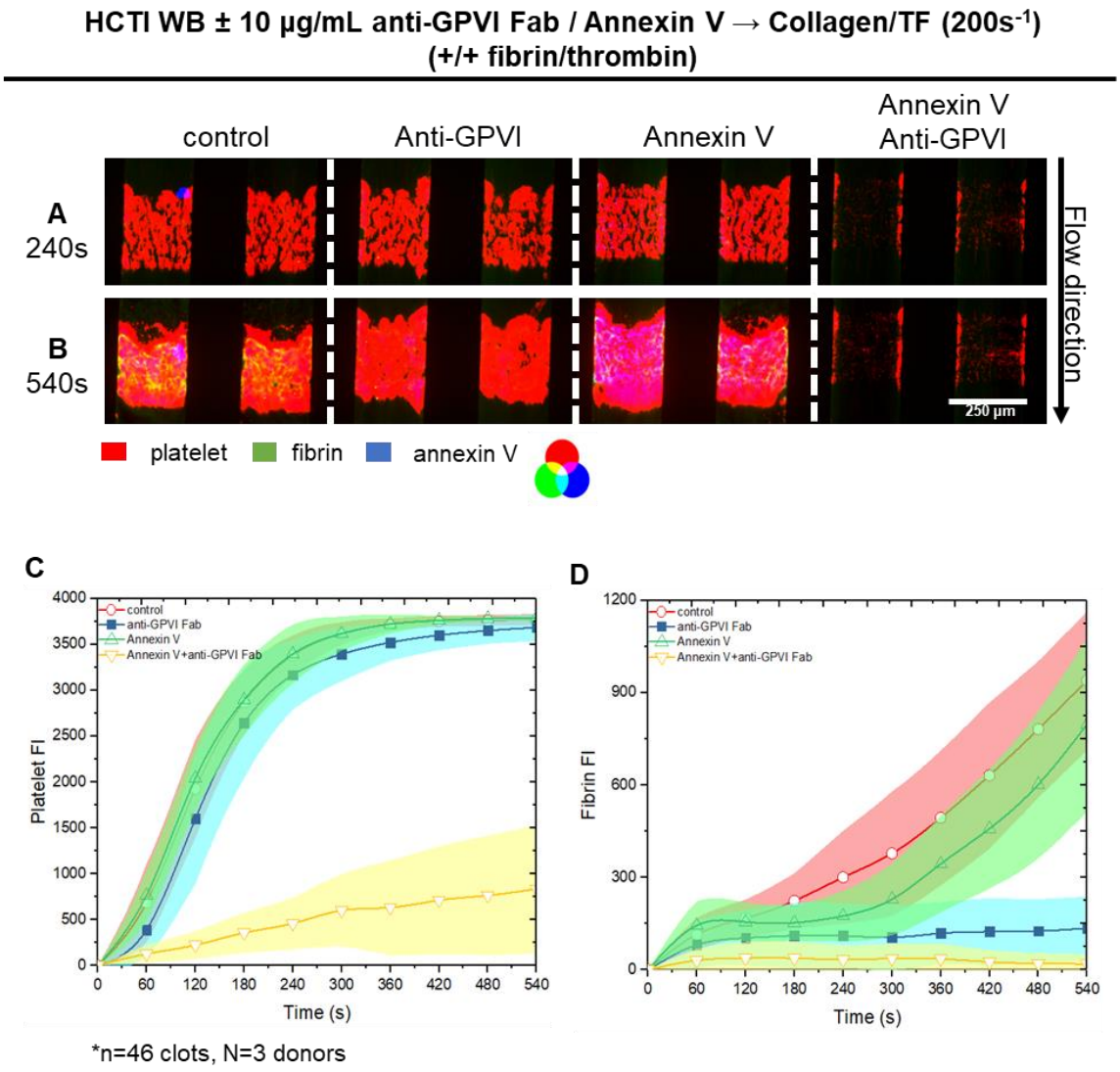

Figure 3-6: Annexin V and Anti-GPVI Fab have an additive inhibitory effect on platelet deposition.

High CTI WB treated with control (HBS), anti-GPVI Fab, Annexin V, or anti-GPVI Fab + Annexin V, was perfused over collagen at 200 s^{-1} for 7 minutes. CD61 and fluorescent fibrinogen fluorophores were added to all channels to label for platelets and fibrin, respectively. In the 4 leftmost channels, no Annexin V fluorophore was added, while in the 4 rightmost channels, Annexin V fluorophore was added to label PS exposure. Overlay images were taken at 90s (A), 225s (B), and 405s (C). Fluorescence intensities for platelets (D) and P-selectin (E) were measured throughout the course of the experiments.

3.4.4 Anti-GPVI Fab inhibits PS exposure in clot development when added at t=0, but has little to no effect on PS exposure when added at later time points

To further investigate the role of anti-GPVI in PS exposure, we performed a series of experiments with an elevated channel microfluidic device (120-μm channel height) at lower initial shear rate (100 s^{-1}) which allows for longer duration experiments without reaching occlusion [26]. We performed a control experiment with the 120-μm device at 100 s^{-1} with the same experimental design as in Fig. 3-6, which yielded similar results (Supp. Fig. S3-1). Importantly, in each of the following experiments on collagen/TF (Figs. 3-7 to 3-10), annexin V was present, in contrast to Figs. 3-3 to 3-5.

We perfused annexin V and CTI-treated WB ± anti-GPVI Fab over collagen/TF (100 s^{-1}) looking at platelet, fibrin, and phosphatidylserine (PS) fluorescence. We observed normal platelet deposition in control and limited platelet deposition with anti-GPVI Fab present (Fig. 3-7A and D), and normal fibrin polymerization in control and limited fibrin polymerization with anti-GPVI Fab (Fig. 3-7B and E). Compared to control, we see essentially no PS exposure when anti-GPVI Fab is present (Fig. 3-7C and F). The difference in platelet deposition between Fig. 3-7D and Fig. 3-3D is caused by the presence of annexin V in Fig. 3-7.

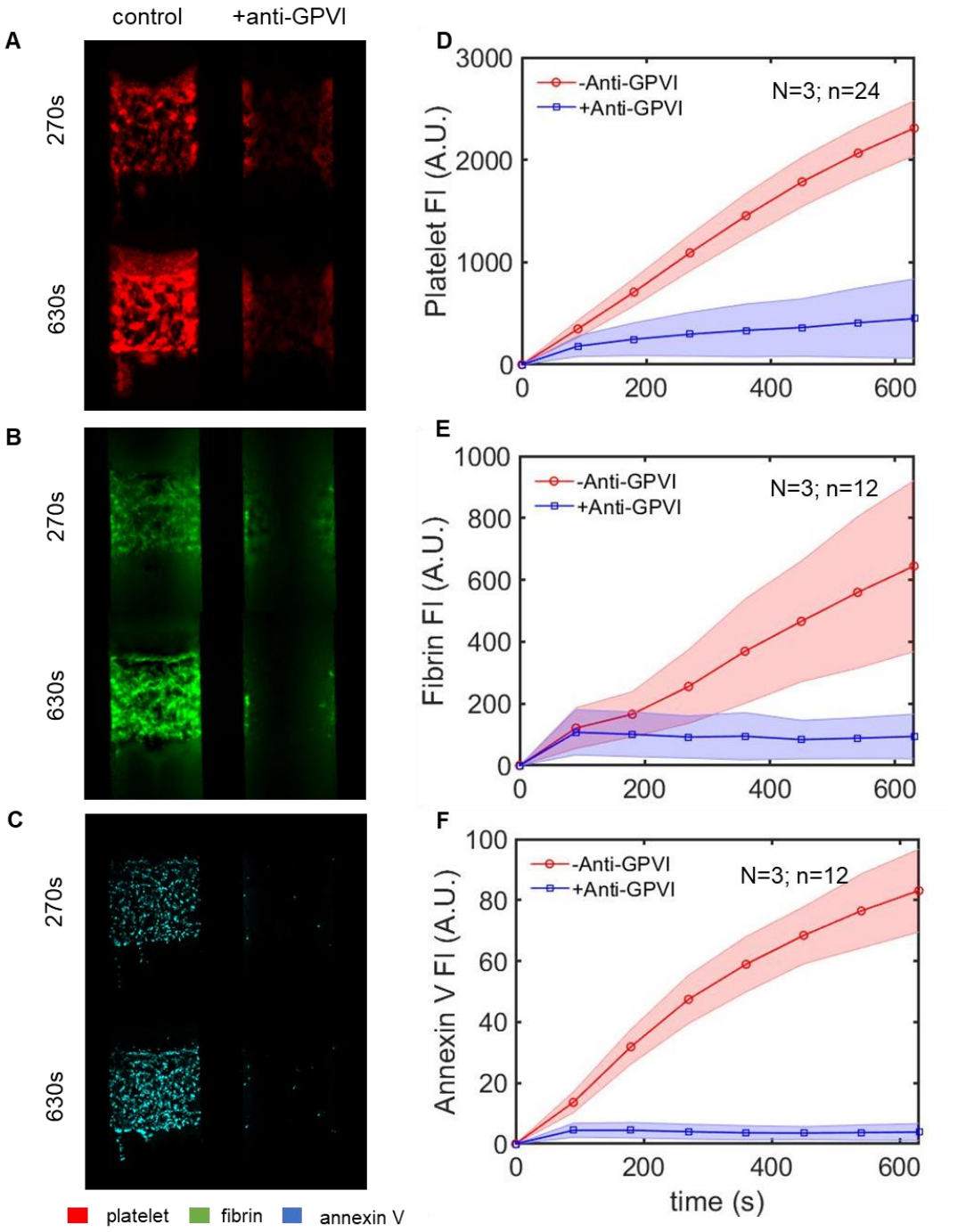

Figure 3-7: Inhibition of GPVI shows significantly decreases PS exposure.

High CTI WB with and without anti-GPVI Fab was perfused over collagen at 100 s^{-1} for 10.5 minutes using a microfluidic device with a 120-μm height. CD61, fluorescence fibrinogen, and Annexin V fluorophores were added to label platelets (A), fibrin (B), and PS exposure (C), respectively, with images taken at 270s and 630s. Fluorescence intensities for platelets (D), fibrin (E), and Annexin V (F) were measured throughout the course of the experiments. (A.U. = arbitrary units)

We then wanted to validate that the limited PS exposure in anti-GPVI channels was indeed due from anti-GPVI Fab rather than limited platelet deposition or fibrin polymerization. To do this, we compared Annexin V FI in the presence of anti-GPVI Fab, GR-144053, or GPRP. GR-144053 inhibits $\alpha_{IIb}\beta_3$ integrin, thereby preventing platelet-platelet interactions and results in a platelet monolayer. We perfused CTI-treated WB ± GR-144053, GPRP, or anti-GPVI Fab over collagen/TF at an initial wall shear rate of 100 s^{-1}. Platelet deposition was normal in control and GPRP, while there was reduced platelet deposition in anti-GPVI, and only a platelet monolayer in GR-144053 (Fig.3-8A and D). Fibrin levels were normal in control and GR-144053, while there was little to no fibrin in GPRP or anti-GPVI (Fig. 3-8B and E). We observed increased PS exposure with GR-144053 or GPRP compared to control, while anti-GPVI Fab once again had essentially no PS exposure (Fig. 3-8C and F).

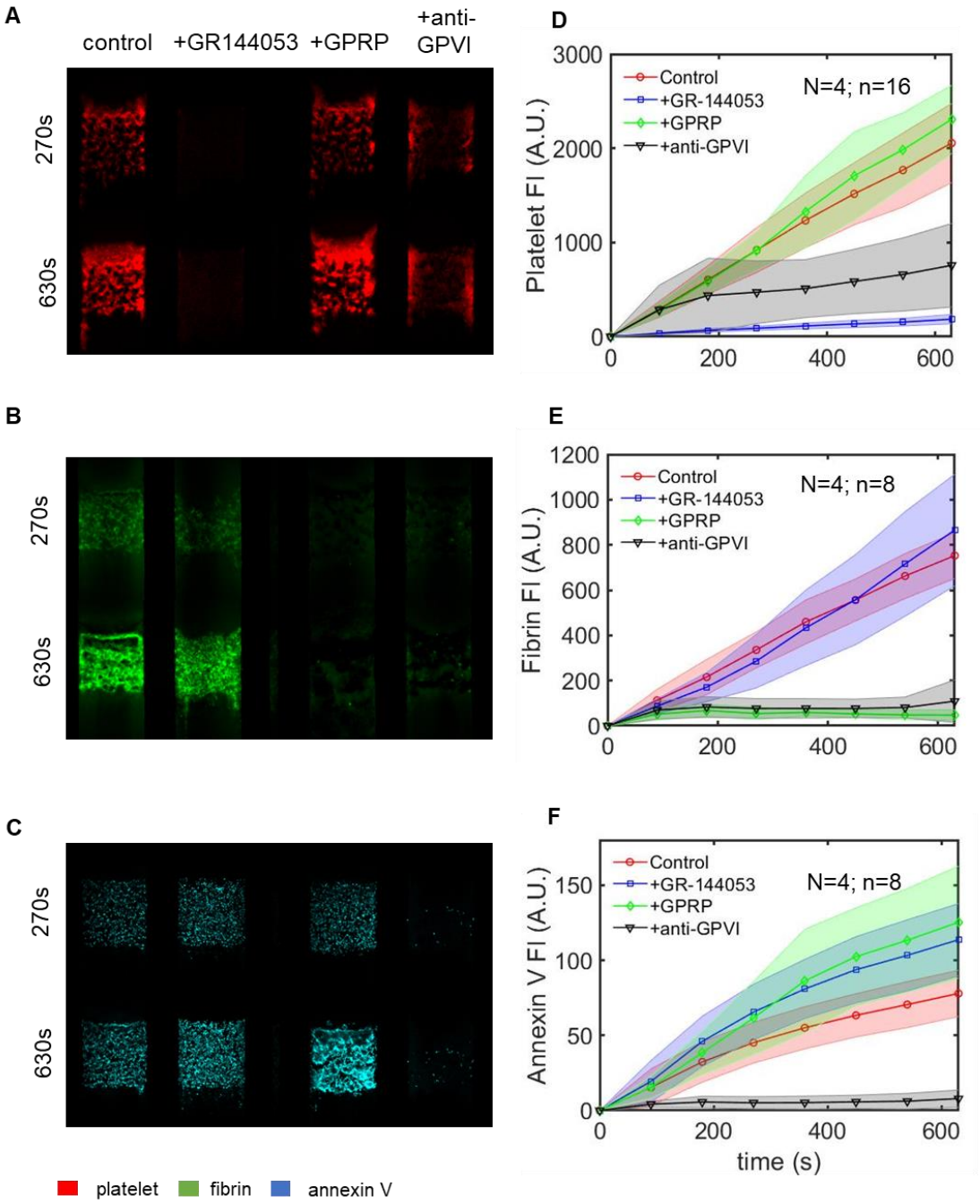

Figure 3-8: Decrease in Annexin V in the presence of anti-GPVI is due from anti-GPVI, not limited platelet deposition or fibrin polymerization.

High CTI WB with control (HBS), GR-144053, GPRP, or anti-GPVI Fab, was perfused over collagen at 100 s^{-1} for 10.5 minutes using a microfluidic device with a 120-μm height. CD61, fluorescence fibrinogen, and Annexin V fluorophores were added to label platelets (A), fibrin (B), and PS exposure (C), respectively, with images taken at 270s and 630s. Fluorescence intensities for platelets (D), fibrin (E), and Annexin V (F) were measured throughout the course of the experiments. (A.U. = arbitrary units)

We next investigated the effect of anti-GPVI Fab addition at different time points to determine if early or late inhibition of GPVI affected PS exposure. We perfused CTI-treated WB under 4 different conditions: (1) control WB with no switch, (2) control WB at 0s, followed by a switch to anti-GPVI WB at 30s, (3) control WB at 0s, followed by a switch to anti-GPVI WB at 90s, and (4) anti-GPVI WB with no switch. We found that platelet deposition was similar in conditions (1), (2), and (3) throughout the experiment (Fig. 3-9A and D), illustrating that anti-GPVI Fab had little to no effect on platelet deposition when control blood was present from the start, consistent with earlier results (Fig. 3-3). Fibrin polymerization was also similar among conditions (1), (2), and (3) throughout the experiment (Fig. 3-9B and E), also illustrating that anti-GPVI Fab had little to no effect on fibrin polymerization when control blood was present initially, again consistent with earlier results (Fig. 3-3). In terms of PS exposure, annexin V binding was fairly similar between conditions (1), (2), and (3), while there was essentially no PS exposure in anti-GPVI Fab at t = 0s condition (4) (Fig. 3-9C and F). These results demonstrate that if control WB is initially present to all platelet interactions with collagen, GPVI signaling, and thrombin generation, the addition of anti-GPVI Fab E12 at later time points has little to no effect on platelet deposition, fibrin polymerization, and PS exposure.

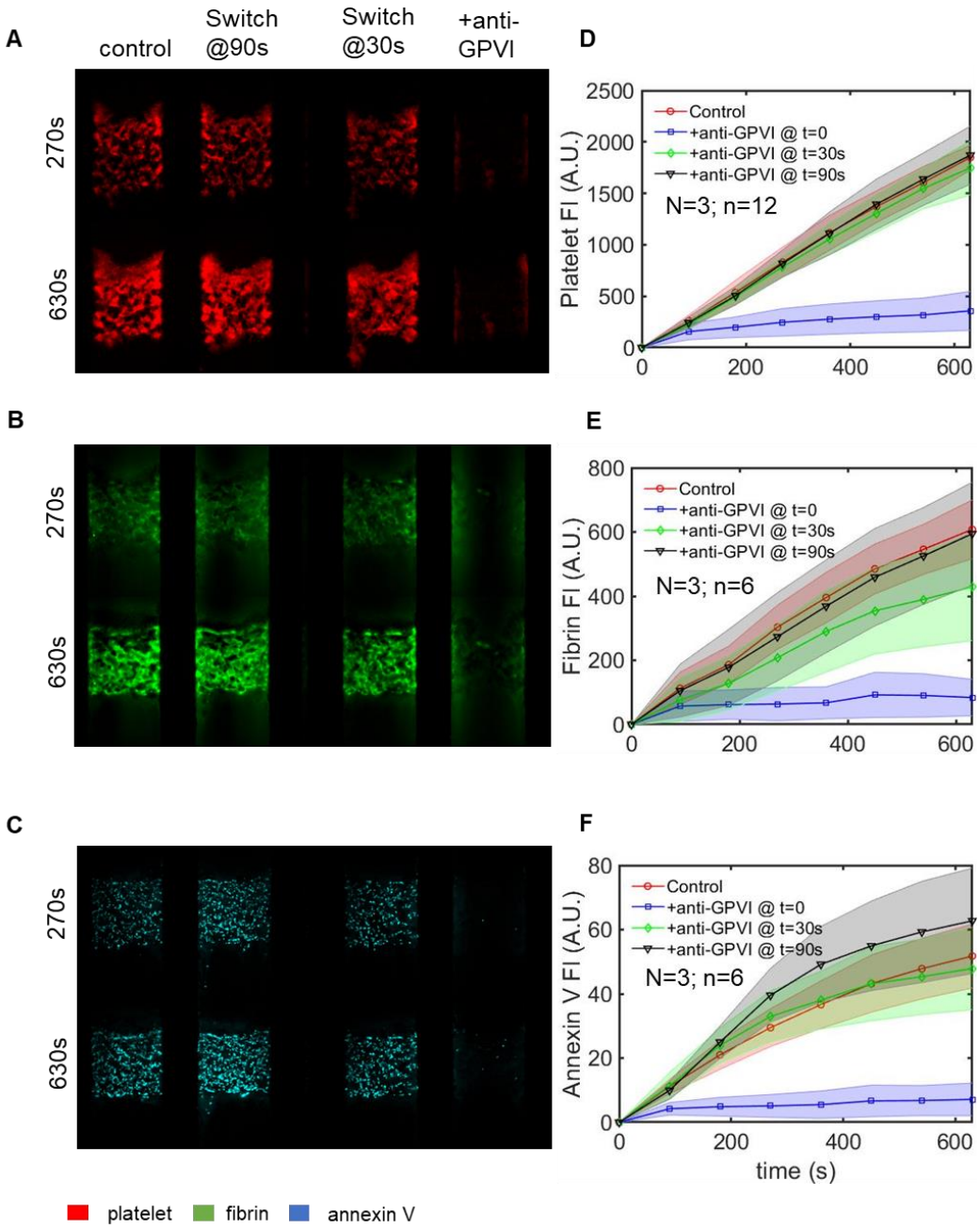

Figure 3-9: Effects of anti-GPVI Fab require its presence from the initiation of clot development in the presence of thrombin.

High CTI WB with or without anti-GPVI Fab was perfused over collagen at 100 s^{-1} for 10.5 minutes using a microfluidic device with a 120-μm height. The two middle channels started with control WB perfusion, with a switch to anti-GPVI WB at either 30s or 90s. CD61, fluorescence fibrinogen, and Annexin V fluorophores were added to label platelets (A), fibrin (B), and PS exposure (C), respectively, with images taken at 270s and 630s. Fluorescence intensities for platelets (D), fibrin (E), and Annexin V (F) were measured throughout the course of the experiments. (A.U. = arbitrary units)

3.4.5 The effects of anti-GPVI Fab are reversible for platelet deposition, fibrin polymerization, and PS exposure when switched to control blood

We wanted to evaluate the effect of switching from anti-GPVI Fab-treated WB back to control WB lacking Fab. We perfused CTI-treated WB again under 4 conditions: (1) control WB with no switch, (2) anti-GPVI WB at t=0s, followed by a switch to control WB at 90s, (3) anti-GPVI WB at t=0s, followed by a switch to control WB at 270s, and (4) anti-GPVI WB with no switch. Platelet deposition in condition (1) formed normally, while there was limited platelet deposition in anti-GPVI condition (4) (Fig. 3-10A and D). In the switch conditions, both conditions initially had limited platelet deposition, but after about 180s post-switch, there was a significant increase in platelet levels in both conditions relative to condition (4). There were statistical differences in final fluorescence values between conditions (2) and (4) ($p = 0.0032$) and between conditions (3) and (4) ($p=0.0014$). After platelets levels began increasing in the switch channels, the platelet clot morphology was restored back to control conditions. In terms of fibrin fluorescence, we again observed normal fibrin formation in condition (1) and essentially no fibrin form in condition (4), as expected and as previously shown. In the switch channels, there was essentially no fibrin polymerization throughout nearly the entirety of the experiment, except at the very end where there was a slight increase in fibrin (Fig. 3-10B and E). Even still, these slight increases were found to be statistically significant compared to anti-GPVI; there were statistical differences in final fibrin fluorescence between conditions (2) and (4) ($p=0.0009$) and between conditions (3) and (4) ($p=0.017$). Lastly, annexin V levels were normal in condition (1) and essentially negligible in condition (4), again in agreement with previous results. In the switch conditions, annexin V was negligible initially, as expected, and then eventually increased after the switch to control WB. Again, there were statistical differences in final annexin V fluorescence between conditions (2) and (4) and between conditions (3) and (4) (both $p<0.0001$). There was again an approximate 180s time lag between the switch and when annexin V levels began increasing in both conditions. This is in line with the platelet restoration time lag.

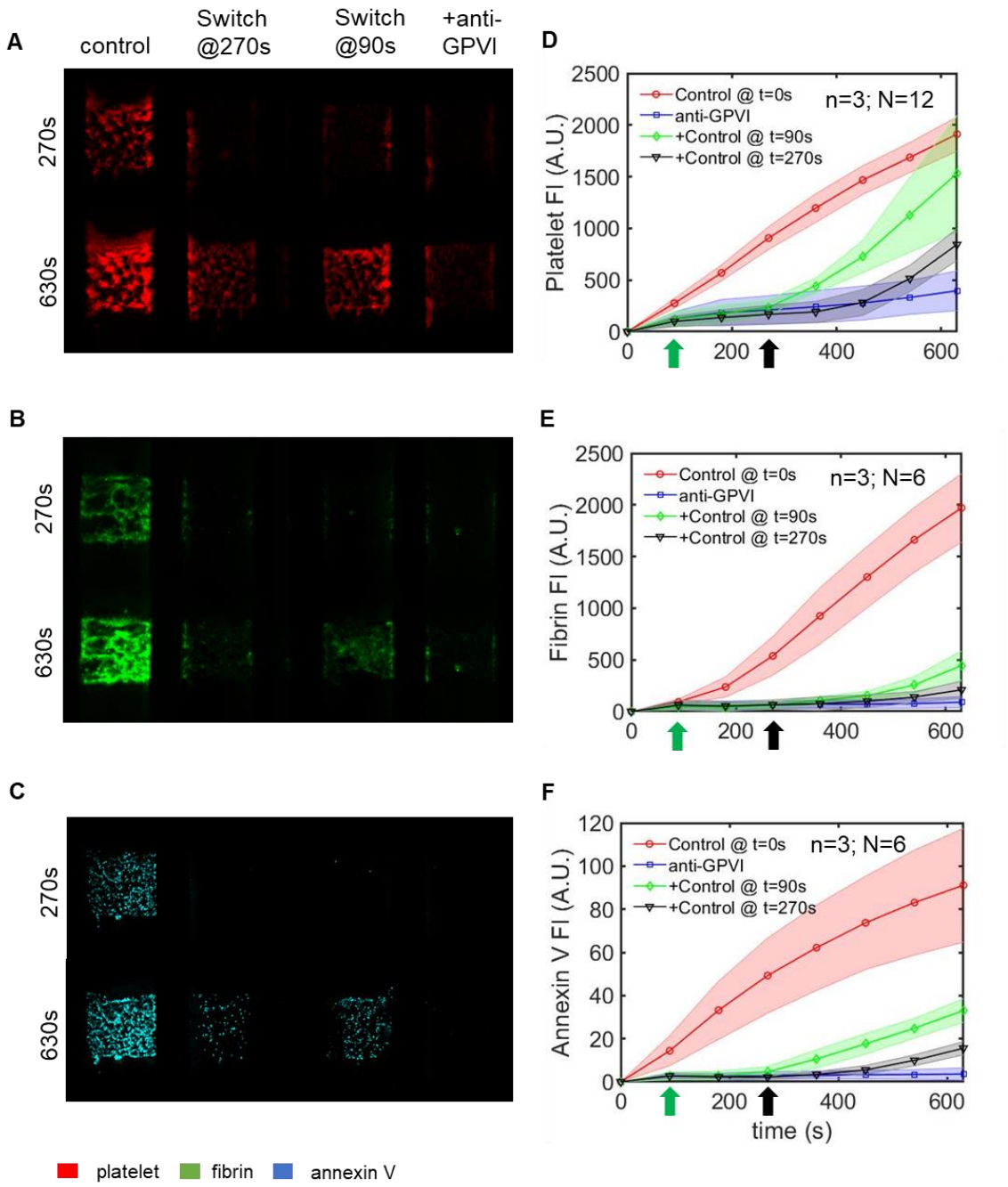

Figure 3-10: Effects of anti-GPVI Fab on clot development are reversible.

High CTI WB with or without anti-GPVI Fab was perfused over collagen at 100 s^{-1} for 10.5 minutes using a microfluidic device with a 120-μm height. The two middle channels started with anti-GPVI WB perfusion, with a switch to control WB at either 90s or 270s. CD61, fluorescence fibrinogen, and Annexin V fluorophores were added to label platelets (A), fibrin (B), and PS exposure (C), respectively, with images taken at 270s and 630s. Fluorescence intensities for platelets (D), fibrin (E), and Annexin V (F) were measured throughout the course of the experiments. (A.U. = arbitrary units)

3.4.6 Anti-GPVI limits platelet deposition when thrombin is inhibited at later time points

We wanted to observe how thrombin inhibition affects platelet deposition at different time points in the presence of anti-GPVI. We perfused CTI-treated WB ± anti-GPVI with a switch to PPACK-treated WB ± anti-GPVI at either 90s, 270s, or 540s over collagen/TF at 100 s^{-1} for 15 minutes (Fig. 3-11). Notably, annexin V was not present in these experiments. In channels 1 and 2, there was only CTI-treated WB, no switch to PPACK, for the entirety of the experiment. The remaining channels 3-8 started with CTI-treated WB, but was then switched to PPACK-treated WB at 90s (channels 7 and 8), 270s (channels 5 and 6), or 540s (channels 3 and 4). “Control” channels (odd channels) did not have anti-GPVI present for the entirety of the experiment, while “anti-GPVI” channels (even channels) had anti-GPVI present for the entirety of the experiment. We see that platelet deposition and fibrin formation are both normal in control (no switch), while platelet deposition is normal for anti-GPVI (no switch), but there is reduced fibrin (Fig. 3-11A, B), as previously shown in Fig. 3-3. When there is switch to PPACK-treated WB at different time points, we see fibrin begin to plateau, or slightly decrease (Fig. 3-11B, Supp. Fig. S3-2). Noticeably, anti-GPVI channels all have relatively low fibrin levels regardless of switch time; however, adding PPACK earlier appears to further reduce/limit fibrin polymerization (Fig. 3-11B). There is mostly normal platelet deposition in “control” channels, although adding PPACK earlier (90s or 270s) appears to slightly reduce platelet deposition compared to adding PPACK later (540s) or not at all (Fig. 3-11A, Supp. Fig. S3-2). Platelet deposition in anti-GPVI channels appears to be heavily reliant on when PPACK is added; anti-GPVI (no switch) has nearly identical platelet deposition to control (no switch). When PPACK is added at 540s, platelet deposition is similar, albeit slightly lower than anti-GPVI (no switch) (Supp. Fig. S3-2). When PPACK is added at 270s, platelet deposition is significantly lower, and when PPACK is added at 90s, platelet deposition is even lower (Fig. 3-11A, Supp. Fig. S3-2).

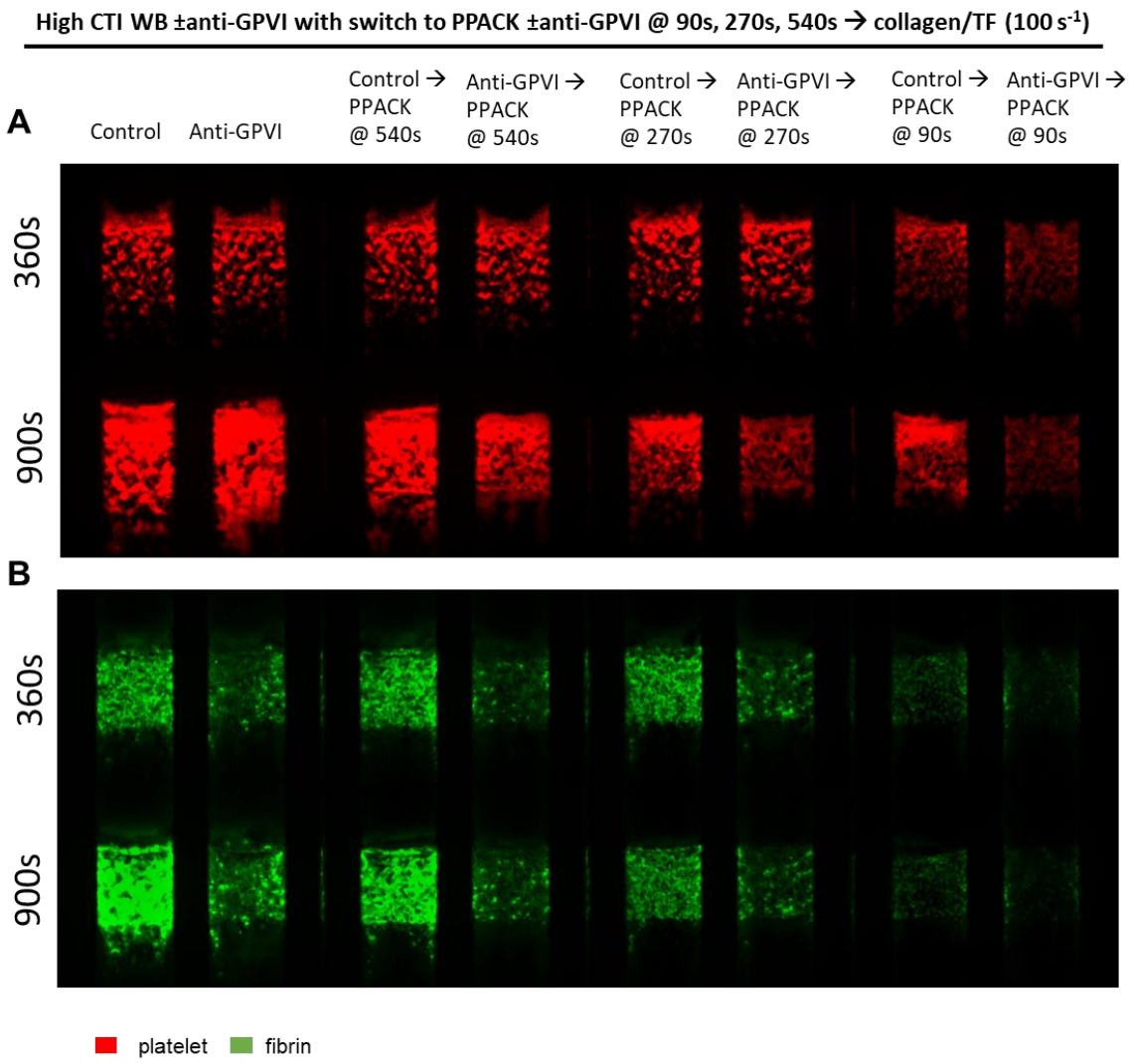

Figure 3-11: Anti-GPVI limits platelet deposition when thrombin is inhibited at later time points.

High CTI WB with or without anti-GPVI Fab, with a switch to PPACK WB with or without anti-GPVI, was perfused over collagen/TF at 100 s^{-1} for 15 minutes using a microfluidic device with a 120-μm height. This experiment had no annexin V present in any channels. In the 2 leftmost channels, CTI WB was present without (channel 1) or with (channel 2) anti-GPVI from t=0s. The remaining channels all started with either CTI-treated control (channels 3, 5, 7) or anti-GPVI (channels 4, 6, and 8) WB, with a switch at either 90s, 270s, or 540s to PPACK-treated WB. In the switch channels (channels 3-8), anti-GPVI or control remained constant throughout the experiment (i.e. channels either did or did not have anti-GPVI for the entire experiment time); the only change was from CTI-treated to PPACK-treated WB. CD61 and fluorescence fibrinogen fluorophores were added to label platelets (A) and fibrin (B) respectively, with images taken at 270s and 630s.

3.4.7 Addition of annexin V to anti-GPVI WB at later time points has no effect on platelet deposition

In Figure 9, we added anti-GPVI at later time points (after t=0s) to WB containing annexin V to see if there is an effect on platelet deposition when annexin V and anti-GPVI are added together, but at later times. Here, we wanted to add annexin V at later time points to anti-GPVI WB. We perfused CTI-treated WB + anti-GPVI (no annexin V) with a switch to anti-GPVI + annexin V at 30s, 90s, 270s, or 540s over collagen/TF at 100 s^{-1} for 15 minutes (Fig. 3-12). In the 4 rightmost channels (channels 1-4), we repeated conditions in figure 6 (here, at 100 s^{-1} instead of 200 s^{-1} and in the 120-µm height device instead of the 60-µm height device), to again confirm that anti-GPVI and annexin V together have a strong inhibitory effect on platelet deposition, but not when added individually (Fig. 3-12A). In the leftmost channels, anti-GPVI is present in all channels throughout the experiment, but annexin V is introduced at different times: 30s (channel 5), 90s (channel 6), 270s (channel 7), or 540s (channel 8). We see nearly identical platelet deposition in channels 5-8, regardless of when annexin V is added (Fig. 3-12A). In terms of fibrin deposition, fibrin is relatively low in channels 5-8 compared to control (channel 1); there does appear to be a slightly increased inhibitory effect when annexin V is added earlier (Fig. 3-12B). Annexin V fluorescence is very low in all switch channels relative to the Annexin V control (channel 2) (Fig. 3-12C). To confirm this reduction was due from anti-GPVI and not from adding annexin V at later time points, we performed a control experiment adding annexin V at later time points without anti-GPVI present (Supp. Fig. S3-4), showing that annexin V FI normally increases significantly when added to WB.

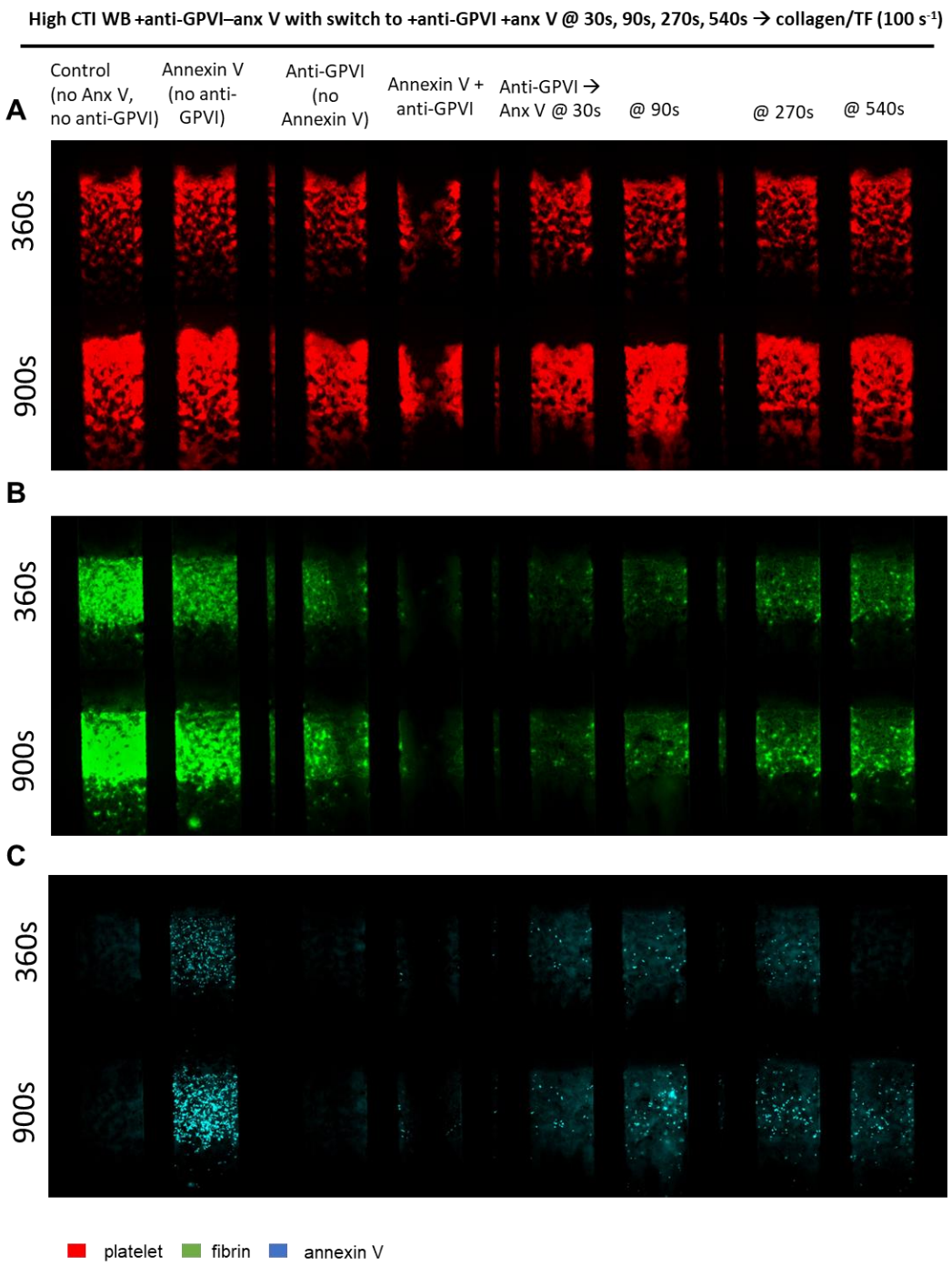

Figure 3-12: Addition of annexin V to anti-GPVI WB at later time points has no effect on platelet deposition.

High CTI WB with anti-GPVI (-anx V), with a switch to anti-GPVI +anx V was perfused over collagen/TF at 100 s^{-1} for 15 minutes using a microfluidic device with a 120-μm height. The 4 rightmost channels were conditions repeated from Fig. 6, as a control for the 4 leftmost channels. In the 4 leftmost channels, anti-GPVI was present from t=0s, and annexin V was not present at t=0s. Annexin V was then added at either 30s, 90s, 270s, or 540s. CD61, fluorescence fibrinogen, and Annexin V fluorophores were added to label platelets (A), fibrin (B), and PS exposure (C), respectively, with images taken at 360s and 900s.

3.4.8 Confocal microscopy confirms fibrin and PS exposure are localized to collagen surface, while platelet deposition occurs throughout the clot thickness

Confocal images show an example clot from the bottom view (Fig. 3-13A), top view (Fig. 3-13B), side view (Fig. 3-13C), and outlet view (Fig. 3-13D). These images illustrate that fibrin and annexin V were predominantly localized near the collagen surface, while platelets are distributed throughout the clot, most clearly visible at the top layer of the clot. We also took example orthogonal slices of the example clot (Fig. 3-13E to G) to further illustrate the localization of fibrin and PS exposure at the collagen surface.

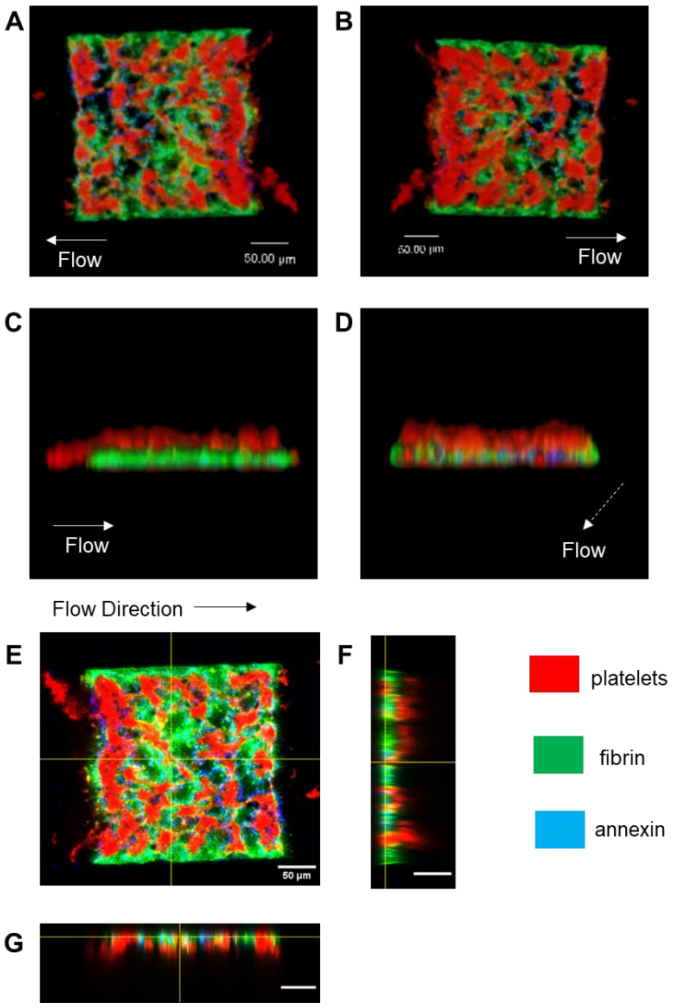

Figure 3-13: Representative 3D images of clot end point.

Z-stack images were taken of preserved clots on a confocal microscope to determine the distribution of platelets (red), fibrin (green) and annexin (blue). (A) Bottom view of clot (on coverslip). (B) Top view of clot. (C) Clot side view. (D) Clot outlet view. (E) Single z plane image of clot with orthogonal slices pointed out (yellow lines). (F) Vertical orthogonal slice from wall to wall of microfluidic device channel. (G) Horizontal orthogonal slice from clot inlet to clot outlet.

3.4.9 3D computer model simulations of clot development illustrate crucial role of the first 90s of clot development in determining collagen-bound platelet deposition

The near complete coverage of collagen with platelets typically requires 90s during clotting at venous shear rate. We explored the formation of the first layer of platelets (in contact with collagen) and the rate of deposition of subsequent layer using numerical computer simulation of thrombus formation in 3 dimensions. The numerical simulations captured individual platelets that deposited and aggregated on the reactive collagen/TF surface, their corresponding activation levels, the spatiotemporal distribution of ADP and TXA2, and the blood velocity profile over the growing clot. The simulations were able to accurately capture the evolution and morphology of the thrombus initiated at the reactive surface. Model predictions agreed well with fluorescent micrographs of thrombus formation over time observed in experiments for cases with and without wall-derived TF, as shown in Fig. 3-14A to C. The simulations showed that almost all platelets in the first platelet monolayer (in contact with the collagen/TF surface) were deposited within the first 150s of blood perfusion without thrombin present, and within the first 90s with thrombin present (Fig. 3-14A to D). Following this initial period, significant platelet deposition occurred in subsequent platelet layers binding platelets, making it difficult for platelets binding the outer clot domain to interact with the collagen surface (Fig. 3-14D). A plot of the cumulative number of platelet-collagen collisions as a function of time showed little to no platelet-collagen collisions after 90s and 150s under the presence and absence of thrombin respectively (Fig. 3-14E).

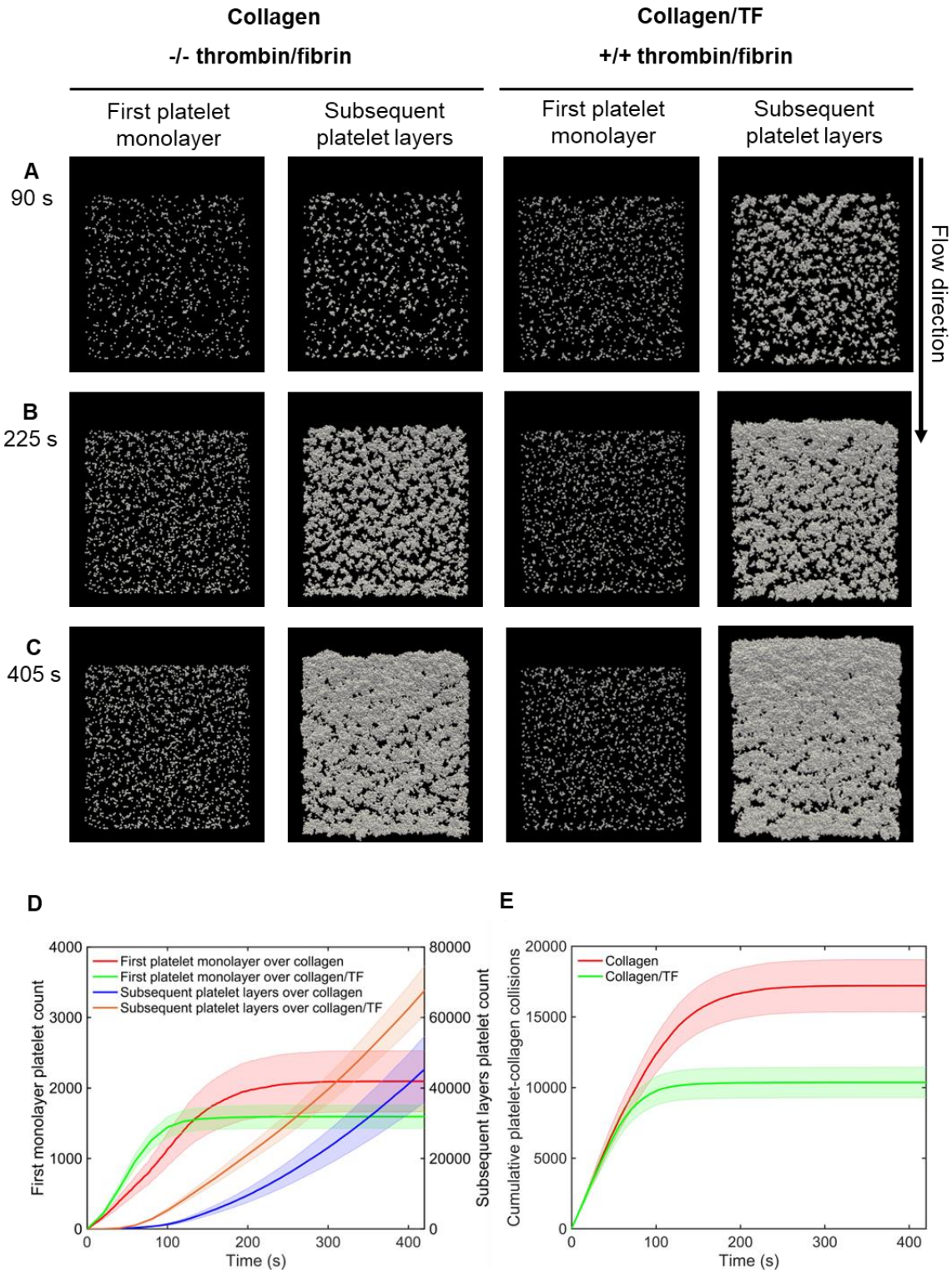

Figure 3-14: Multiscale simulations of platelet aggregation under flow over collagen/TF.

The first monolayer of deposited platelets and subsequent platelet layers are shown after (A) 90 s, (B) 225 s, and (C) 400 s of perfusion. (D) Dynamics of deposited platelet count in the first platelet monolayer and subsequent platelet players, and (E) cumulative platelet-collagen collisions observed over time.

3.5 Discussion

We performed a series of *in vitro* experiments with human blood using a novel, direct GPVI inhibitor to demonstrate the role GPVI plays in primary and secondary platelet deposition and fibrin polymerization. We first showed that anti-GPVI Fab significantly reduced platelet deposition on collagen when thrombin was not present, demonstrating the role of GPVI in both primary and secondary platelet deposition. With thrombin present, anti-GPVI Fab treated and control blood had similar platelet deposition, although fibrin was inhibited with anti-GPVI Fab present. To confirm thrombin, not fibrin, contributed to this platelet deposition with anti-GPVI Fab present, we used GPRP to show that platelet deposition was still similar between anti-GPVI and control. P-selectin levels were lower for anti-GPVI than for control, further supporting the role of free, available thrombin in contributing to platelet deposition. In the presence of thrombin, the combination of annexin V fluorophore and anti-GPVI Fab still managed to reduce platelet deposition significantly lower than control, annexin V alone, or anti-GPVI alone, suggesting that thrombin generated specifically via PS exposure may play a significant role in contributing to platelet aggregation in the presence of anti-GPVI Fab.

We observed that anti-GPVI Fab significantly reduced annexin V fluorescence nearly to background levels. To confirm this was due from anti-GPVI Fab rather than reduced platelet aggregation or fibrin inhibition, we compared the annexin V signals of anti-GPVI, GR-144053, and GPRP in the presence of thrombin. We saw that platelet monolayers (caused by GR-144053) and fibrin inhibition (caused by GPRP) resulted in similar or increased annexin V fluorescence, while annexin V fluorescence in the anti-GPVI condition remained near background levels. This demonstrated the potent effect of anti-GPVI and annexin V in limiting PS exposure. To better understand this synergistic effect, we performed two experiments to evaluate annexin V fluorescence: (1) switching from control blood to anti-GPVI blood, and (2) switching from anti-GPVI blood to control blood. When control blood was present at the beginning of the experiment, platelet deposition, fibrin polymerization, and PS exposure occurred normally, even when anti-GPVI Fab was present as early as 30s. When anti-GPVI blood was present at the beginning of the experiment, but there was a switch to control blood, platelets, fibrin, and annexin V slowly

begin to increase after the switch. This demonstrated that the effects of anti-GPVI Fab seem to be reversible, while anti-GPVI Fab does not seem to be effective (in the presence of thrombin) if it first becomes present after control clotting has already been initiated.

Without thrombin, platelets will not deposit further if GPVI is inhibited, and formed platelet aggregates will undergo slight erosion based on shear or presence of anti-GPVI Fab, or both. This observation supports a role for GPVI signaling in a platelet deposit that is fibrin independent. When thrombin is present, however, GPVI plays very little in secondary deposition, and fibrin polymerization was not affected for channels switched to anti-GPVI treated WB. From our results with GPRP (Fig. 4), we can confirm the robust activation of platelets was likely induced by the presence of thrombin, regardless of the presence of anti-GPVI Fab.

There was a synergistic effect of inhibition of GPVI and inhibition of exposed PS on lowering platelet deposition in clot development. Increased PS exposure in GR-144053 compared to control further demonstrates the significance of collagen in stimulating PS exposure, since essentially all platelets in GR-144053 are bound and stimulated via collagen. Increased PS exposure in the presence of GPRP compared to control demonstrates the role of freely available thrombin to contribute to PS exposure, and we have previously shown this before (80). Therefore, when collagen interactions are inhibited by anti-GPVI Fab and freely available thrombin is reduced by annexin V, it follows that there is very little measurable PS exposure. Our results support the significant role for thrombin generated via PS exposure in stimulating platelet deposition and continued buildup when GPVI is inhibited. Since annexin V binds exposed PS on the platelet surface (81,82), and PS allows for formation of the prothrombinase complex for conversion of prothrombin to thrombin catalyzed by Factor Xa (16), annexin V binding to PS may have reduced the generation of thrombin at the beginning of the clot growth, thus resulting in limited platelet stimulation via thrombin. Blocking collagen binding and inhibiting thrombin generation are both crucial for attenuating subsequent platelet deposition.

In our perfusion-switch experiments with annexin V present, our results in Figure 3-10 suggest that the time lag between the switch and increase in platelet fluorescence may consist of the removal of GPVI-inhibited platelets with control platelets. In addition, the time lag for fibrin

formation to be restored takes longer than for platelet deposition, which is logical since platelet deposition precedes fibrin polymerization in control conditions, and is in agreement with thrombin kinetics (68,83). These results suggest switching from anti-GPVI WB to control WB nearly allows for clot restoration in terms of platelet deposition and morphology, fibrin polymerization, and PS exposure. This is not the case when control WB is switched to anti-GPVI WB, where we see platelet deposition, fibrin polymerization, and annexin V remain similar to control throughout the experiment (Fig. 3-9). These results are in agreement with simulation results from our 3D model (Fig. 3-14), which illustrates that the collagen surface is essentially fully covered by the first 90 seconds of perfusion when thrombin is present. This initial layer of platelet deposition is crucial for directing the development of the full clot, as seen in Fig. 3-10 when anti-GPVI WB is replaced with control WB, allowing normal clot development to be restored.

Many of our findings are consistent with previous studies investigating GPVI deficiency/inhibition. Munnix et. al. studied the effects of an anti-GPVI JAQ1 Fab on platelet deposition and PS exposure in PPACK-treated WB over collagen, and in citrated mouse blood (+$CaCl_2$ +TF) over collagen at 1000 s^{-1} (38). They also observed a significant decrease in platelet deposition with JAQ1 in anti-coagulated WB over collagen, similar to what we've seen with E12 (Fig. 3-2). Additionally, they also observed a significant decrease in Annexin V exposure with JAQ1, similar to what was observed with E12 (Fig. 3-7). However, they also observed a decrease in platelet deposition with JAQ1 in the presence of thrombin (38), while we did not see this change in platelet deposition (Fig. 3-3). The reason for this should be studied further to better understand why E12 does not cause a decrease in platelet deposition in the presence of thrombin.

Our results are also in agreement with Navarro, et al., where they perfused citrated whole blood + anti-GPVI Fab EMF-1 over collagen or collagen/TF at 1000 s^{-1} (84). Over collagen/TF, their results show that when EMF-1 is added at t=0 min, annexin V FI is significantly lower and fibrin polymerization is strongly inhibited compared to vehicle; however, when EMF-1 is added at t=2 min, annexin V and fibrin polymerization is at least restored, in accordance with our results in Figures 3-3 and 3-9 (84). Over collagen (thrombin not available), they observed significant inhibition of platelet deposition when EMF-1 was added at t=0 min, but only slightly reduced

platelet deposition when EMF-1 was added at t=2 min, in agreement with our results in Figure 3-2 (84). However, it should be noted that Navarro, et al. experimental results were performed at arterial shear rates, as opposed to our venous shear rates in this study.

Our results are also in agreement with experiments performed with GPVI-deficient blood. Nagy, et. al. demonstrated a critical role for GPVI in platelet aggregation, but not adhesion under non-coagulating conditions, and a critical role of GPVI in PS exposure, but not thrombus formation, under coagulating conditions (72). As they explain, a reason for this finding may be due to the presence of integrin $\alpha_2\beta_1$, a secondary collagen receptor, which can support platelet adhesion to collagen under flow (85–87). Nagy, et. al. also show fibrin generation was inhibited in GPVI-deficient blood, in agreement with our findings in Figure 3-3, and that thrombin is reduced, but still present, in GPVI-deficient blood compared to control, which supports our findings in Figure 3-3 and 3-4, where we show reduced P-selectin display in anti-GPVI conditions relative to control; reduced thrombin levels in anti-GPVI conditions may explain this decrease in P-selectin.

While we see similarities between E12 and other modes of GPVI inhibition, we also observe differences. Noticeably, although we observed some inhibition of platelet deposition, we did not see long term inhibition of platelet deposition at arterial flow rates (Supp. Fig. S3-S5). This is in contrast with studies that have evaluated GPVI inhibition previously (84,88,89). Additionally, Fab E12 did not significantly inhibit platelet deposition when fibrin had already formed (Fig. 3-3), which does not agree with previous GPVI inhibitors (90). These differences may suggest that E12 is a more sensitive inhibitor of GPVI than previous anti-GPVI inhibitors, with its mechanism of action more relevant to cases that may require moderate modulation of platelet deposition.

Here, we investigated the effect of E12 in thrombin-free or thrombin-rich environments. However, there exists conditions where there are low or moderate levels of thrombin. As van der Meijden et. al. showed, collagen can contribute to FXII-induced intrinsic pathway coagulation. Additional experiments should be investigated in the future to determine the effect of E12 on platelet deposition, fibrin formation, and PS exposure in environments where there are low to moderate thrombin levels (e.g. perfuse CTI-treated WB + E12 over collagen).

We have shown that anti-GPVI Fab has a potent effect on platelet deposition when thrombin is not present. With thrombin present, anti-GPVI does not limit platelet deposition, as thrombin is the most likely cause of normal platelet deposition. With our perfusion-switch experimental design, we show that the initial layer of platelets is crucial for clot development, as switching from control to anti-GPVI WB has little to no effect on the clot, while switching from anti-GPVI WB to control WB restores normal clot development. Together, our results demonstrate a deeper understanding of the role GPVI plays in primary and secondary deposition (both in the presence and absence of thrombin), fibrin polymerization, alpha-granule release, and PS exposure.

CHAPTER 4 – FUTURE WORK

4.1 NAC facilitating VWF strands cleavage and dissolving thrombus plug under arterial shear

As cardiovascular disease remains the most leading cause of death in the US (2), recent studies regarding arteriole thrombosis proposed a possible solution by administering N-acetylcysteine (NAC) in hope to reduce the size of ultra-long VWF (ULVWF) (91) to mitigate, cure or prevent arteriole thrombosis (92). NAC has been proven to be a low-cost, safe, generic, and promising drug (93) for many diseases including mucolytic therapy (94), kidney disease (95), chronic obstructive pulmonary disease (96), etc.; however, although the antithrombic efficacy of NAC has been confirmed in various studies (91,92,97), the cause of its efficacy should not be concluded hastily to its ability to disintegrate ULVWF, since experiment results also have shown that NAC cannot digest VWF that was already formed under pathological shear rate (98). Therefore, understanding the antithrombotic effect of NAC requires a more wholistic perspective that includes the interactions between platelet, VWF, and all other factors that attribute to thrombosis formation.

Experiments for *in vitro* simulation of pathological environment for formation of VWF and its responses to different treatment was conducted using 8-channel device with a shear inducing region (60μm×1000μm×45μm, W×L×H) with a square post (30μm×30μm) in the middle of each flow chamber. Platelet-free plasma (PFP) prepared from EDTA or PPACK treated whole blood was flown through the chambers and ULVWF fibers were attached on the post upon pathological wall shear rate (> 10,000 s^{-1}). Anti-VWF was flowed for staining at a lower shear rate (3300 s^{-1}), followed by epifluorescence microscopy. Once sufficient staining is achieved, HBS with or without 30 mM NAC will be flown through the channels with the same shear rate (3300 s^{-1}), and the integrity of VWF strands will be observed under the microscope for 380 s. Through the course of the whole experiment, no visual disintegration of VWF strands was observed through eight fibers formed this way, and the normalized florescent intensity of the fiber (intensity over time/initial intensity) didn't change, as shown in Figure 4-1.

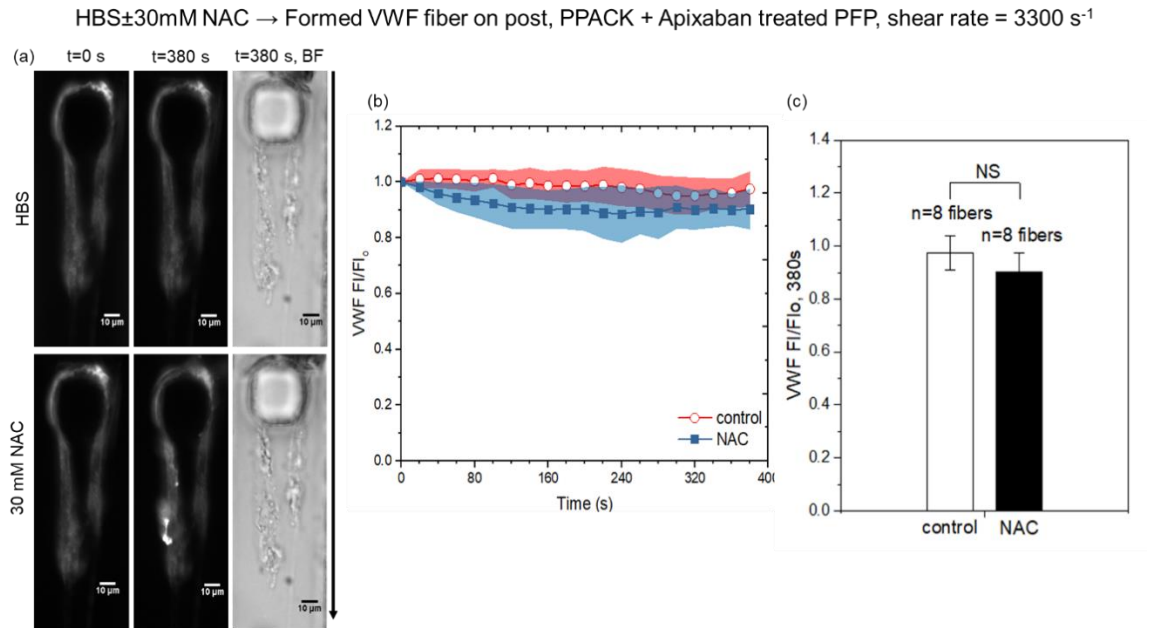

Figure 4-1: VWF fiber integrity upon treatment of NAC

Both visual observations and analysis of fluorescent integrity showed NAC doesn't digest VWF fiber at 30 mM

Experiments for *in vitro* simulation of arteriole thrombosis formation and the antithrombotic efficacy of NAC was conducted using 8-channel device with a shear inducing region (60 μm×2000 μm×70 μm, W×L×H) in the middle of each flow chamber. Experiment conducted to ensure that NAC had no effect on VWF coated on glass slide before adding VWF into activation strip (Supp. Fig. S4-1). Device was vacuum-mounted perpendicularly to collagen/VWF surfaces forming 8 parallel-spaced prothrombotic patches (60 μm×250μm). PPACK-treated blood was perfused across the 8 channels by withdrawal through a single outlet under pathological wall shear rate (5,100 s^{-1}). Similar perfusion-switch experiment was conducted that once a significant thrombosis is formed (100 s), whole blood with 30mM NAC was switched in some channels to observe the antithrombotic effect of NAC. Platelet and VWF were fluorescently tagged for epifluorescence microscopy. Images were captured with a charged coupled device camera and were analyzed with ImageJ software. As shown in Figure 4-2, upon treatment of NAC treated whole blood, thrombus plug significantly reduced size and both platelet and VWF signal showed decrease, yet the ratio of platelet/VWF signal showed increase for switched streams, meaning that VWF gets cleaned from the plug, but more platelets remained.

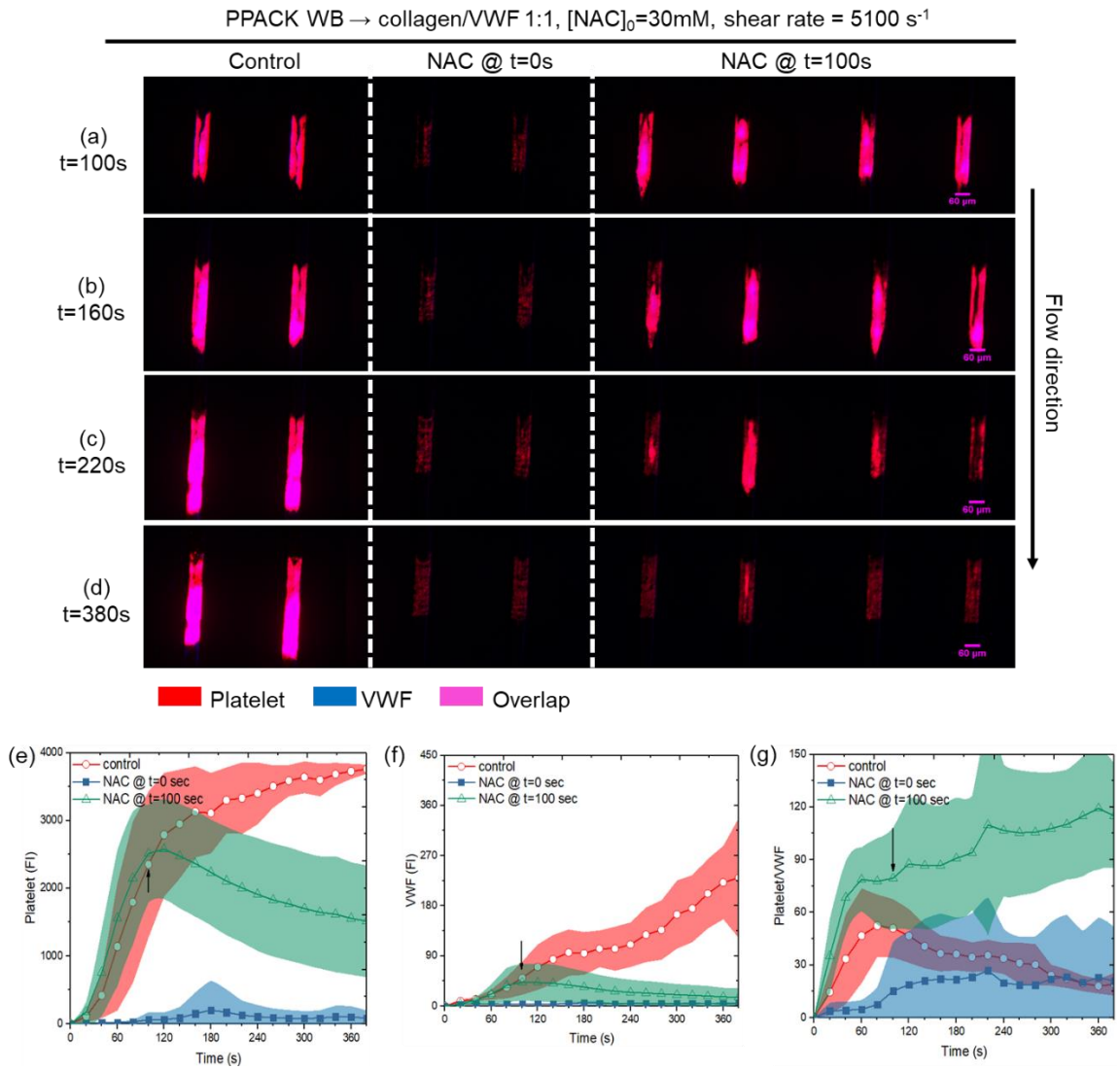

Figure 4-2: Anti-thrombus effect of NAC treated whole blood under pathological shear rate

NAC treated whole blood showed hindered primary platelet deposition on collagen/VWF activation strip, while built-up thrombus plug reduced in size and eventually disappeared upon switching to NAC treated whole blood (a, b, c, and d). Fluorescent signals for platelet (e) and VWF (f) showed decrease up on switching too (shown by arrow), but the ratio of platelet/VWF signal increased for switched streams (g), indicating that most thrombus left was platelet.

Although VWF is the dominating fiber for platelet attraction under arterial flow, it is still helpful to study if NAC facilitates platelet inhibition under venous flow or has any effect on fibrin formation. Thus, similar perfusion flow experiment was done with switch time at 90 seconds, and the result suggests that NAC inhibits platelet deposition and fibrin polymerization under venous

flow as well, as shown in Figure 4-3. This suggests that either NAC has the effect of directly preventing fibrin polymerization, or inhibiting thrombin formation through platelet inhibition, or both.

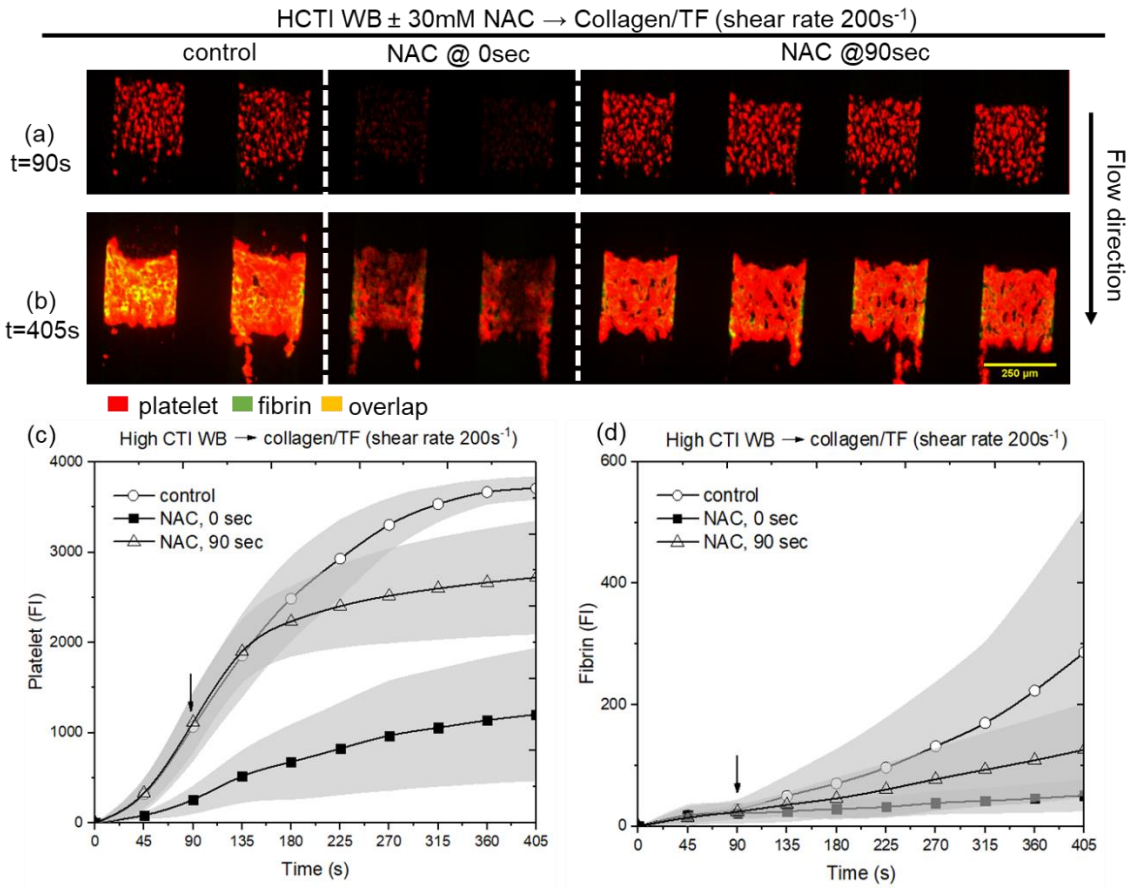

Figure 4-3: Perfusion-switch experiment with NAC inhibited platelets under venous shear rate

NAC treated whole blood showed moderate platelet inhibition, and platelets in switched stream stopped developing after 90 s (a, b, and c). Fibrin polymerization was inhibited as well for both NAC treated stream and switched stream (a, b, and d).

Calcium assay was used to testify if NAC treated platelets were inhibited effectively, and the results show that for most agonists, NAC had inhibitory effect on platelet, although there isn't much difference shown with Convulxin. Besides, since previous experiments showed that cystine had similar anti-thrombus effects (Supp. Fig. S4-2), similar calcium assay experiment was used for cystine as well (Figure 4-4). For most agonists, it showed similar trend as NAC, but for U46619 it showed a higher calcium level than control. Convulxin, as expected, showed no differences from control.

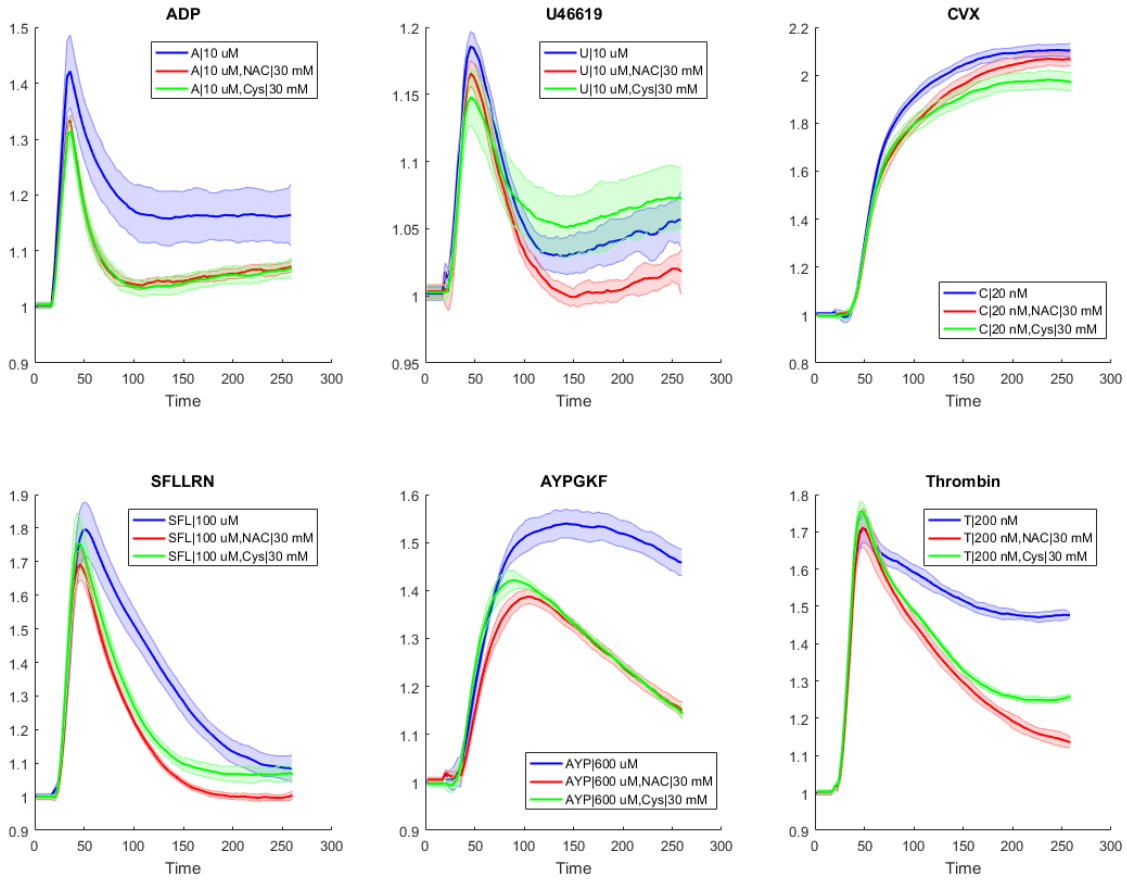

Figure 4-4: Calcium assay data for NAC and cystine

For agonists ADP, SFLLRN, AYPGKF and thrombin, both NAC and cystine showed decrease in calcium level compared to control, while for convulxin there is no clear difference, and cystine showed higher level of calcium compared to control.

Based on our observation, NAC does have the potential to be an anti-thrombus drug to alleviate arterial thrombus blockage. However, whether it will react with other common anti-thrombus drugs, such as tPA, remains a question. Thus, experiment was done on whole blood treated with either tPA, NAC, or both, to see their response on the activation surface. Since tPA is used for fibrin digestion, which is targeting venous thrombus formation, both pathological arterial shear rate (5,100 s^{-1}) (Supp. Fig. S4-3) and venous shear rate (200 s^{-1}) (Supp. Fig. S4-4) was studied. Both experiments showed that NAC and tPA doesn't offset each other's anti-thrombus effect, showing the potential of NAC to be subscribed at the same time for patients. Future works

could be done on understanding the mechanisms of NAC on platelet and VWF to evaluate the potential of this molecule under a clinical setting.

4.2 Anti-GPVI fab as a GPVI-inhibitor under arterial shear and its role for thrombus development

Based on the previous experiments, the inhibitory effects of anti-GPVI fab on platelet deposition and thrombin generation was testified under venous shear rate. However, since GPVI is the first responder for collagen contact, such experiments should be done under arterial shear rate as well. In Chapter 3, experiments were done under arterial conditions (1,000 s-1 shear rate) with collagen strip as the activating surface, where no thrombin nor fibrin were present in the system; the results were shown in Supp. Fig. S3-9.

Given GPVI's dominant role in arterial shear region, additional experiment will be helpful using the same shear rate with collagen/VWF activation strip, to better reveal the function of GPVI with the effect of VWF, and the role of VWF in arterial clot growth. Furthermore, similar experiments could be done with a collagen/TF activation strip, so that the role of thrombin under arterial shear rate could be revealed as well.

Chapter 3 also mentioned the differences between primary and secondary platelet deposition and how it was modulated by GPVI. To better distinguish the stages of clot growth contributed by these two dispositions, whole blood used for these two stages could be labeled with different fluorescent signal, facilitated by confocal imaging. The distinguish layers of platelet could quantify the critical roles of different platelets at stages for clot development under both venous and arterial shear rate.

APPENDIX – SUPPLEMENTAL FIGURES

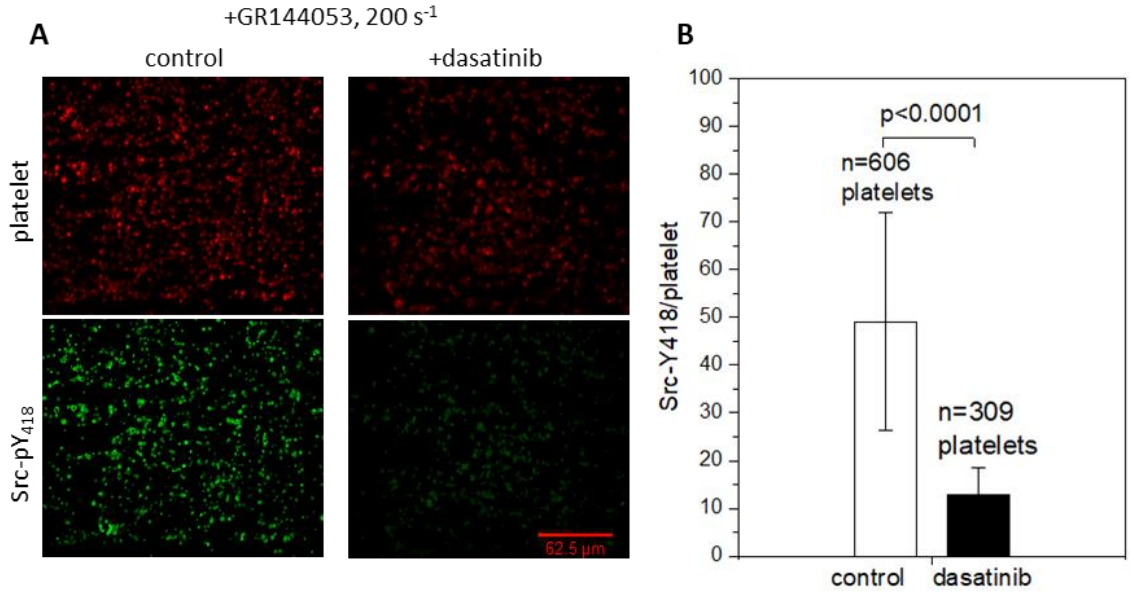

Supplemental Figure S2-1: Post-stain images of clot monolayers for PPACK blood flow over collagen at venous shear rate (200 s^{-1}) at 6.75 minutes.

Images were taken under 40× for both conditions without and with dasatinib for platelet and Src-pY418 (A). Bar chart of Src-pY418 intensity for both conditions was plotted for a better comparison (B).

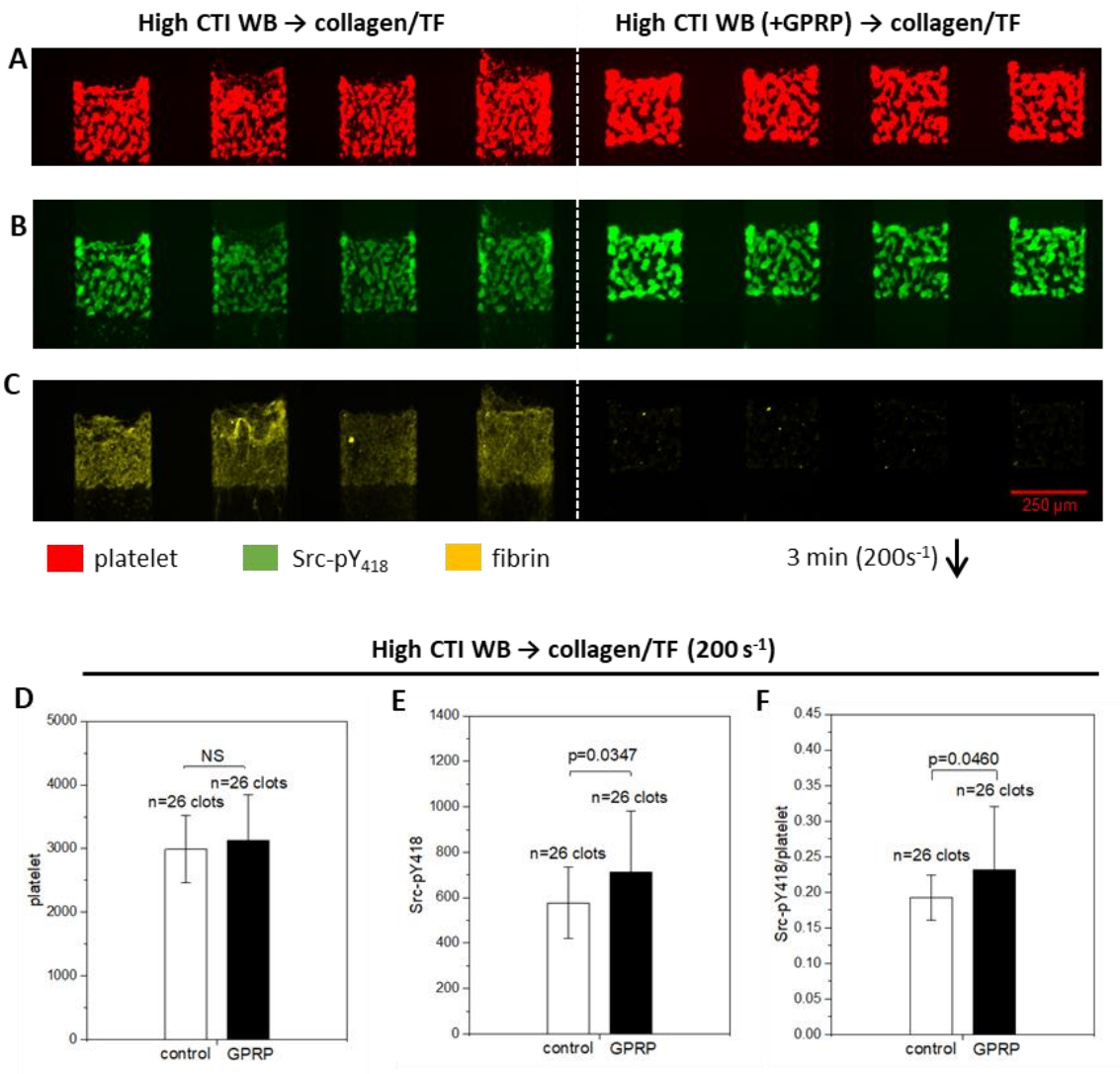

Supplemental Figure S2-2: Post-stain images of clots for high CTI blood with/without GPRP flown over collagen incubated with TF at venous shear rate (200 s^{-1}) at 3 minutes.

Images were taken for platelet (A), Src-pY418 (B) and fibrin (C) for both conditions under 10×; the left four channels are for high CTI blood, and the right four channels are for high CTI blood with GPRP. The platelet (D) and Src-pY18 (E) intensities were measured for both conditions, and the ratio of the two was calculated (F). Thicker clots obtained at 6 min endpoint were more occlusive of the channel and more difficult to rinse and to prepare for fluorescence staining, therefore an endpoint of 3 min was used for post-staining experiments.

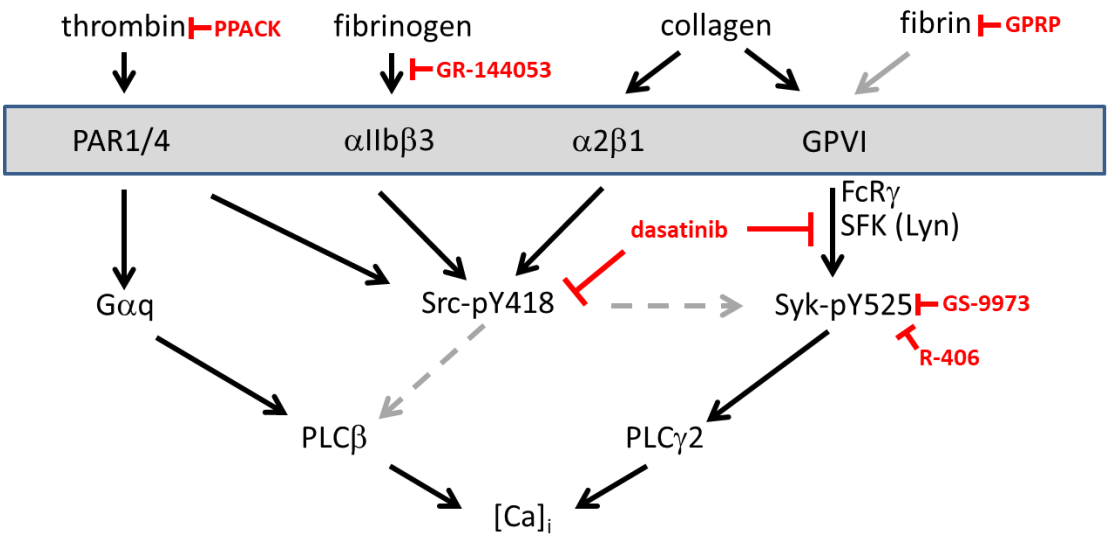

Supplemental Figure S2-3: Summary figure of Syk/Src activation cascade, with inhibitors at different sites.

We can see more interactions between proteins and kinases at downstream that lead to platelet activation in different ways.

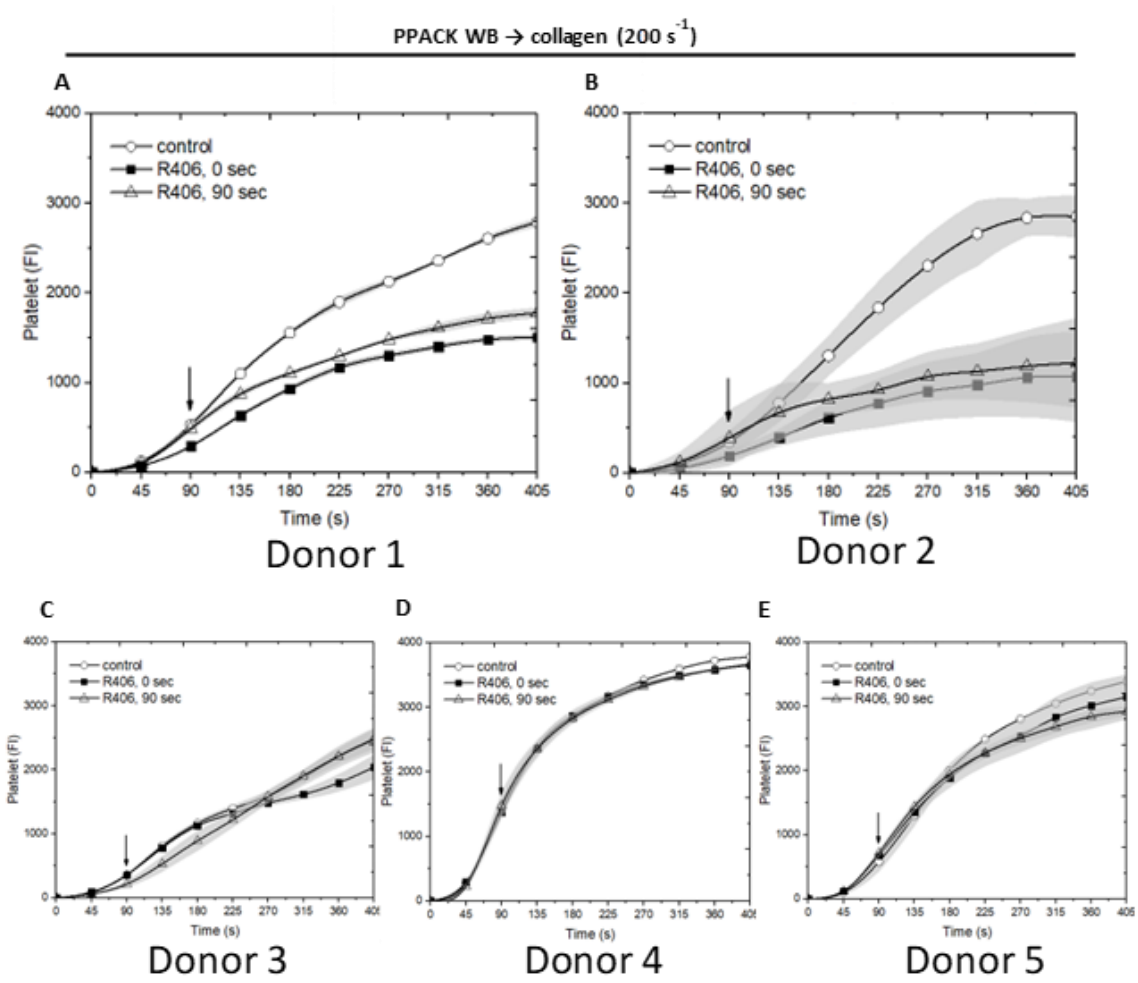

Supplemental Figure S2-4: Donor responses to R-406 for PPACK treated whole blood perfused under venous shear rate.

We can see inhibition effect of R-406 is very strongly donor dependent. More cases showed no inhibition in our assay.

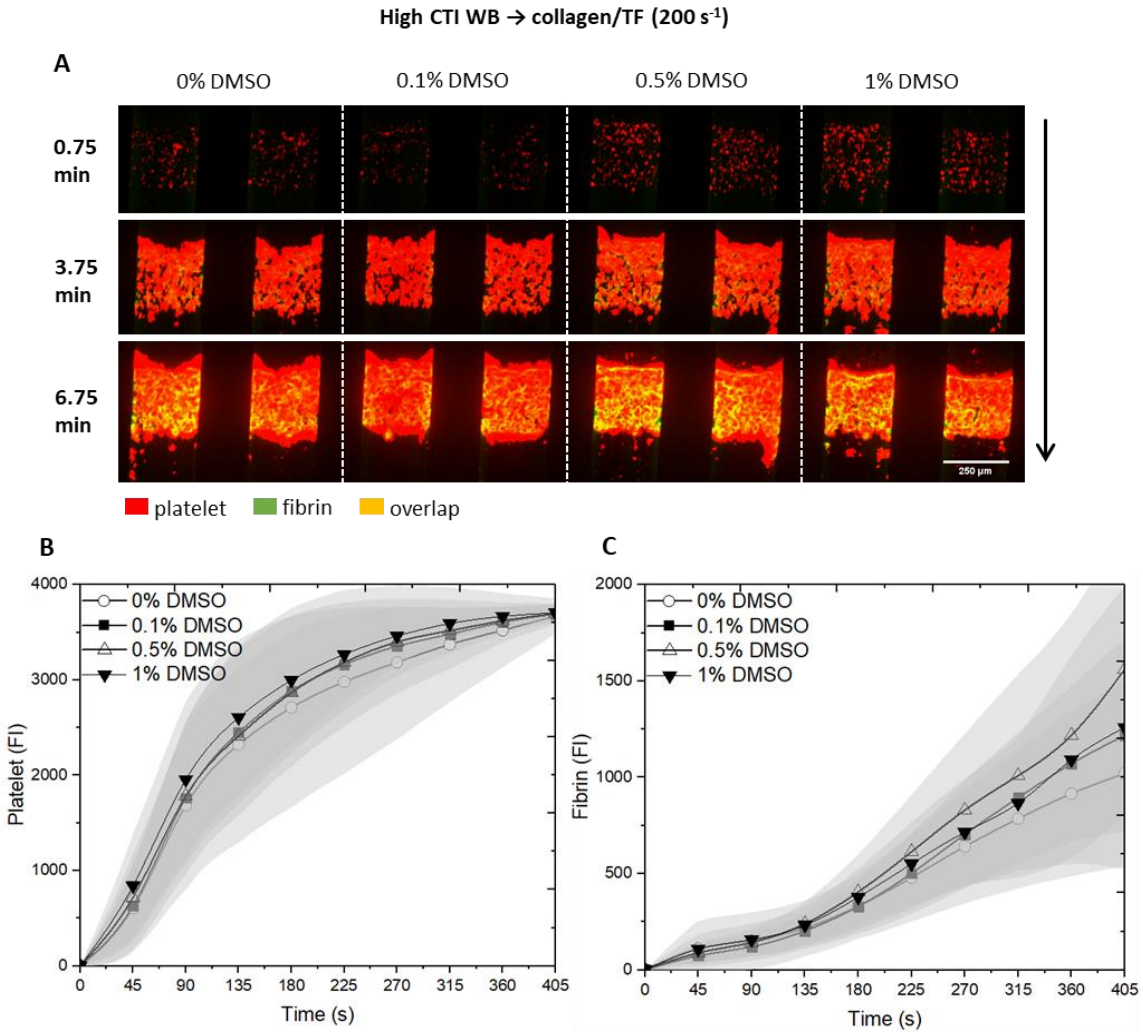

Supplemental Figure S2-5: The dose response of DMSO at different concentrations in WB under 1% v/v.

No difference was shown for either platelet or fibrin signal.

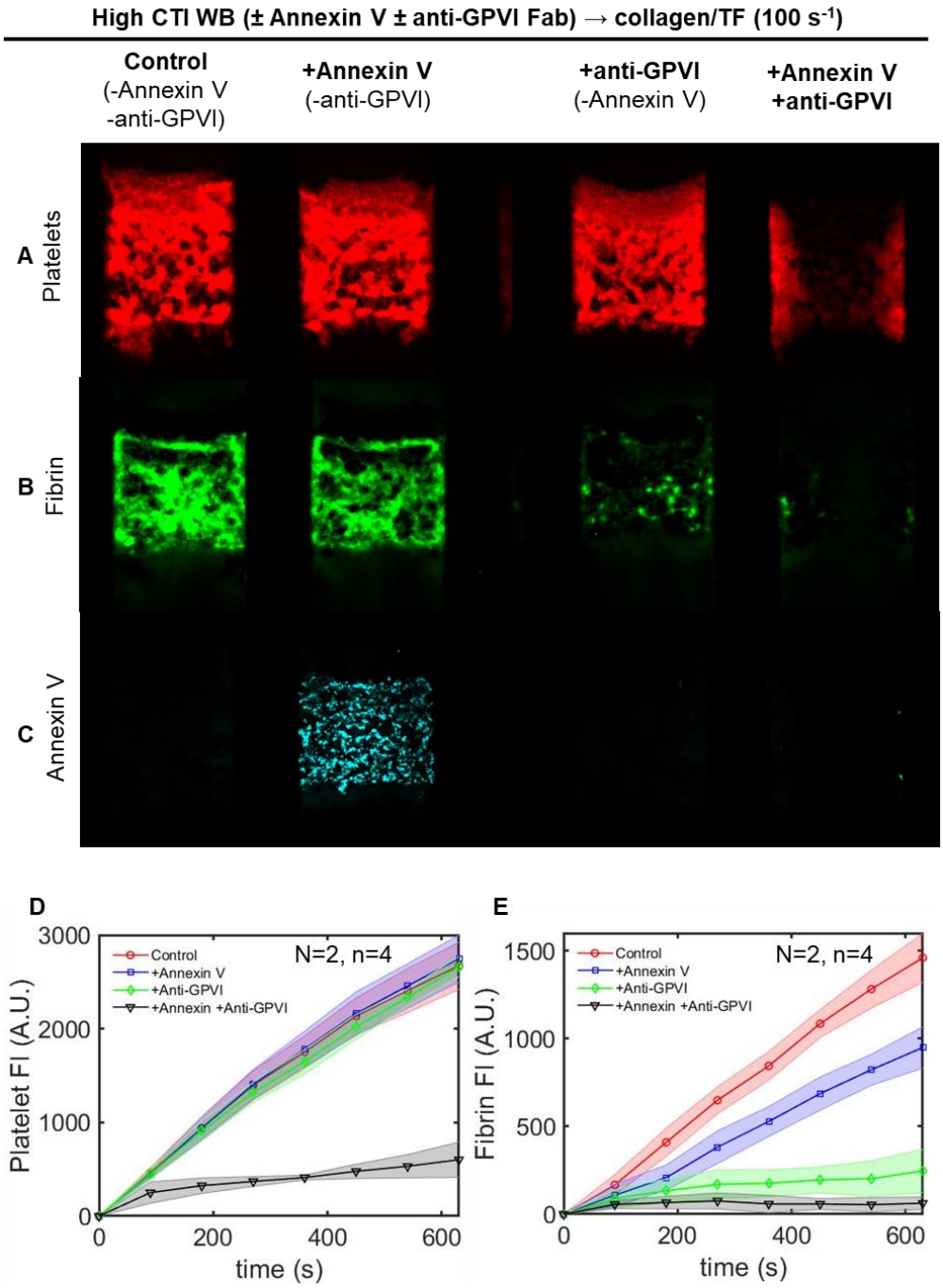

Supplemental Figure S3-1: Annexin V and anti-GPVI Fab have additive effect on limiting platelet deposition (at 100 s^{-1} in 120-µm device).

High CTI WB, with and without Annexin V and anti-GPVI, was perfused over collagen/TF at 100 s^{-1} in the 120-µm channel height device, with CD61, fluorescent fibrinogen, and Annexin V fluorophores added for platelets (A), fibrin (B), and Annexin V (C). Annexin V was not added in channels with (-Annexin V). Representative images were taken at the end of the experiment (10.5 min). Fluorophores were measured throughout the course of the experiment for platelet fluorescence (D) and fibrin fluorescence (E). These data were taken under the same conditions as in Figure 6, except for the flow rate and channel height. Representative data are from 2 individual donors (N = 2) and 4 individual clots (n = 4). (A.U. = arbitrary units).

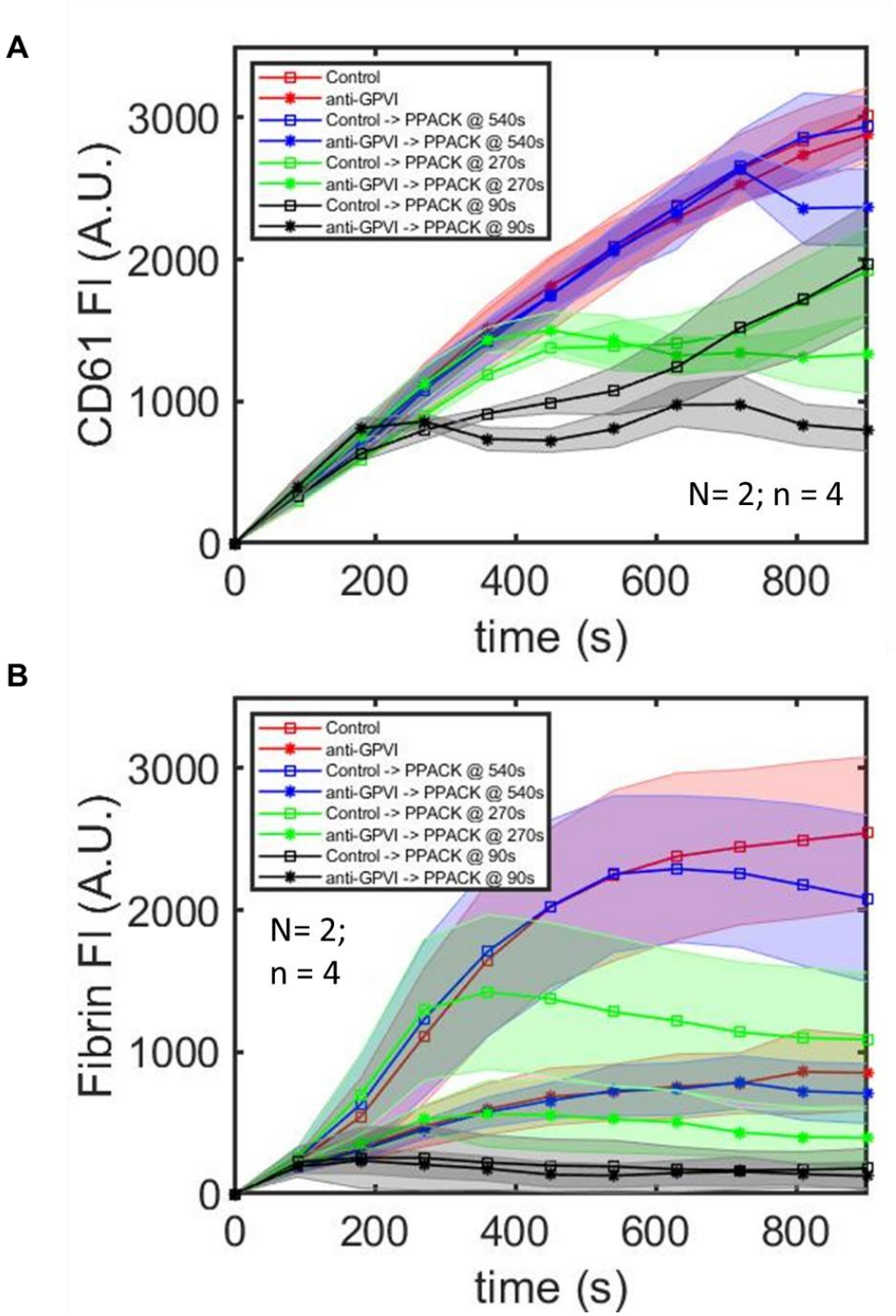

Supplemental Figure S3-2: Quantitative fluorescence data from Figure 3-11.

High CTI WB with or without anti-GPVI Fab, with a switch to PPACK WB with or without anti-GPVI, was perfused over collagen/TF at 100 s^{-1} for 15 minutes using a microfluidic device with a 120-μm height. Fluorescence intensities for platelets (A) and fibrin (B) were measured throughout the course of the experiments. (A.U. = arbitrary units)

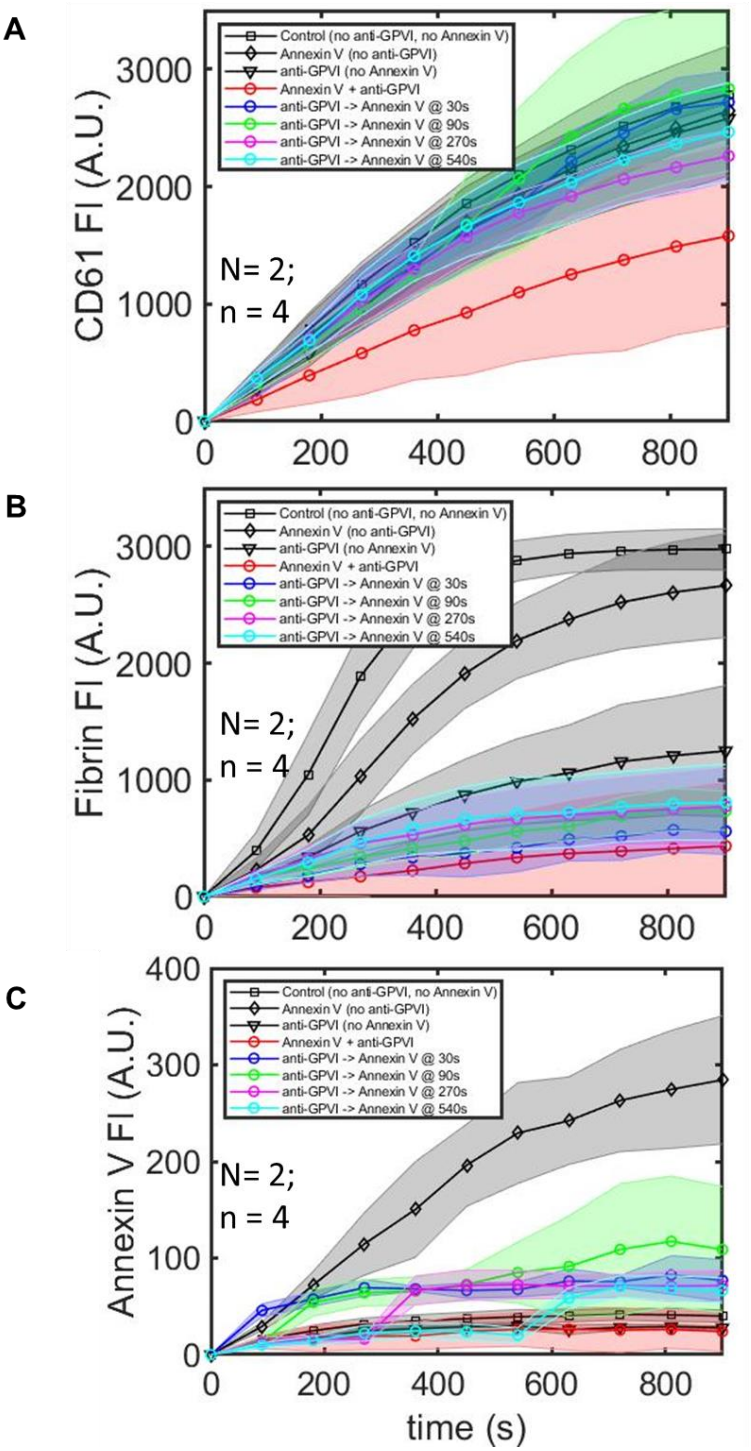

Supplemental Figure S3-3: Quantitative fluorescence data from Figure 3-12.

High CTI WB with anti-GPVI (-anx V), with a switch to anti-GPVI +anx V was perfused over collagen/TF at 100 s^{-1} for 15 minutes using a microfluidic device with a 120-µm height. Fluorescence intensities for platelets (A), fibrin (B), and annexin V (C) were measured throughout the course of the experiments.

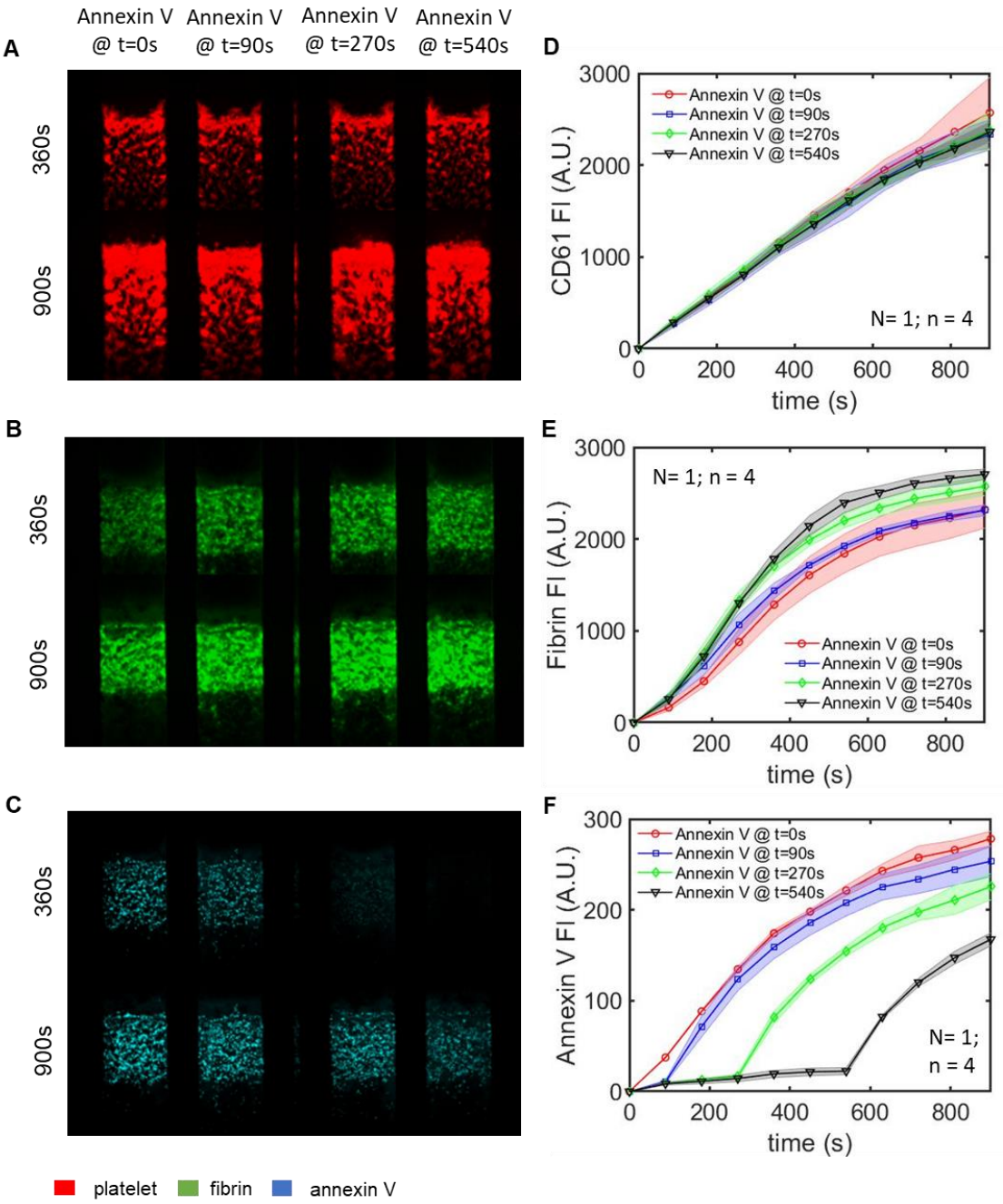

Supplemental Figure S3-4: Annexin V has a slight inhibitory effect on fibrin polymerization when added at different times.

High CTI WB with or without a switch to annexin V at either 90s, 270s, or 540s was perfused over collagen/TF at 100 s^{-1} for 15 minutes using a microfluidic device with a 120-μm height. CD61, fluorescence fibrinogen, and annexin V fluorophores were added to label platelets (A), fibrin (B), and PS exposure (C), respectively, with images taken at 360s and 900s. Fluorescence intensities for platelets (D), fibrin (E), and Annexin V (F) were measured throughout the course of the experiments. (A.U. = arbitrary units)

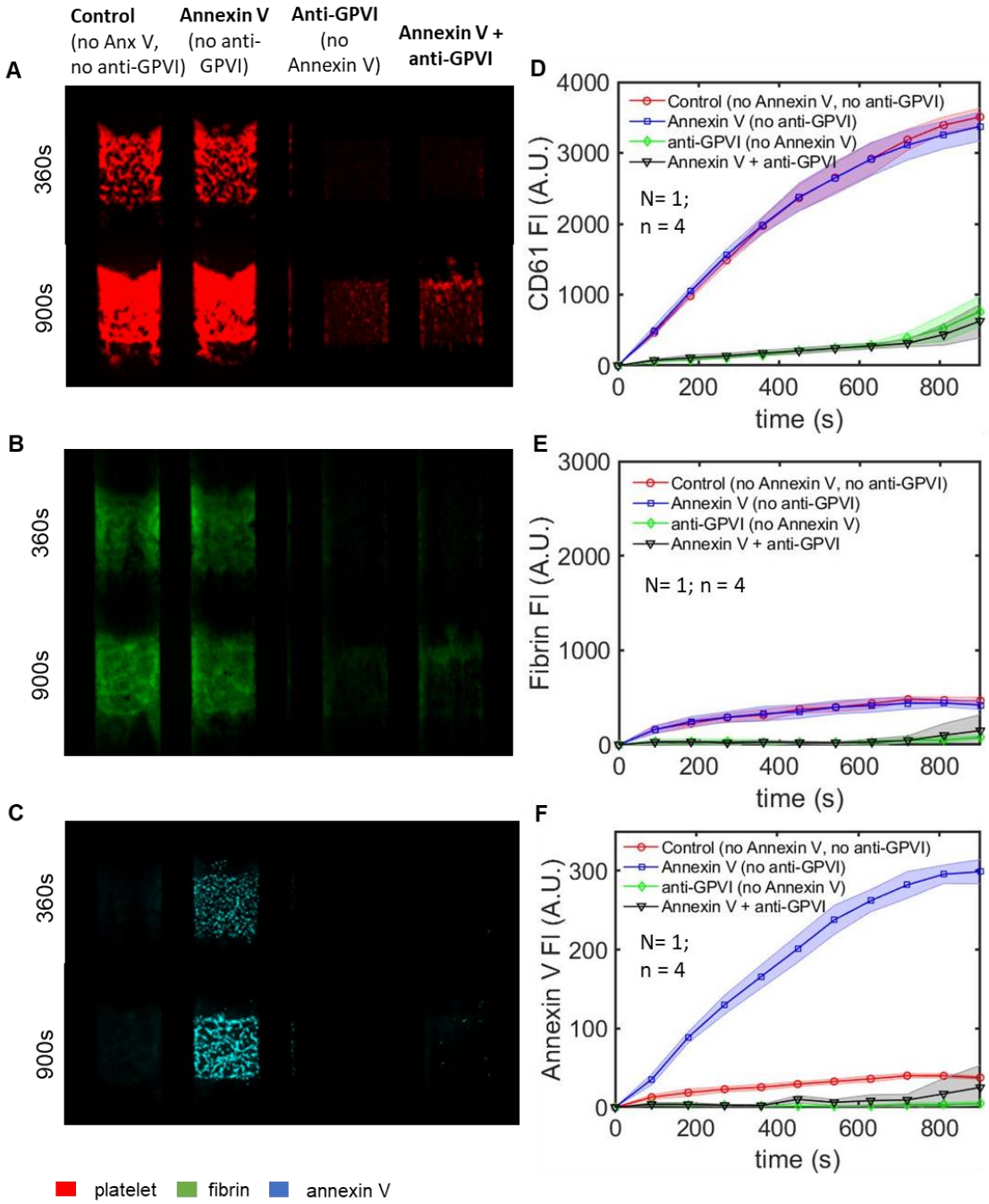

Supplemental Figure S3-5: Thrombin inhibition blocks platelet deposition when anti-GPVI is present, regardless of annexin V presence or absence.

PPACK-treated WB with or without anti-GPVI Fab and with or without annexin V was perfused over collagen at 100 s^{-1} for 15 minutes using a microfluidic device with a 120-μm height. CD61, fluorescence fibrinogen, and annexin V fluorophores were added to label platelets (A), fibrin (B), and PS exposure (C), respectively, with images taken at 360s and 900s. Fluorescence intensities for platelets (D), fibrin (E), and Annexin V (F) were measured throughout the course of the experiments. (A.U. = arbitrary units)

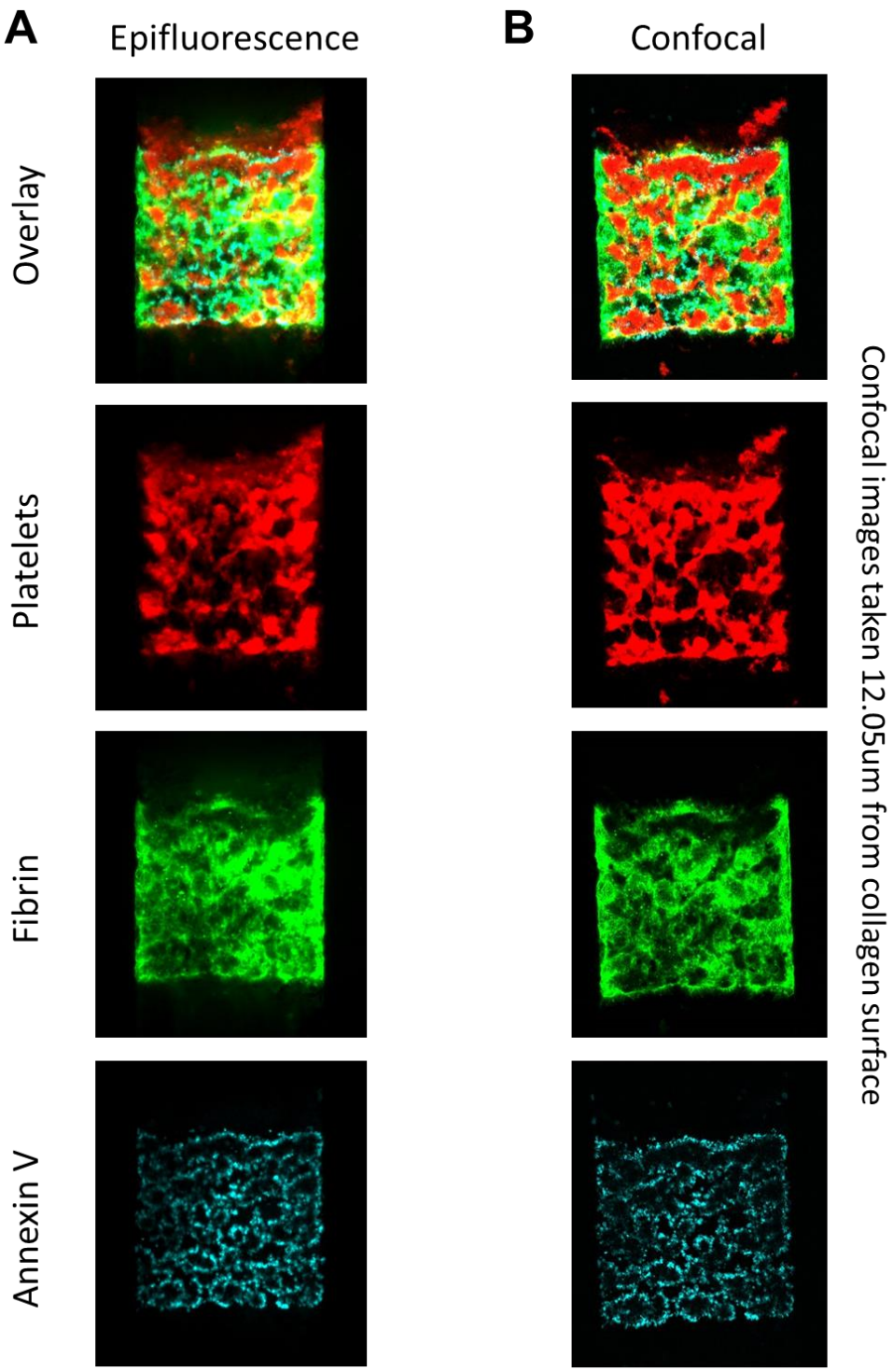

Supplemental Figure S3-6: Comparison of Epifluorescence and Confocal Images.

High CTI WB was perfused over collagen/TF for 7.5 min, with images taken using the epifluorescence microscope at 7.5 min (A). Then clots were fixed, as described in Methods, and taken to image using the confocal microscope (B). Representative confocal images are from 12.05 μm above the collagen surface. Images include individual fluorophores for platelets, fibrin, and Annexin V, as well as an overlay of all three.

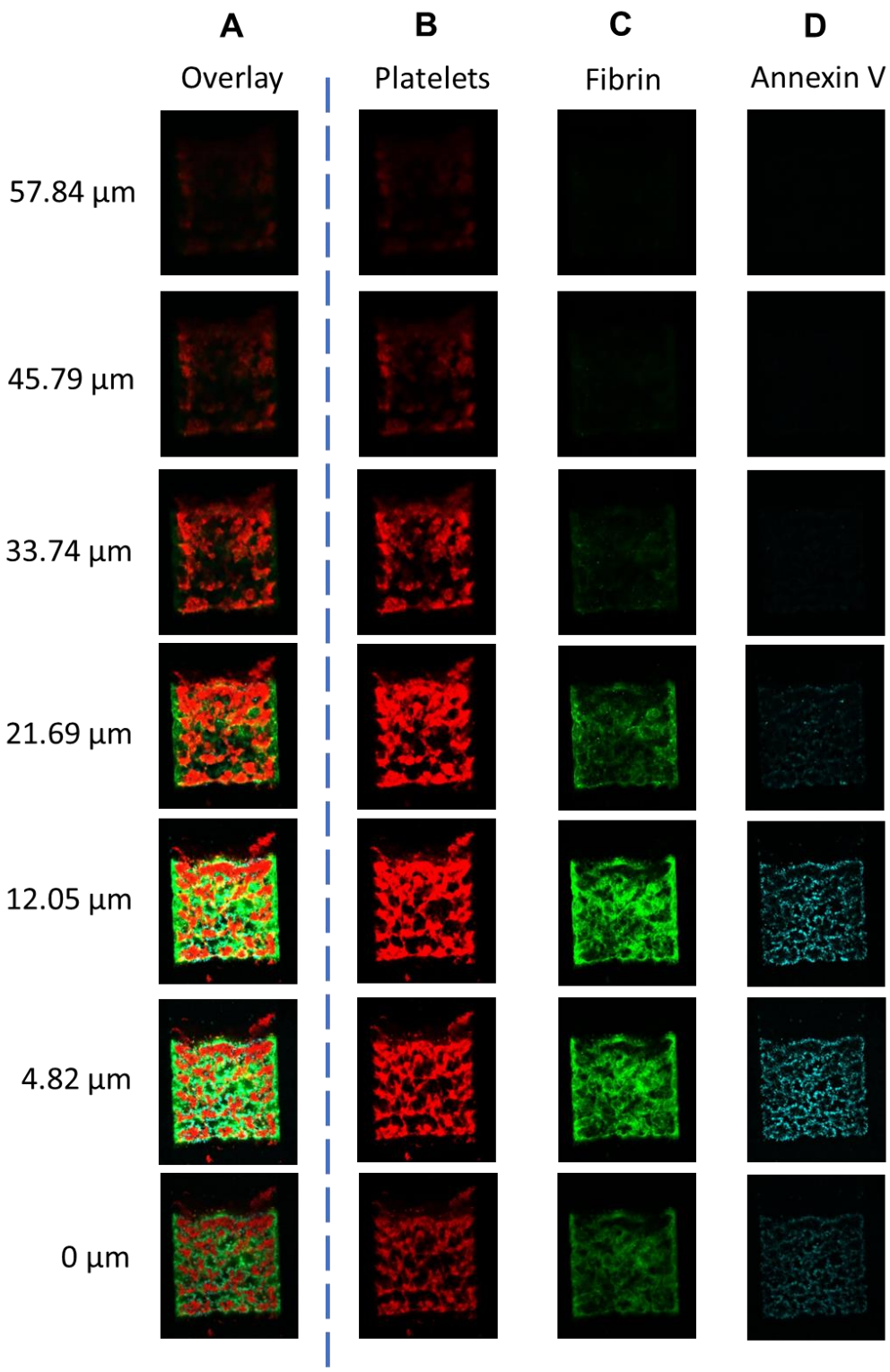

Supplemental Figure S3-7: Confocal images at different heights in the z-direction.

Images from the same clot in Supp. Fig. S3-2 were taken at different heights in the z-direction, starting at the glass surface (0 µm) up to 57.84 µm above the glass surface. Images for overlay (A), platelets (B), fibrin (C), and Annexin V (D) are included.

A

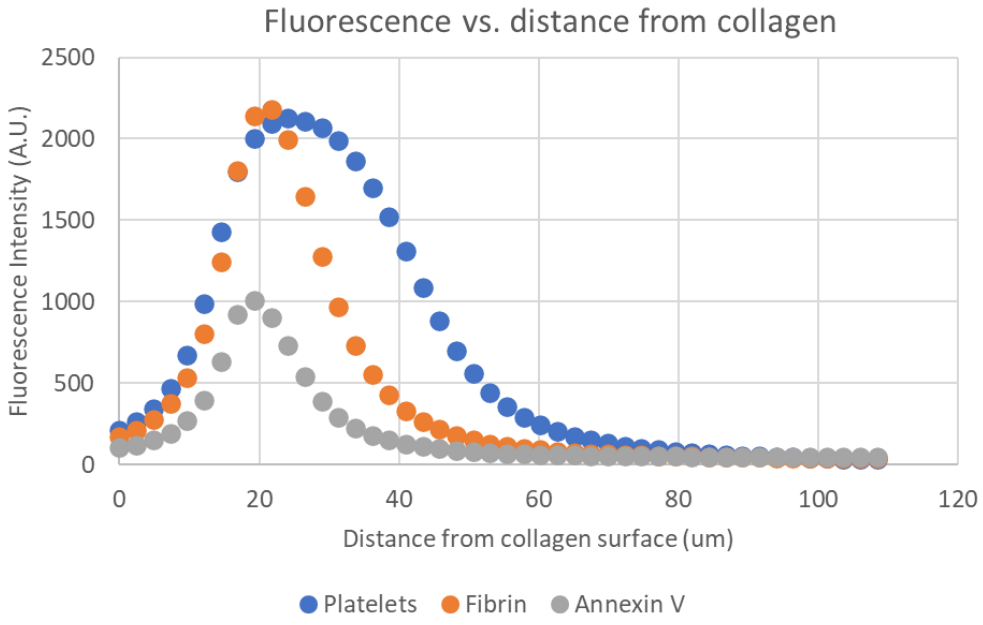

B

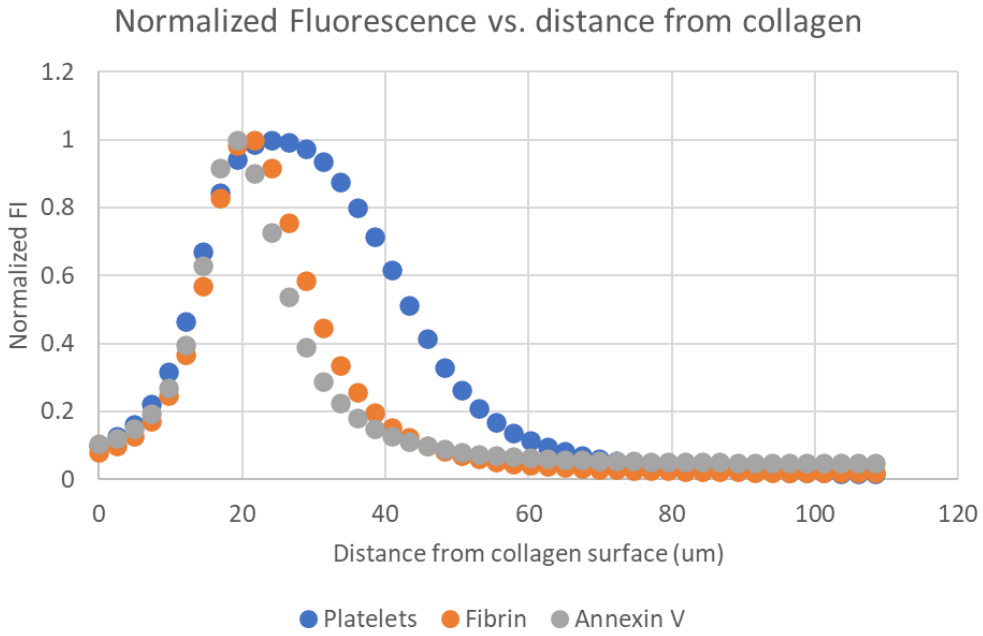

Supplemental Figure S3-8: Quantitative analysis of confocal images at different heights in the z-direction.

Images from the same clot in Supp. Fig. 3 were quantitatively analyzed for the fluorescence intensity for platelets (blue), fibrin (orange), and Annexin V (grey) at different heights in the z-direction (A). Fluorescence values in each data set in (A) were divided by the respective maximum value in each individual data set to yield a normalized fluorescence intensity among the different fluorophore labels (B). (A.U.= arbitrary units)

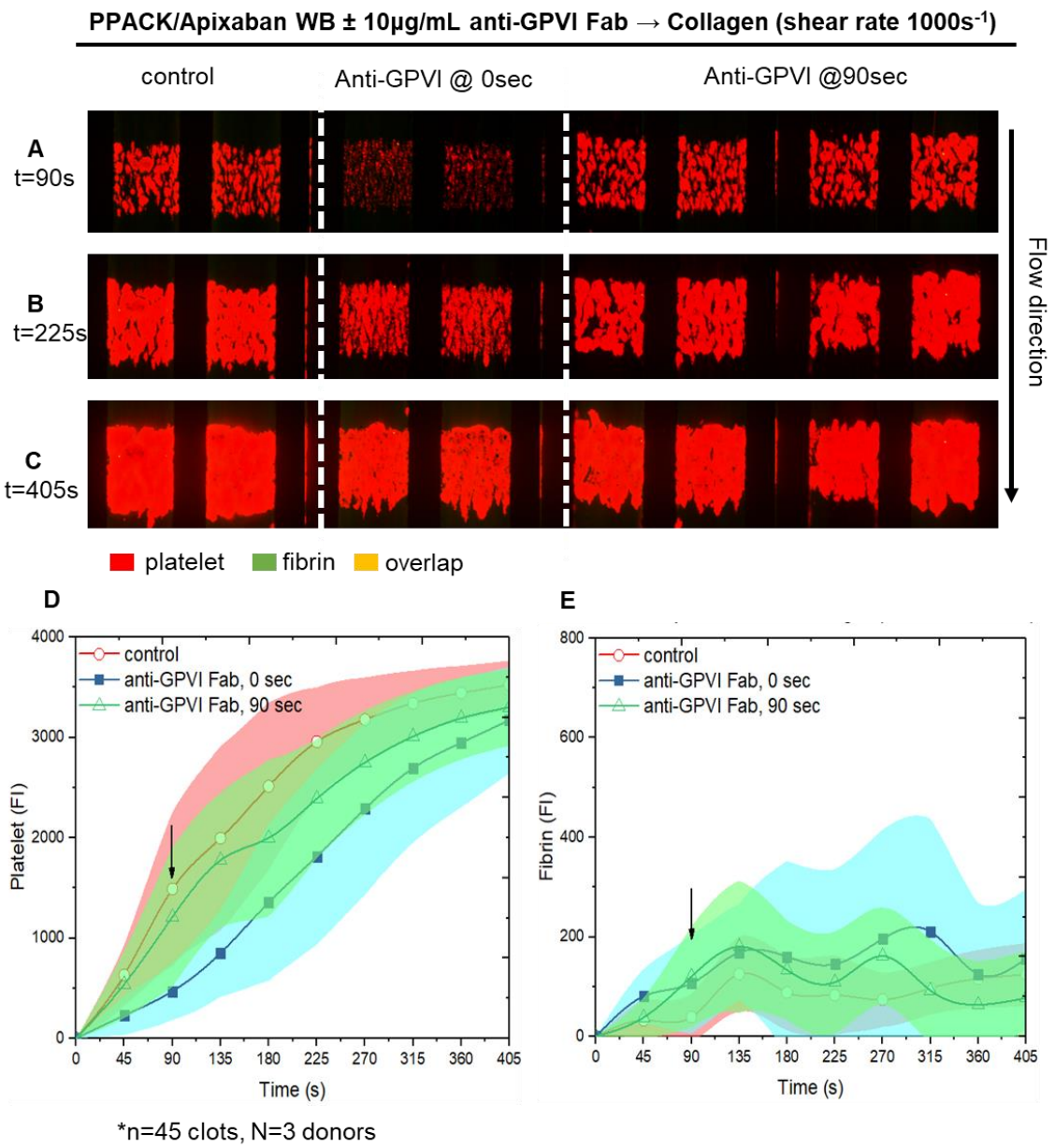

Supplemental Figure S3-9: Inhibition of GPVI via E12 at arterial shear rates does not decrease, but delays, platelet deposition when neither thrombin nor fibrin are present.

PPACK/Apixaban WB with and without anti-GPVI Fab was perfused over collagen at 1000 s^{-1} for 7 minutes. In the right 4 channels, control WB was perfused for 90 seconds, with a perfusion switch to anti-GPVI WB at 90s. CD61 and fluorescence fibrinogen fluorophores were added to label platelets and fibrin, respectively, with overlay images taken at 90s (A), 225s (B), and 405s (C). Fluorescence intensities for platelets (D) and fibrin (E) were measured throughout the course of the experiments.

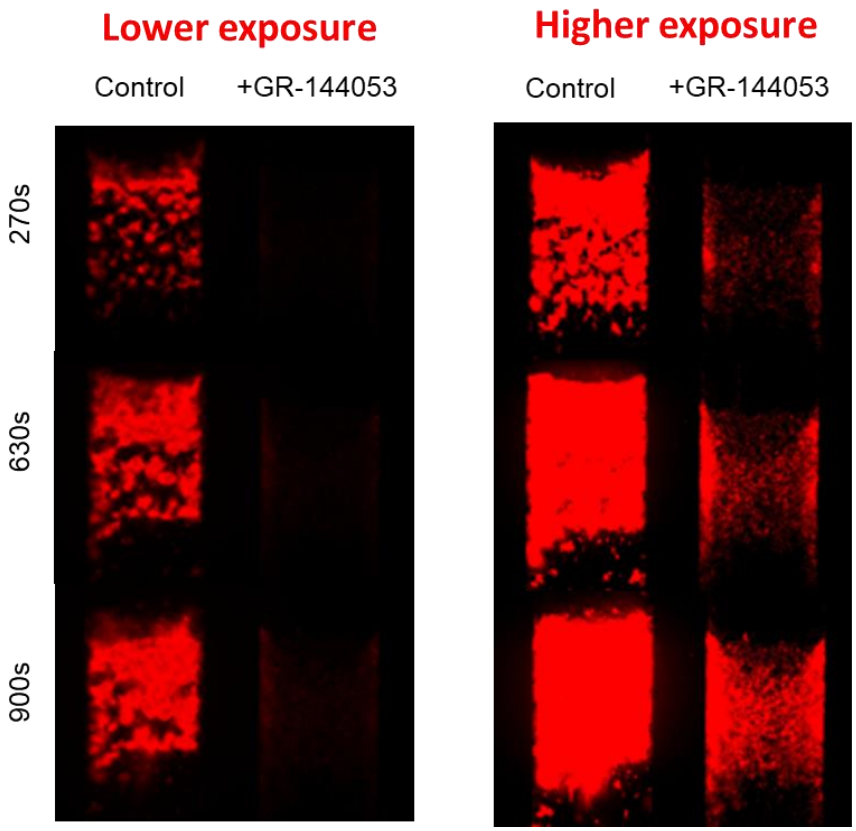

Supplemental Figure S3-10: Platelet monolayer forms in the presence of GR-144053.

High CTI WB with or without GR-144053 was perfused over collagen/TF at 100 s^{-1} for 15 minutes using a microfluidic device with a 120-µm height. GR-144053 results in a monolayer of platelets forming on collagen, but this is difficult to see at normal exposure. Here, we increased exposure of images on the left (typical exposure) to the resulting images on the right (i.e. images on the left and right are of the same clots). The resulting images on the right better illustrate the presence of platelets on collagen in the presence of GR-144053.

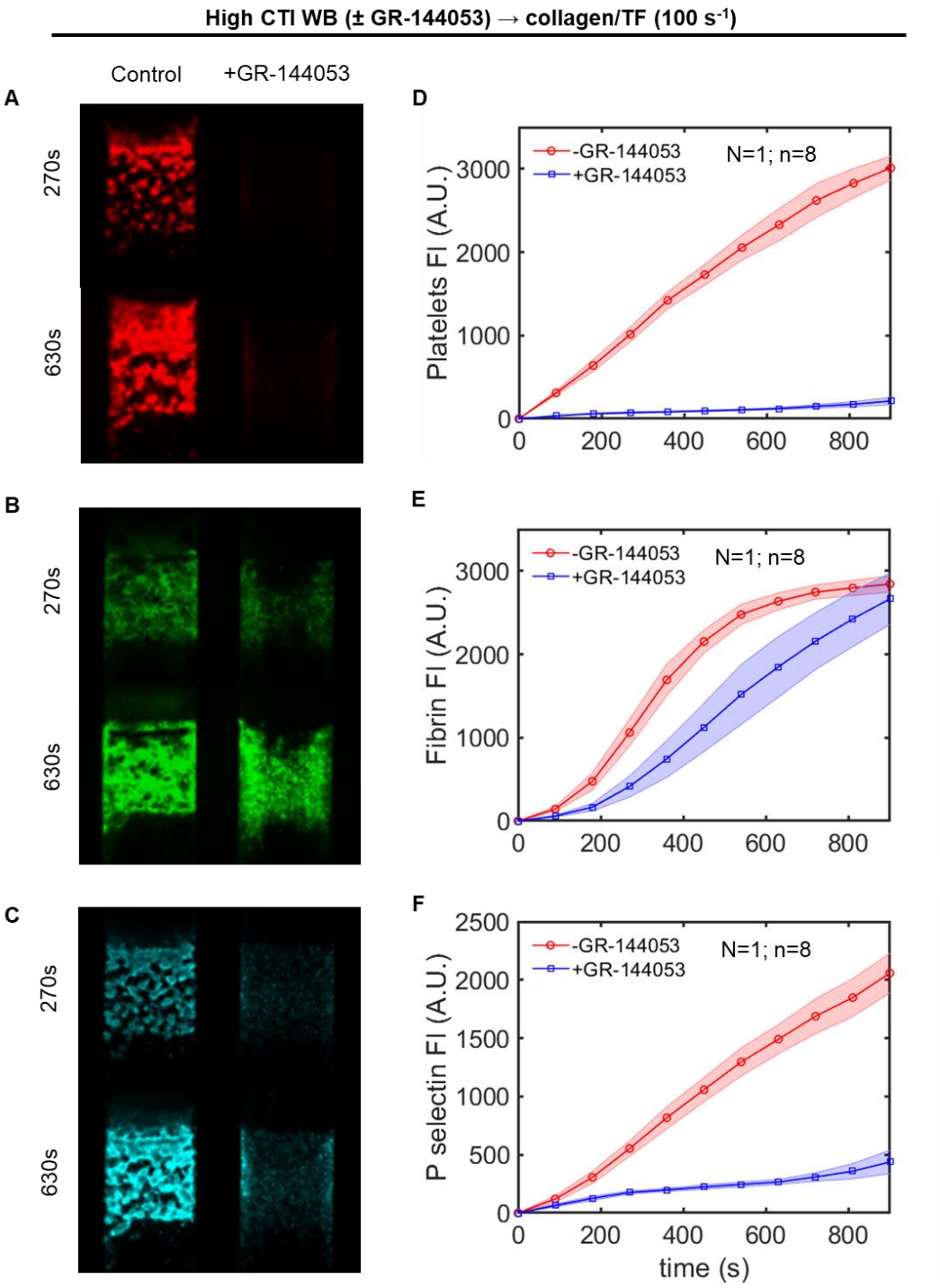

Supplemental Figure S3-11: P-selectin staining of platelets treated with GR-144053.

High CTI WB with or without GR-144053 was perfused over collagen/TF at 100 s^{-1} for 15 minutes using a microfluidic device with a 120-µm height. CD61, fluorescence fibrinogen, and P-selectin fluorophores were added to label platelets (A), fibrin (B), and alpha-granule release (C), respectively, with images taken at 270s and 630s. Fluorescence intensities for platelets (D), fibrin (E), and P-selectin (F) were measured throughout the course of the experiments. (A.U. = arbitrary units)

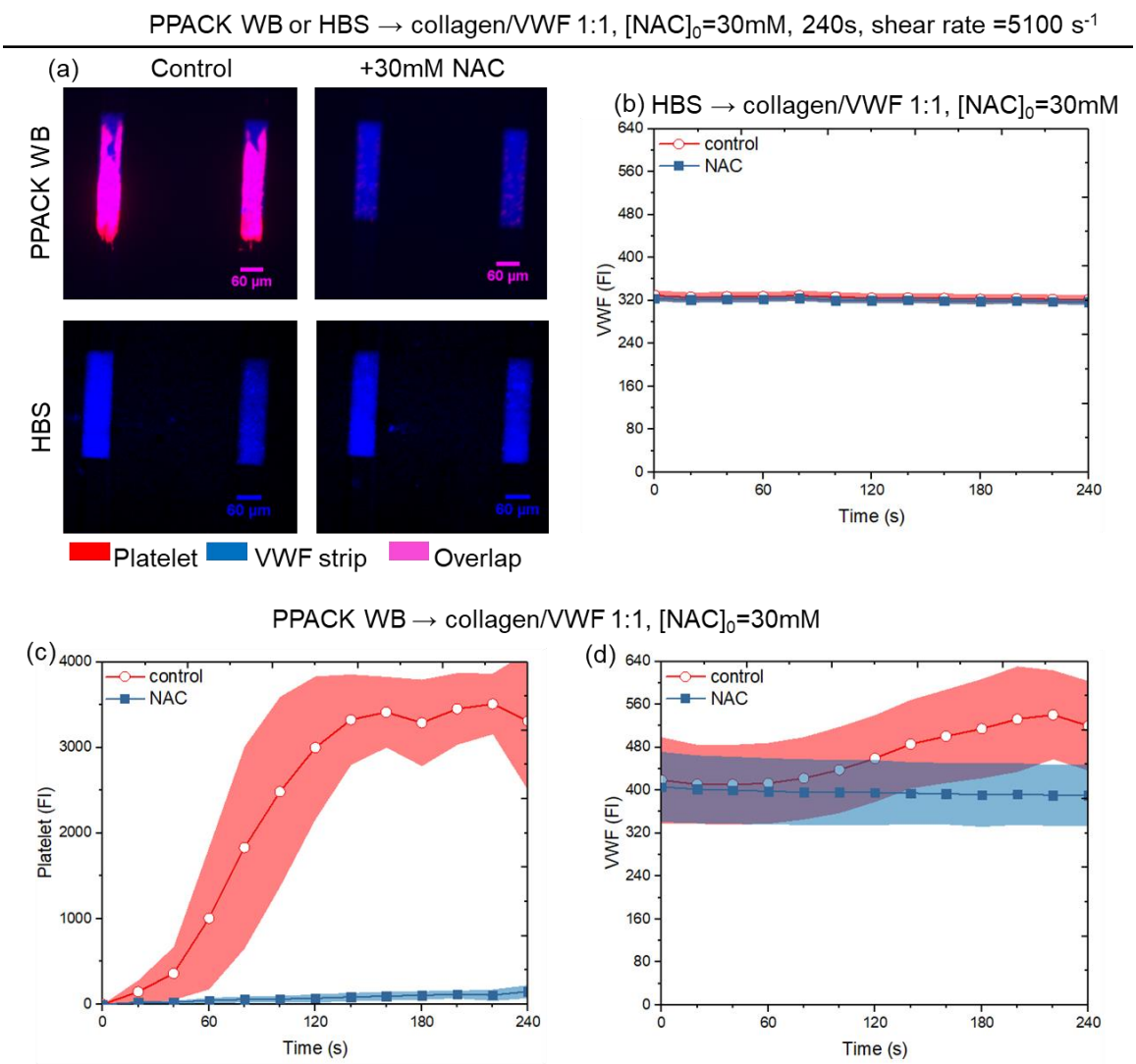

Supplemental Figure S4-1: NAC had no effect on VWF coated on glass slide before adding VWF into activation strip.

PPACK treated whole blood and HBS with and without NAC was flown over pre-stained VWF activation strip at 5100 s^{-1} for 240s and no reduction of VWF signal was observed on both images (a) and quantified fluorescent intensity graphs (b, c and d). Control whole blood showed an expected increase in platelet (c) and VWF (d).

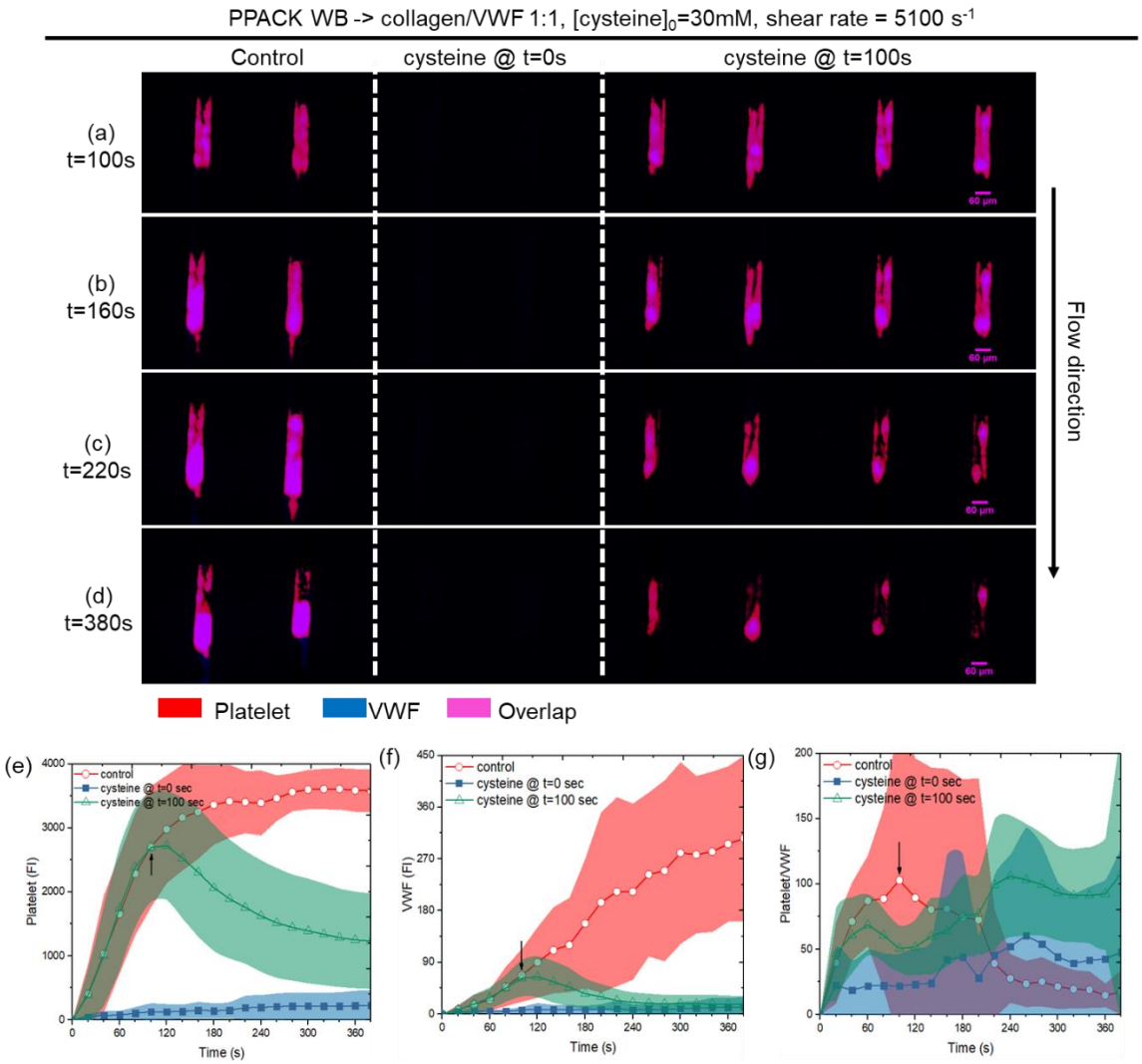

Supplemental Figure S4-2: Anti-thrombus effect of cysteine treated whole blood under pathological shear rate shows similar results of NAC

Cysteine treated whole blood showed similar hindered primary platelet deposition on collagen/VWF activation strip, as well as anti-thrombus effects (a, b, c, and d). Fluorescent signals for platelet (e) and VWF (f) showed decrease up on switching too (shown by arrow), but the ratio of platelet/VWF signal is hard to visualize (g), indicating that free thiol in both cysteine and NAC might have similar function but still has some differences.

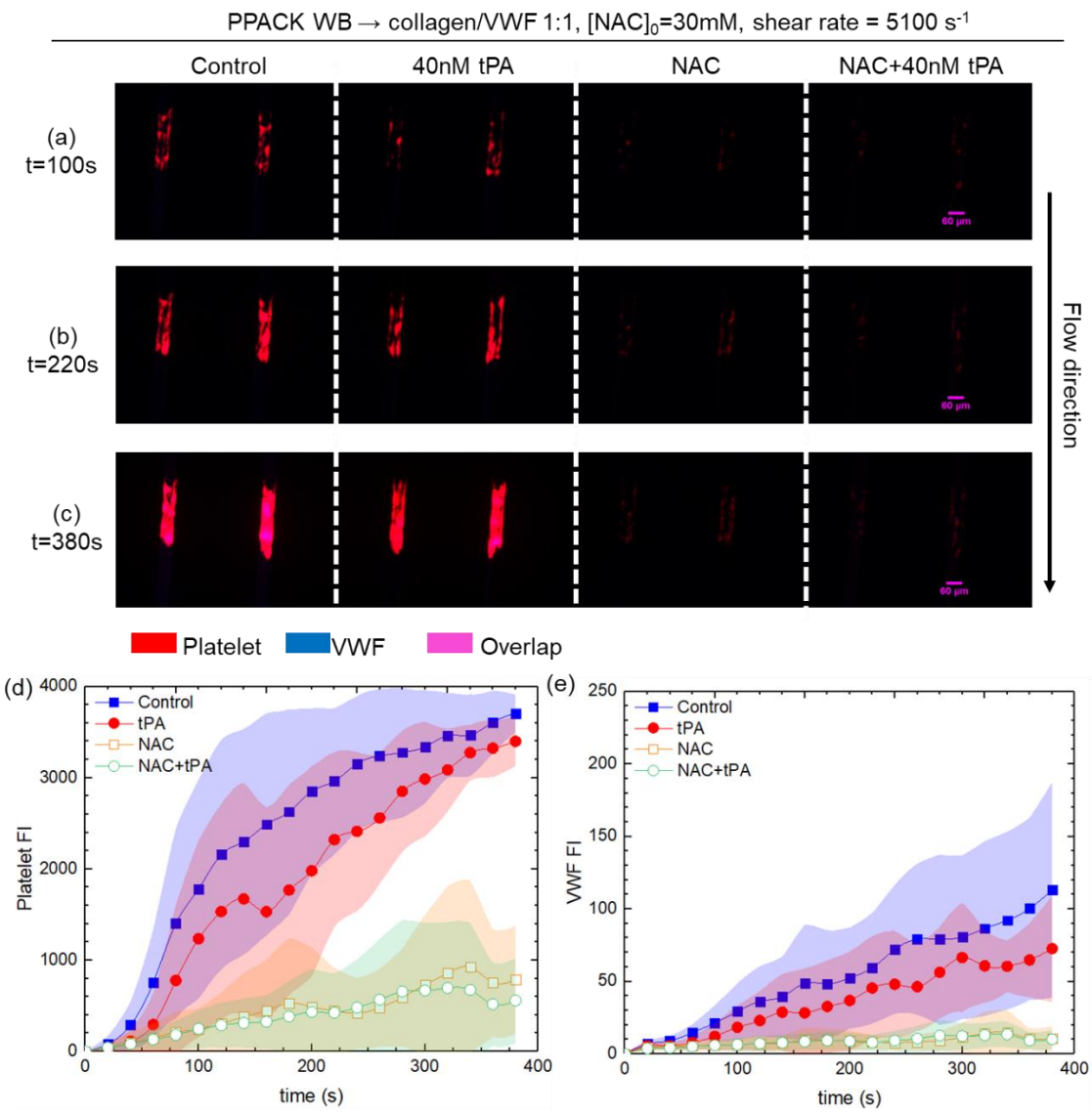

Supplemental Figure S4-3: NAC does not interact with tPA under arterial shear rate

PPACK treated whole blood with NAC, tPA, or both, were flowed under pathological shear rate (5100 s^{-1}) to see if coexistence of tPA and NAC would impede the anti-thrombus effect of NAC. Both images (a, b and c) and fluorescent signals for platelet (d) and VWF (e) showed NAC has a strong anti-thrombus effect with or without tPA, meaning that they could be used together clinically.

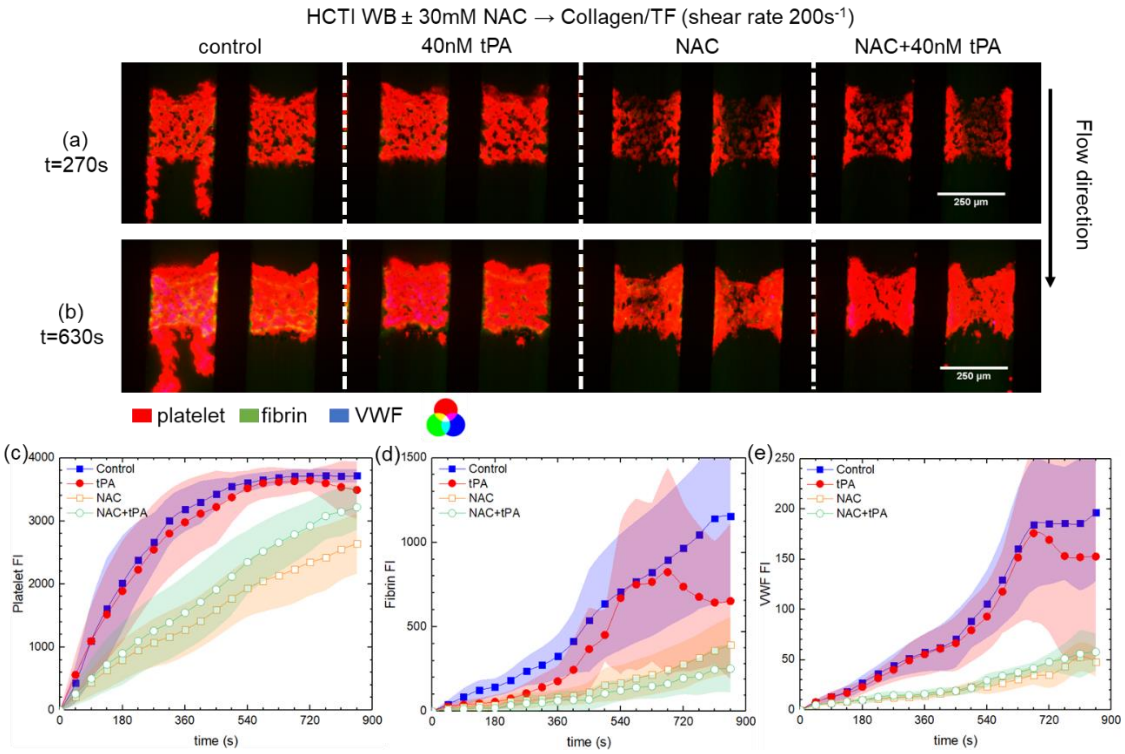

Supplemental Figure S4-4: NAC does not interact with tPA under arterial shear rate

PPACK treated whole blood with NAC, tPA, or both, were flowed under venous shear rate (5100 s^{-1}) to see if coexistence of tPA and NAC would impede the anti-thrombus effect of NAC. Both images (a, b) and fluorescent signals for platelet (c), fibrin (d) and VWF (e) showed NAC has a strong anti-thrombus effect with or without tPA, meaning that they could be used together clinically.

BIBLIOGRAPHY

1. Smeets MWJ. Erythrocytes and von Willebrand Factor in Venous Thrombosis. 2018.
2. Lozano R, Naghavi M, Foreman K, Lim S, Shibuya K, Aboyans V, et al. Global and regional mortality from 235 causes of death for 20 age groups in 1990 and 2010: A systematic analysis for the Global Burden of Disease Study 2010. Lancet. 2012;380(9859):2095–128.
3. Stefanini L, Bergmeier W. Negative regulators of platelet activation and adhesion. J Thromb Haemost. 2017;220–30.
4. Lehmann M, Schoeman RM, Krohl PJ, Wallbank AM, Samaniuk JR, Jandrot-Perrus M, et al. Platelets drive thrombus propagation in a hematocrit and glycoprotein VI-dependent manner in an in vitro venous thrombosis model. Arterioscler Thromb Vasc Biol. 2018;38(5):1052–62.
5. Zhu S, Herbig BA, Yu X, Chen J, Diamond SL. Contact pathway function during human whole blood clotting on procoagulant surfaces. Front Med. 2018;5(JUL):1–8.
6. Beckman JD, Holle LA, Wolberg AS. Factor XIII cotreatment with hemostatic agents in hemophilia A increases fibrin α-chain crosslinking. J Thromb Haemost. 2018;16(1):131–41.
7. Reininger AJ, Bernlochner I, Penz SM, Ravanat C, Smethurst P, Farndale RW, et al. A 2-Step Mechanism of Arterial Thrombus Formation Induced by Human Atherosclerotic Plaques. J Am Coll Cardiol. 2010;55(11):1147–58.
8. Brass LF. Thrombin and Platelet Activation. Chest. 124(3).
9. Boilard E, Duchez AC, Brisson A. The diversity of platelet microparticles. Curr Opin Hematol. 2015;22(5):437–44.
10. Li Z, Delaney MK, O'Brien KA, Du X. Signaling during platelet adhesion and activation. Arterioscler Thromb Vasc Biol. 2010;30(12):2341–9.
11. Yun SH, Sim EH, Goh RY, Park JI, Han JY. Platelet activation: The mechanisms and potential biomarkers. Biomed Res Int. 2016;2016:10–4.
12. Zhang P, Du J, Zhao L, Wang X, Zhang Y, Yan R, et al. The role of intraplatelet reactive oxygen species in the regulation of platelet glycoprotein Ibα ectodomain shedding.

Thromb Res. 2013;132(6):696–701.

13. van der Meijden PEJ, Heemskerk JWM. Platelet biology and functions: new concepts and clinical perspectives. Nat Rev Cardiol. 2019;16(3):166–79.

14. España F, Ratnoff OD. The role of prekallikrein and high-molecular-weight kininogen in the contact activation of Hageman factor (factor XII) by sulfatides and other agents. J Lab Clin Med. 1983 Oct;102(4):487–99.

15. Van Der Meijden PEJ, Munnix ICA, Auger JM, Govers-Riemslag JWP, Cosemans JMEM, Kuijpers MJE, et al. Dual role of collagen in factor XII-dependent thrombus formation. Blood. 2009;114(4):881–90.

16. Majumder R, Weinreb G, Lentz BR. Efficient thrombin generation requires molecular phosphatidylserine, not a membrane surface. Biochemistry. 2005;44(51):16998–7006.

17. Muthard RW, Welsh JD, Brass LF, Diamond SL. Fibrin, γ′-Fibrinogen, and Transclot Pressure Gradient Control Hemostatic Clot Growth during Human Blood Flow over a Collagen/Tissue Factor Wound. Arterioscler Thromb Vasc Biol. 2015;35(3):645–54.

18. Zhang D, Ebrahim M, Adler K, Blanchet X, Jamasbi J, Megens RTA, et al. Glycoprotein VI is not a Functional Platelet Receptor for Fibrin Formed in Plasma or Blood. Thromb Haemost. 2020;120(6):977–93.

19. Massberg S, Gawaz M, Grüner S, Schulte V, Konrad I, Zohlnhöfer D, et al. A crucial role of glycoprotein VI for platelet recruitment to the injured arterial wall in vivo. J Exp Med. 2003;197(1):41–9.

20. Iba T, Levy JH. Inflammation and thrombosis: roles of neutrophils, platelets and endothelial cells and their interactions in thrombus formation during sepsis. J Thromb Haemost. 2018;16(2):231–41.

21. Stalker TJ, Wu J, Morgans A, Traxler EA, Wang L, Chatterjee MS, et al. Endothelial cell specific adhesion molecule (ESAM) localizes to platelet-platelet contacts and regulates thrombus formation in vivo. J Thromb Haemost. 2009;7(11):1886–96.

22. Lee MY, Diamond SL. A Human Platelet Calcium Calculator Trained by Pairwise Agonist Scanning. PLoS Comput Biol. 2015;11(2):1–24.

23. Maloney SF, Brass LF, Diamond SL. P2Y12 or P2Y1 inhibitors reduce platelet deposition in a microfluidic model of thrombosis while apyrase lacks efficacy under flow conditions. Integr Biol. 2010;2(4):183–92.

24. Branchford BR, Stalker TJ, Law L, Acevedo G, Sather S, Brzezinski C, et al. The small-molecule MERTK inhibitor UNC2025 decreases platelet activation and prevents thrombosis. J Thromb Haemost. 2018;16(2):352–63.

25. Zhu S, Welsh JD, Brass LF, Diamond SL. Platelet-targeting thiol reduction sensor detects thiol isomerase activity on activated platelets in mouse and human blood under flow. J Thromb Haemost. 2016;14(5):1070–81.

26. Perrella G, Nagy M, Watson SP, Heemskerk JWM. Platelet gpvi (glycoprotein vi) and thrombotic complications in the venous system. Arterioscler Thromb Vasc Biol. 2021;(November):2681–92.

27. Alshehri OM, Hughes CE, Montague S, Watson SK, Frampton J, Bender M, et al. Fibrin activates GPVI in human and mouse platelets. Blood. 2015;126(13):1601–8.

28. Lee MY, Verni CC, Herbig BA, Diamond SL. Soluble fibrin causes an acquired platelet glycoprotein VI signaling defect: implications for coagulopathy. J Thromb Haemost. 2017;15(12):2396–407.

29. Zhu S, Travers RJ, Morrissey JH, Diamond SL. FXIa and platelet polyphosphate as therapeutic targets during human blood clotting on collagen/tissue factor surfaces under flow. Blood. 2015;126(12):1494–502.

30. Zhu S, Chen J, Diamond SL. Establishing the Transient Mass Balance of ThrombosisHighlights. Arterioscler Thromb Vasc Biol [Internet]. 2018;38(7):1528–36. Available from: http://atvb.ahajournals.org/lookup/doi/10.1161/ATVBAHA.118.310906

31. Yu X, Tan J, Diamond SL. Hemodynamic force triggers rapid NETosis within sterile thrombotic occlusions. J Thromb Haemost. 2018;16(2):316–29.

32. Zhang Y, Diamond SL. Src family kinases inhibition by dasatinib blocks initial and subsequent platelet deposition on collagen under flow, but lacks efficacy with thrombin generation. Thromb Res. 2020;192(May):141–51.

33. Keating GM. Dasatinib: A Review in Chronic Myeloid Leukaemia and Ph+ Acute Lymphoblastic Leukaemia. Drugs. 2017;77(1):85–96.

34. Li R, Grosser T, Diamond SL. Microfluidic whole blood testing of platelet response to pharmacological agents. Platelets. 2017;28(5):457–62.

35. Senis YA, Mazharian A, Mori J. Src family kinases: At the forefront of platelet activation. Blood. 2014;124(13):2013–24.

36. Sharman J, Hawkins M, Kolibaba K, Boxer M, Klein L, Wu M, et al. An open-label phase 2 trial of entospletinib (GS-9973), a selective spleen tyrosine kinase inhibitor, in chronic lymphocytic leukemia. Blood. 2015;125(15):2336–43.

37. Currie KS, Kropf JE, Lee T, Blomgren P, Xu J, Zhao Z, et al. Discovery of GS-9973, a selective and orally efficacious inhibitor of spleen tyrosine kinase. J Med Chem. 2014;57(9):3856–73.

38. Munnix ICA, Strehl A, Kuijpers MJE, Auger JM, Van Der Meijden PEJ, Van Zandvoort MAM, et al. The glycoprotein VI-phospholipase Cγ2 signaling pathway controls thrombus formation induced by collagen and tissue factor in vitro and in vivo. Arterioscler Thromb Vasc Biol. 2005;25(12):2673–8.

39. Talpaz M, Shah NP, Kantarjian H, Donato N, Nicoll J, Paquette R, et al. Dasatinib in Imatinib-Resistant Philadelphia Chromosome–Positive Leukemias. N Engl J Med. 2006;354(24):2531–41.

40. Sasaki K, Jabbour EJ, Ravandi F, Short NJ, Thomas DA, Garcia-Manero G, et al. Hyper-CVAD plus ponatinib versus hyper-CVAD plus dasatinib as frontline therapy for patients with Philadelphia chromosome-positive acute lymphoblastic leukemia: A propensity score analysis. Cancer. 2016;122(23):3650–6.

41. Andorsky DJ, Kolibaba KS, Assouline S, Forero-Torres A, Jones V, Klein LM, et al. An open-label phase 2 trial of entospletinib in indolent non-Hodgkin lymphoma and mantle cell lymphoma. Br J Haematol. 2019;184(2):215–22.

42. Flinn IW, Bartlett NL, Blum KA, Ardeshna KM, Lacasce AS, Flowers CR, et al. A phase II trial to evaluate the efficacy of fostamatinib in patients with relapsed or refractory diffuse

large B-cell lymphoma (DLBCL). Eur J Cancer. 2016;54:11–7.

43. Bajpai M. Fostamatinib, a Syk inhibitor prodrug for the treatment of inflammatory diseases. IDrugs. 2009 Mar;12(3):174–85.

44. Burke JM, Shustov A, Essell J, Patel-Donnelly D, Yang J, Chen R, et al. An Open-label, Phase II Trial of Entospletinib (GS-9973), a Selective Spleen Tyrosine Kinase Inhibitor, in Diffuse Large B-cell Lymphoma. Clin Lymphoma, Myeloma Leuk. 2018;18(8):e327–31.

45. Duran GE, Sikic BI. The Syk inhibitor R406 is a modulator of P-glycoprotein (ABCB1)-mediated multidrug resistance. PLoS One. 2019;14(1):1–14.

46. Kostos L, Burbury K, Srivastava G, Prince HM. Gastrointestinal bleeding in a chronic myeloid leukaemia patient precipitated by dasatinib-induced platelet dysfunction: Case report. Platelets. 2015;26(8):809–11.

47. Gratacap M-P, Martin V, Valera M-C, Sophie A, Garcia C, Sie P, et al. The new tyrosine-kinase inhibitor and anticancer drug dasatinib reversibly affects platelet activation in vitro and in vivo. Blood. 2009;114(9):1884–92.

48. Totani L, Amore C, Di Santo A, Dell'Elba G, Piccoli A, Martelli N, et al. Roflumilast inhibits leukocyte-platelet interactions and prevents the prothrombotic functions of polymorphonuclear leukocytes and monocytes. J Thromb Haemost. 2016;14(1):191–204.

49. Van Eeuwijk JMM, Stegner D, Lamb DJ, Kraft P, Beck S, Thielmann I, et al. The novel oral Syk inhibitor, Bl1002494, protects mice from arterial thrombosis and thromboinflammatory brain infarction. Arterioscler Thromb Vasc Biol. 2016;36(6):1247–53.

50. Clarke AS, Rousseau E, Wang K, Kim JY, Murray BP, Bannister R, et al. Effects of GS-9876, a novel spleen tyrosine kinase inhibitor, on platelet function and systemic hemostasis. Thromb Res. 2018;170(May):109–18.

51. Andre P, Morooka T, Sim D, Abe K, Lowell C, Nanda N, et al. Critical role for Syk in responses to vascular injury. Blood. 2011;118(18):5000–10.

52. Schmaier AA, Zou Z, Kazlauskas A, Emert-Sedlak L, Fong KP, Neeves KB, et al. Molecular priming of Lyn by GPVI enables an immune receptor to adopt a hemostatic role. Proc Natl Acad Sci. 2009;106(50):21167–72.

53. Jooss NJ, Simone I De, Provenzale I, Fern DI, Brouns SLN, Farndale RW, et al. Role of Platelet Glycoprotein VI and Tyrosine Kinase Syk in Thrombus Formation on Collagen-Like Surfaces. Int J Mol Sci. 2019;20(2788):1–20.

54. Belair DG, Le NN, Murphy WL. Regulating VEGF signaling in platelet concentrates: Via specific VEGF sequestering. Biomater Sci. 2016;4(5):819–25.

55. Ruggeri ZM, Zarpellon A, Roberts JR, Mc Clintock RA, Jing H, Mendolicchio GL. Unravelling the mechanism and significance of thrombin binding to platelet glycoprotein Ib. Thromb Haemost. 2010;104(5):894–902.

56. Onselaer M, Hardy AT, Wilson C, Sanchez X, Babar AK, Miller JLC, et al. Fibrin and D-dimer bind to monomeric GPVI. Blood Adv. 2017;1(19):1495–504.

57. Pollitt AY, Poulter NS, Gitz E, Navarro-Nuñez L, Wang YJ, Hughes CE, et al. Syk and src family kinases regulate c-type lectin receptor 2 (clec-2)-mediated clustering of podoplanin and platelet adhesion to lymphatic endothelial cells. J Biol Chem. 2014;289(52):35695–710.

58. Mazharian A, Ghevaert C, Zhang L, Massberg S, Watson SP. Dasatinib enhances megakaryocyte differentiation but inhibits platelet formation. Blood. 2011;117(19):5198–206.

59. Colace T V., Muthard RW, Diamond SL. Thrombus growth and embolism on tissue factor-bearing collagen surfaces under flow: Role of thrombin with and without fibrin. Arterioscler Thromb Vasc Biol. 2012;32(6):1466–76.

60. Sharman J, Hawkins M, Kolibaba K, Boxer M, Klein L, Wu M, et al. An open-label phase 2 trial of entospletinib (GS-9973), a selective spleen tyrosine kinase inhibitor, in chronic lymphocytic leukemia. Blood. 2015;125(15):2336–43.

61. Spalton JC, Mori J, Pollitt AY, Hughes CE, Eble JA, Watson SP. The novel Syk inhibitor R406 reveals mechanistic differences in the initiation of GPVI and CLEC-2 signaling in platelets. J Thromb Haemost. 2009;7(7):1192–9.

62. Fasbender F, Claus M, Wingert S, Sandusky M, Watzl C. Differential requirements for Src-family kinases in SYK or ZAP70-mediated SLP-76 phosphorylation in lymphocytes. Front

Immunol. 2017;8(JUL):1–9.

63. Loren CP, Aslan JE, Rigg RA, Nowak MS, Healy LD, Gruber A, et al. The BCR-ABL inhibitor ponatinib inhibits platelet immunoreceptor tyrosine-based activation motif (ITAM) signaling, platelet activation and aggregate formation under shear. Thromb Res. 2015;135(1):155–60.

64. Blair TA, III ALF. Platelet surface marker analysis by mass cytometry. Platelets. 2019;0(0):1–8.

65. Nieswandt B, Schulte V, Bergmeier W, Mokhtari-Nejad R, Rackebrandt K, Cazenave JP, et al. Long-term antithrombotic protection by in vivo depletion of platelet glycoprotein VI in mice. J Exp Med. 2001;193(4):459–69.

66. Schuhmann MK, Kraft P, Bieber M, Kollikowski AM, Schulze H, Nieswandt B, et al. Targeting platelet GPVI plus rt-PA administration but not α2β1-mediated collagen binding protects against ischemic brain damage in mice. Int J Mol Sci. 2019;20(8):1–7.

67. Rayes J, Watson SP, Nieswandt B. Functional significance of the platelet immune receptors GPVI and CLEC-2. J Clin Invest. 2019;129(1).

68. Ahmed MU, Kaneva V, Loyau S, Nechipurenko D, Receveur N, Le Bris M, et al. Pharmacological Blockade of Glycoprotein VI Promotes Thrombus Disaggregation in the Absence of Thrombin. Arterioscler Thromb Vasc Biol. 2020;(September):2127–42.

69. Mangin PH, Onselaer MB, Receveur N, Le Lay N, Hardy AT, Wilson C, et al. Immobilized fibrinogen activates human platelets through glycoprotein VI. Haematologica. 2018;103(5):898–907.

70. Dubois C, Panicot-Dubois L, Merrill-Skoloff G, Furie B, Furie BC. Glycoprotein VI-dependent and -independent pathways of thrombus formation in vivo. Blood. 2006;107(10):3902–6.

71. Mangin P, Yap CL, Nonne C, Sturgeon SA, Goncalves I, Yuan Y, et al. Thrombin overcomes the thrombosis defect associated with platelet GPVI/FcRγ deficiency. Blood. 2006;107(11):4346–53.

72. Nagy M, Perrella G, Dalby A, Becerra MF, Quintanilla LG, Pike JA, et al. Flow studies on

human GPVI-deficient blood under coagulating and noncoagulating conditions. Blood Adv. 2020;4(13):2953–61.

73. Dobie G, Kuriri FA, Omar MMA, Alanazi F, Gazwani AM, Tang CPS, et al. Ibrutinib, but not zanubrutinib, induces platelet receptor shedding of GPIb-IX-V complex and integrin αIIbβ3 in mice and humans. Blood Adv. 2019;3(24):4298–311.

74. Vielreicher M, Harms G, Butt E, Walter U, Obergfell A. Dynamic interaction between Src and C-terminal Src kinase in integrin αIIbβ3-mediated signaling to the cytoskeleton. J Biol Chem. 2007;282(46):33623–31.

75. DeCortin ME, Brass LF, Diamond SL. Core and shell platelets of a thrombus: A new microfluidic assay to study mechanics and biochemistry. Res Pract Thromb Haemost. 2020;4(7):1158–66.

76. Flamm MH, Colace T V., Chatterjee MS, Jing H, Zhou S, Jaeger D, et al. Multiscale prediction of patient-specific platelet function under flow. Blood. 2012;120(1):190–8.

77. Lu Y, Lee MY, Zhu S, Sinno T, Diamond SL. Multiscale simulation of thrombus growth and vessel occlusion triggered by collagen/tissue factor using a data-driven model of combinatorial platelet signalling. Math Med Biol. 2017;34(4):523–46.

78. Shankar KN, Zhang Y, Sinno T, Diamond SL. A three-dimensional multiscale model for the prediction of thrombus growth under flow with single-platelet resolution. PLoS Comput Biol. 2022;18(1):1–19.

79. Chen J, Diamond SL. Reduced model to predict thrombin and fibrin during thrombosis on collagen/tissue factor under venous flow: Roles of γ'-fibrin and factor XIa. PLoS Comput Biol. 2019;15(8):1–16.

80. Trigani KT, Diamond SL. Intrathrombus Fibrin Attenuates Spatial Sorting of Phosphatidylserine Exposing Platelets during Clotting under Flow. Thromb Haemost. 2020;

81. Reutelingsperger CPM, Van Heerde WL. Annexin V, the regulator of phosphatidylserine-catalyzed inflammation and coagulation during apoptosis. Cell Mol Life Sci. 1997;53(6):527–32.

82. Stuart MC, Bevers EM, Comfurius P, Zwaal RF, Reutelingsperger CP, Frederik PM.

Ultrastructural detection of surface exposed phosphatidylserine on activated blood platelets. Thromb Haemost. 1995 Oct;74(4):1145–51.

83. Zhu S, Lu Y, Sinno T, Diamond SL. Dynamics of thrombin generation and flux from clots during whole human blood flow over collagen/tissue factor surfaces. J Biol Chem. 2016;291(44):23027–35.

84. Navarro S, Stegner D, Nieswandt B, Heemskerk JWM, Kuijpers MJE. Temporal roles of platelet and coagulation pathways in collagen- and tissue factor-induced thrombus formation. Int J Mol Sci. 2022;23(1).

85. Siljander PRM, Munnix ICA, Smethurst PA, Deckmyn H, Lindhout T, Ouwehand WH, et al. Platelet receptor interplay regulates collagen-induced thrombus formation in flowing human blood. Blood. 2004;103(4):1333–41.

86. Nissinen L, Koivunen J, Käpylä J, Salmela M, Nieminen J, Jokinen J, et al. Novel α2β1 integrin inhibitors reveal that integrin binding to collagen under shear stress conditions does not require receptor preactivation. J Biol Chem. 2012;287(53):44694–702.

87. Santoro SA, Walsh JJ, Staatz WD, Baranski KJ. Distinct determinants on collagen support α2β1 integrin-mediated platelet adhesion and platelet activation. Mol Biol Cell. 1991;2(11):905–13.

88. Lecut C, Feeney LA, Kingsbury G, Hopkins J, Lanza F, Gachet C, et al. Human platelet glycoprotein VI function is antagonized by monoclonal antibody-derived fab fragments. J Thromb Haemost. 2003;1(12):2653–62.

89. Jadoui S, Le Chapelain O, Ollivier V, Mostefa-Kara A, Di Meglio L, Dupont S, et al. Glenzocimab does not impact glycoprotein VI-dependent inflammatory hemostasis. Haematologica. 2021;106(7):2000–3.

90. Mammadova-Bach E, Ollivier V, Loyau S, Schaff M, Dumont B, Favier R, et al. Platelet glycoprotein VI binds to polymerized fibrin and promotes thrombin generation. Blood. 2015;126(5):683–91.

91. Chen J, Reheman A, Gushiken FC, Nolasco L, Fu X, Moake JL, et al. N-acetylcysteine reduces the size and activity of von Willebrand factor in human plasma and mice. J Clin

Invest. 2011;121(2):593–603.

92. De Lizarrondo SM, Gakuba C, Herbig BA, Repessé Y, Ali C, Denis C V., et al. Potent thrombolytic effect of N-acetylcysteine on arterial thrombi. Circulation. 2017;136(7):646–60.

93. WHO. World health organization model list of essential medicines. Ment Holist Heal Some Int Perspect. 2019;119–34.

94. Sadowska AM, Verbraecken J, Darquennes K, De Backer W. Role for N-acetylcysteine in the management of COPD. Int J Chron Obstruct Pulmon Dis. 2006;1(2):99–106.

95. Kellum JA, Lameire N, Aspelin P, Barsoum RS, Burdmann EA, Goldstein SL, et al. Kidney disease: Improving global outcomes (KDIGO) acute kidney injury work group. KDIGO clinical practice guideline for acute kidney injury. Kidney Int Suppl. 2012;2(1):1–138.

96. Santus P, Corsico A, Solidoro P, Braido F, Di Marco F, Scichilone N. Oxidative stress and respiratory system: Pharmacological and clinical reappraisal of N-acetylcysteine. COPD J Chronic Obstr Pulm Dis. 2014;11(6):705–17.

97. Lillicrap D. Thrombolytic potential of N-acetylcysteine: Evidence for significant benefit in mitigating arterial thrombosis. Circulation. 2017;136(7):661–3.

98. Herbig BA, Diamond SL. Pathological von Willebrand factor fibers resist tissue plasminogen activator and ADAMTS13 while promoting the contact pathway and shear-induced platelet activation. J Thromb Haemost. 2015;13(9):1699–708.